www.oftalmoloji.org

E-ISSN: 2149-8709

TURKISH JOURNAL OF OPHTHALMOLOGY

TURKISH JOURNAL OF OPHTHALMOLOGY TJO

May June 2022
52 Volume
Issue 3

galenos

TURKISH JOURNAL OF OPHTHALMOLOGY

TJO

www.oftalmoloji.org

Publishing House
Molla Gürani Mah. Kaçamak Sokak No: 21,
34093 Fındıkzade-İstanbul-Turkey
Publisher Certificate Number: 14521
Phone: +90 212 621 99 25 **Fax:** +90 212 621 99 27
E-mail: info@galenos.com.tr
Online Publishing Date: June 2022
International scientific journal published bimonthly.
E-ISSN: 2149-8709

The Turkish Journal of Ophthalmology is an official journal of the Turkish Ophthalmological Association.

On Behalf of the Turkish Ophthalmological Association Owner

Ziya KAPRAN
Private Practice, İstanbul, Turkey

TURKISH JOURNAL OF OPHTHALMOLOGY

TJO

www.oftalmoloji.org

ABOUT US

The Turkish Journal of Ophthalmology is the only scientific periodical publication of the Turkish Ophthalmological Association and has been published since January 1929. The Journal was first published in Turkish and French in an effort to bring Turkish ophthalmological research to the international scientific audience. Despite temporary interruptions in publication over the intervening decades due to various challenges, the Turkish Journal of Ophthalmology has been published continually from 1971 to the present.

The Journal currently publishes articles in Turkish and English after an independent, unbiased double-blind peer review process. Issues are published electronically six times a year, with occasional special issues.

The aim of the Turkish Journal of Ophthalmology is to publish original research articles of the highest scientific and clinical value at an international level. It also features review articles, case reports, editorial commentary, letters to the editor, educational contributions, and congress/meeting announcements.

The target audience of the Turkish Journal of Ophthalmology includes physicians working in the various areas of ophthalmology and all other health professionals interested in these issues.

The Journal's publication policies are based on the Recommendations for the Conduct, Reporting, Editing, and Publication of Scholarly Work in Medical Journals from the International Committee of Medical Journal Editors (ICMJE) (2013, archived at http://www.icmje.org/).

The Turkish Journal of Ophthalmology is indexed in the **PubMed/MEDLINE, PubMed Central (PMC), Web of Science-Emerging Sources Citation Index (ESCI), Scopus, TÜBİTAK/ULAKBİM, Directory of Open Access Journals (DOAJ), EBSCO Database, Gale, CINAHL, Proquest, Embase, British Library, Index Copernicus, J-Gate, IdealOnline, Türk Medline, Hinari, GOALI, ARDI, OARE, AGORA, and Turkish Citation Index.**

Open Access Policy

This journal provides immediate open access to its content on the principle that making research freely available to the public supports a greater global exchange of knowledge.

Author(s) and copyright owner(s) grant access to all users for the articles published in the Turkish Journal of Ophthalmology as free of charge.

Open Access Policy is based on rules of Budapest Open Access Initiative (BOAI). By "open access" to [peer-reviewed research literature], we mean its free availability on the public internet, permitting any users to read, download, copy, distribute, print, search, or link to the full texts of these articles, crawl them for indexing, pass them as data to software, or use them for any other lawful purpose, without financial, legal, or technical barriers other than those inseparable from gaining access to the internet itself.

Copyright

Turkish Journal of Ophtalmology is an open access publication, and the journal's publication model is based on Budapest Open Access Initiative (BOAI) declaration.

All published content is available online, free of charge at www.oftalmoloji.org/.

Subscription Information

The full text of all issues of the Journal can be accessed free of charge at www.oftalmoloji.org.

Contact Information

Editor-in-Chief, Banu Bozkurt, MD, Professor of Ophthalmology

Turkish Journal of Ophthalmology
Avrupa Konutları Kale, Maltepe Mah. Yedikule Çırpıcı Yolu Sk. 9. Blok No: 2 Kat:1 Ofis:1 Zeytinburnu-İstanbul-Türkiye
Phone: +90 212 801 44 36/37
Fax: +90 212 801 44 39
Website: https://www.oftalmoloji.org/
E-mail: dergi@oftalmoloji.org - sekreter@oftalmoloji.org

Secretary: Selvinaz Arslan

Advertising

Inquiries regarding advertising should be directed to the Editor-in-Chief via the Journal's secretariat.

Advertisement

Applications for advertisement should be addressed to the editorial office.

Address: Avrupa Konutları Kale, Maltepe Mah. Yedikule Çırpıcı Yolu Sk. 9. Block No: 2 Floor:1 Office:1 Zeytinburnu-Istanbul-Turkey
Phone: +90 212 801 44 36/37; **Fax:** +90 212 801 44 39
Website: www.oftalmoloji.org
E-mail: dergi@oftalmoloji.org - sekreter@oftalmoloji.org

Publisher Contact Information

Galenos Publishing House, Ltd. Şti.
Address: Molla Gürani Mah. Kaçamak Sk. No: 21, 34093 Fındıkzade-İstanbul-Türkiye
Phone: +90 212 621 99 25;
Fax: +90 212 621 99 27
E-mail: info@galenos.com.tr

Information for Authors

Instructions for authors can be found on the Journal website and at www.oftalmoloji.org.

Material Disclaimer

The opinions and reports stated in all articles published in the Turkish Journal of Ophthalmology are the views of the author(s). They do not reflect the opinions of the Editor-in-Chief, editorial board, or publisher, and these parties accept no responsibility for these articles.

OPEN ACCESS

TURKISH JOURNAL OF OPHTHALMOLOGY

TJO

www.oftalmoloji.org

INSTRUCTIONS TO AUTHORS

The Turkish Journal of Ophthalmology is the official periodical of the Turkish Ophthalmological Association and accepts manuscripts written in Turkish and English. Each issue is published electronically in both Turkish and English. Manuscripts submitted in Turkish should be consistent with the Turkish Dictionary and Writing Guide ("Türkçe Sözlüğü ve Yazım Kılavuzu") of the Turkish Language Association, and care should be taken to use the Turkish forms of words. The Turkish Journal of Ophthalmology charges no submission or manuscript processing fee.

Contributions submitted to the Journal must be original and not published elsewhere or under consideration for publication by another journal.

Reviewed and accepted manuscripts are translated either from Turkish to English or from English to Turkish by the Journal through a professional translation service. Prior to publication, the translations are sent to the authors for approval or correction requests, to be returned within 3 days. If no response is received from the corresponding author within this period, the translation is checked and approved by the editorial board.

Turkish Journal of Ophthalmology is abbreviated as TJO, but should be denoted as Turk J Ophthalmol when referenced. In the international index and database, the journal is registered as Turkish Journal of Ophthalmology, abbreviated as Turk J Ophthalmol.

Scientific and ethical liability for a contribution remains with the author(s) and copyright is held by TJO. Authors are responsible for article contents and accuracy of the references. Manuscripts submitted for publication must be accompanied by the Copyright Transfer Form signed by all contributing authors. By submitting this form, the authors guarantee that the manuscript and the data therein are not previously published or being evaluated for publication elsewhere and declare their scientific contribution and liability.

All manuscripts submitted to TJO are screened for plagiarism using iThenticate. Results indicating plagiarism may result in manuscripts being returned or rejected.

Experimental, clinical and drug studies requiring approval by an ethics committee must be submitted to TJO with an ethics committee approval report confirming that the study was conducted in accordance with international agreements and the Helsinki Declaration (2013 revision) (https://www.wma.net/policies-post/wma-declaration-of-helsinki-ethical-principles-for-medical-research-involving-human-subjects). Information regarding ethical approval and patient informed consent for the study should be indicated in the Materials and Methods section. For experimental animal studies, the authors should include a statement confirming that the study procedures were in accordance with animal rights as per the Guide for the Care and Use of Laboratory Animals (http://oacu.od.nih.gov/regs/guide/guide.pdf) and that animal ethics committee approval was obtained.

If an article includes any direct or indirect commercial connections or if any institution provided material support for the research, authors must include a statement in the cover letter stating that they have no commercial relationship with the relevant product, drug, pharmaceutical company, etc. or specifying the nature of their relationship (consultant, other agreements).

All individuals and organizations from which the authors received any form of assistance and other support should be declared, and the Conflicts of Interest Form should be used to explain any conflicts of interest.

All contributions are evaluated by the editor-in-chief, associate editors, and independent referees.

The Turkish Journal of Ophthalmology uses an independent, unbiased, double-blind peer review process. Manuscripts are received and reviewed by the editor-in-chief, who directs them to the appropriate section editor. The section editor sends the manuscript to three independent referees. Referees are selected by the editorial board from among national and international experts in the area relevant to the study. The referees accept or reject the invitation to review the manuscript within two weeks. If they accept, they are expected to return their decision within 21 days. The associate editor reviews the referees' decisions, adds their own feedback, and returns the manuscript to the editor-in-chief, who makes the final decision. In case of disagreement among referees, the editor can assign a new referee.

The editor-in-chief, associate editors, biostatistics consultant, and English language editor may make minor changes to accepted manuscripts before publication, provided they do not fundamentally change the text.

In case of a potential scientific error or suspicion/allegation of ethical infringement in research submitted for evaluation, the Journal reserves the right to submit the manuscript to the supporting institutions or other authorities for investigation. The Journal accepts the responsibility of properly following-up on the issue but does not undertake any responsibility for the actual investigation or any power of decision regarding errors.

The editorial policies and general guidelines for manuscript preparation specified below are based on the "Recommendations for the Conduct, Reporting, Editing, and Publication of Scholarly Work in Medical Journals" from the International Committee of Medical Journal Editors (ICMJE) (2013, archived at http://www.icmje.org/).

Research articles, systematic reviews, and meta-analyses should be prepared according to the relevant guidelines:

CONSORT statement for randomized controlled trials (Moher D, Schultz KF, Altman D, for the CONSORT Group. The CONSORT statement revised recommendations for improving the quality of reports of parallel group randomized trials. JAMA 2001; 285: 1987-91) (http://www.consort-statement.org/);

PRISMA statement of preferred reporting items for systematic reviews and meta-analyses (Moher D, Liberati A, Tetzlaff J, Altman DG, The PRISMA Group. Preferred Reporting Items for Systematic Reviews and Meta-Analyses: The PRISMA Statement. PLoS Med 2009; 6(7): e1000097.) (http://www.prisma-statement.org/);

STARD checklist for the reporting of studies of diagnostic accuracy (Bossuyt PM, Reitsma JB, Bruns DE, Gatsonis CA, Glasziou PP, Irwig LM, et al., for the STARD Group. Towards complete and accurate reporting of studies of diagnostic accuracy: the STARD initiative. Ann Intern Med 2003;138:40-4.) (http://www.stard-statement.org/);

STROBE statement, a checklist of items that should be included in reports of observational studies (http://www.strobe-statement.org/);

MOOSE guidelines for meta-analysis and systemic reviews of observational studies (Stroup DF, Berlin JA, Morton SC, et al. Meta-analysis of observational studies in epidemiology: a proposal for reporting Meta-analysis of observational Studies in Epidemiology (MOOSE) group. JAMA 2000; 283: 2008-12).

GENERAL GUIDELINES

All submissions to TJO are made electronically through the Journal Agent website (http://journalagent.com/tjo/). After creating an account, authors can use this system for the online submission and review process. Manuscripts collected in the system are archived according to the rules of the ICMJE, Index Medicus (Medline/PubMed) and Ulakbim-Turkish Medicine Index.

Format: Manuscripts should be prepared using Microsoft Word, size A4 with 2.5 cm margins on all sides, 12 pt Arial font, and 1.5 line spacing.

Abbreviations: Abbreviations should be defined at first mention and used consistently throughout the text thereafter. Internationally accepted abbreviations should be used; refer to scientific writing guides as necessary.

Cover letter: The cover letter should include the manuscript type, a statement confirming that the article is not under consideration for publication by another journal, declaration of all sources of funding and equipment (if applicable) and a conflict of interest statement. In addition, the authors should confirm that articles submitted in English have undergone language editing and that original research articles have been reviewed by a biostatistician.

REFERENCES

Authors are solely responsible for the accuracy of all references.

In-text citations: References should be indicated as a superscript immediately after the period/full stop of the relevant sentence. If the author(s) of a reference is/are indicated at the beginning of the sentence, this reference should be written in superscript immediately after the author's name. Relevant research conducted in Turkey or by Turkish investigators should be cited when possible.

Citing presentations given at scientific meetings, unpublished manuscripts, theses, Internet addresses, and personal interviews or experiences should be avoided. If such references are used, they should be indicated in parentheses at the end of the relevant sentence in the text, without a reference number and written in full, in order to clarify their nature.

References section: References should be numbered consecutively in the order in which they are first mentioned in the text. All authors should be listed regardless of number. The titles of journals should be abbreviated according to the style used in the Index Medicus.

Reference Format

Journal: Last name(s) of the author(s) and initials, article title, publication title and its original abbreviation, publication date, volume, the inclusive page numbers.

Example:

Collin JR, Rathbun JE. Involutional entropion: a review with evaluation of a procedure. Arch Ophthalmol. 1978;96:1058-1064.

TURKISH JOURNAL OF OPHTHALMOLOGY

TJO

www.oftalmoloji.org

INSTRUCTIONS TO AUTHORS

Book: Last name(s) of the author(s) and initials, chapter title, book editors, book title, edition, place of publication, date of publication and inclusive page numbers of the extract cited. Example:
Herbert L. The Infectious Diseases (1st ed). Philadelphia; Mosby Harcourt; 1999:11;1-8.
Book Chapter: Last name(s) of the author(s) and initials, chapter title, book editors, book title, edition, place of publication, date of publication and inclusive page numbers of the cited piece. Example:
O'Brien TP, Green WR. Periocular Infections. In: Feigin RD, Cherry JD, eds. Textbook of Pediatric Infectious Diseases (4th ed). Philadelphia; W.B. Saunders Company;1998:1273-1278.
Books in which the editor and author are the same person: Last name(s) of the author(s) and initials, chapter title, book editors, book title, edition, place of publication, date of publication and inclusive page numbers of the cited piece. Example:
Solcia E, Capella C, Kloppel G. Tumors of the exocrine pancreas. In: Solcia E, Capella C, Kloppel G, eds. Tumors of the Pancreas. 2nd ed. Washington: Armed Forces Institute of Pathology; 1997:145-210.

FIGURES, TABLES, GRAPHICS, AND IMAGES

All visual materials together with their legends should be located on separate pages following the main text.
Images: Images (pictures) should be numbered and include a brief title. Permission to reproduce pictures that were published elsewhere must be included. All pictures should be of the highest quality possible, in JPEG format, and at a minimum resolution of 300 dpi.
Tables, Graphics, Figures: All tables, graphics or figures should be enumerated according to their sequence within the text and a brief descriptive caption should be written. Any abbreviations used should be defined in the accompanying legend. Tables in particular should be explanatory and facilitate readers' understanding of the manuscript, and should not repeat data presented in the main text.

BIOSTATISTICS

To ensure controllability of research findings, the study design, study sample, and methodological approaches and practices should be explained with appropriate sources referenced.
The "p" value defined as the limit of significance along with appropriate indicators of measurement error and uncertainty (confidence interval, etc.) should be specified. Statistical terms, abbreviations, and symbols used in the article should be described and the software used should be stated. Statistical terminology (random, significant, correlation, etc.) should not be used in non-statistical contexts.
All data and analysis results should be presented as tables and figures and summarized in the text of the Results section. Details of the biostatistical methods and procedures used should be presented in the Materials and Methods section or under a separate Statistics heading before the Results section.

MANUSCRIPT TYPES

Original Research Articles

Includes clinical studies, clinical observations, new techniques, and experimental and in vitro studies. Original research articles should include a title, structured abstract, keywords relevant to the content of the article, and introduction, materials and methods, results, discussion, study limitations, conclusion, references, tables/figures/images, and acknowledgements sections. The title, abstract, and keywords should be written in both Turkish and English. The manuscript should be formatted as specified in the guidelines above and should not exceed sixteen A4 pages.
Title Page: This page should include the manuscript title, short title, and author name(s) and affiliation(s). The following descriptions should be stated in the given order:
1. Title of the manuscript (Turkish and English), as concise and explanatory as possible, including no abbreviations, up to 135 characters
2. Short title (Turkish and English), up to 60 characters
3. Each author's full name (without abbreviations and academic titles) and affiliation
4. The corresponding author's name, postal address, e-mail address, and phone and fax numbers
5. If the study was presented at a congress and its abstract was published in the congress abstract book, please provide the date and location of the relevant scientific meeting.
Abstract: The article should be summarized in a Turkish abstract not exceeding 250 words and a corresponding English abstract up to 285 words in length. References should not be cited in the abstract. The use of abbreviations should be avoided as much as possible; any abbreviations in the abstract should be defined and used independently of those used in the main text. For original research articles, the structured abstract should include the following 5 subheadings:
Objectives: The aim of the study should be clearly stated.
Materials and Methods: The study should be described, including selection criteria, design (randomized, retrospective/prospective, etc.), and statistical methods applied, if applicable.
Results: The main results of the study should be stated and the statistical significance level should be indicated.
Conclusion: The results of the study should be summarized and the clinical applicability of the results should be defined.
Keywords: The abstract should be followed by 3 to 5 keywords. Keywords in English should be consistent with the Medical Subject Headings (MESH) terms (www.nlm.nih.gov/mesh/MBrowser.html). Turkish keywords should be direct translations of MESH terms.
The main text of the article should include the following headings:
Introduction: Should consist of a brief background to the subject and the study objective(s), supported by information from the literature.
Materials and Methods: The study plan should be clearly described, including whether the study was randomized and retrospective or prospective, the inclusion and exclusion criteria applied, the patient/sample number and characteristics, and statistical methods used.
Results: The results of the study should be stated, with tables/figures given in numerical order; the results should be evaluated according to the statistical analysis methods applied. See the Tables, Graphics, Figures, And Images section of the General Guidelines for details about the preparation of visual material.
Discussion: The study results should be discussed in terms of their favorable and unfavorable aspects and they should be compared with the literature. The conclusion of the study should be highlighted.
Study Limitations: This section should state which data and analyses could not be included in the study, discuss limitations of the study, and give recommendations for future studies.
Conclusion: Highlights the results obtained and conclusions that can be drawn from the study.
Acknowledgements: Any technical or financial support or editorial contributions (statistical analysis, English/Turkish evaluation) towards the study should appear at the end of the article.
References: Authors are responsible for the accuracy of the references. See the General Guidelines for details about the usage and formatting required.

Case Reports

Case reports should present cases which are rarely seen, feature novelty in diagnosis and treatment, and contribute to our current knowledge. The first page should include the title in Turkish and English, an unstructured Turkish summary up to 150 words in length and a corresponding English abstract not exceeding 175 words, and keywords in both languages. The main text should include the introduction, case presentation, discussion, and references. The entire text should not exceed 5 pages (A4, formatted as specified above).

Review Articles

Review articles can address any aspect of clinical or basic ophthalmology and should be written in a format that describes, discusses, and analyzes the current state of knowledge or clinical use based on the latest evidence and offers directions for future research. Most review articles are invited, but uninvited review submissions are also welcome. Contacting the section editor is recommended before submitting a review.
Reviews articles analyze topics in depth, independently, and without bias. The first section should include Turkish and English titles, unstructured summaries, and keywords. All cited literature should be referenced. The entire text should not exceed 25 pages (A4, formatted as specified above).

Letters to the Editor

Letters to the Editor should be short commentaries related to current developments in ophthalmology and their scientific and social aspects, or may ask questions or offer further contributions in response to articles published in the Journal. Letters do not include a title or an abstract, should not exceed 1,000 words, and can have up to 5 references.

CORRESPONDENCE

All correspondence should be directed to the Journal's secretariat:
Post: Turkish Ophthalmological Association
Avrupa Konutları Kale, Maltepe Mah. Yedikule Çırpıcı Yolu Sk. 9. Blok No: 2 Kat:1 Ofis:1 Zeytinburnu-İstanbul-Turkey
Phone: +90 212 801 44 36/37 Fax: +90 212 801 44 39
Web Page: www.oftalmoloji.org
E-mail: dergi@oftalmoloji.org / sekreter@oftalmoloji.org

TURKISH JOURNAL OF OPHTHALMOLOGY

TJO

www.oftalmoloji.org

CONTENTS

TURKISH JOURNAL OF OPHTHALMOLOGY

TJO

www.oftalmoloji.org

EDITORIAL

2022 Issue 3 at a Glance:

Esteemed colleagues,

In the third issue of 2022, the Turkish Journal of Ophthalmology presents 8 original studies, 3 case reports, and a letter to the editor with a reply from the authors.

A clinical study by Kıyat et al. titled "Dry Eye and Meibomian Gland Dysfunction in Patients with Neovascular Age-Related Macular Degeneration Receiving Intravitreal Injection Therapy" aimed to evaluate the meibomian glands and presence of dry eye in 60 eyes of 30 patients receiving intravitreal injection therapy for neovascular age-related macular degeneration. Each patient received intravitreal injection therapy in one eye (Group 1), while the fellow healthy eye received no treatment (Group 2). Mean Schirmer 1 and tear film break-up time were found to be lower in Group 1. Group 1 did not differ significantly from Group 2 in terms of mean Oxford score or upper eyelid meibography score, whereas their lower eyelid meibography score was significantly higher.

In their study titled "Palliative Efficacy of Intrastromal Amniotic Membrane Procedure in Symptomatic Bullous Keratopathy Patients," Furundaoturan et al. evaluated the results of intrastromal human amniotic membrane implantation performed for palliation in patients with symptomatic bullous keratopathy and limited visual potential. They stated that this method may be an alternative approach to keratoplasty in patients with poor visual prognosis after corneal transplantation.

Another study by Furundaoturan et al. titled "Evaluation of Choroidal Vascular Index in Amblyopic Patients" aimed to compare subfoveal choroidal thickness (SFCT) and choroidal vascular index (CVI) between patients with hyperopic or strabismic amblyopia and healthy eyes. The study included 17 patients diagnosed with strabismic amblyopia (Group 1), 29 patients diagnosed with hyperopic amblyopia (Group 2), and 16 eyes of 16 healthy volunteers (Group 3). SFCT was significantly increased in the amblyopic eyes of Group 2 patients compared to Group 3, while CVI was significantly lower in the Group 2 amblyopic eyes compared to fellow eyes and Group 3.

In their study titled "Hedgehog Signal Defect Leading to Familial Exudative Vitreoretinopathy-Like Disease and Gastrointestinal Malformation," Şahinoğlu Keşkek et al. described a new genetic link between familial exudative vitreoretinopathy-like disease and malformations of the gastrointestinal tract, and emphasized the importance of the hedgehog pathway in the development of the retinal vascular system and intestines.

In a study titled "Survey of Intravitreal Injection Preferences for the Treatment of Age-Related Macular Degeneration and Macular Edema Among Members of the Turkish Ophthalmological Association," Karabaş et al. conducted an anonymous internet-based survey with members of the Turkish Ophthalmological Association to analyze ophthalmologists' current preferences for the treatment of age-related macular degeneration and macular edema and evaluate the off-label use of bevacizumab in Turkey. They determined that ophthalmologists used bevacizumab as a first-line agent in patients with age-related macular degeneration, diabetic macular edema, and retinal vein occlusion when the current legal regulations were considered, but the participants' preference for bevacizumab decreased when economic and legal restrictions were disregarded.

Altınbay et al. conducted a study titled "Comparison of Reading Test Parameters from the Print and Tablet Application Forms of the Minnesota Low Vision Reading Test" including a total of 116 individuals (92 with normal vision and 24 with low vision). They compared reading parameters measured using the printed card and tablet application forms of the Turkish version of the Minnesota Low Vision Reading Test (MNREAD-TR) in individuals with normal vision and low vision and found that both forms gave similar results for reading acuity and critical print size in individuals with normal vision and for reading acuity and reading accessibility index in individuals with low vision.

In their study titled "Investigation of the Role of Convolutional Neural Network Architectures in the Diagnosis of Glaucoma using Colored Fundus Photography," Atalay et al. evaluated the performance of convolutional neural network (CNN) architectures in differentiating glaucomatous eyes from normal eyes and showed that appropriately designed and trained CNNs can distinguish glaucomatous fundus photographs from normal ones with high accuracy, even with a small number of fundus photographs.

In a study titled "Effectiveness, Sensitivity, and Specificity of Intraocular Lens Power Calculation Formulas for Short Eyes," Stopyra compared intraocular lens power calculation formulas in terms of absolute error (AE) and receiver operating characteristic curves in eyes with an axial length shorter than 22.0 mm. The author reported that the Hoffer Q formula gave the lowest AE level and emphasized that this formula could be recommended for the calculation of IOL power in hyperopic eyes.

TURKISH JOURNAL OF OPHTHALMOLOGY

TJO

www.oftalmoloji.org

EDITORIAL

The first case in the case reports section of this issue is from Athanasiadis et al. and titled "Descemet Stripping Endothelial Keratoplasty in Congenital Aniridia: An Interesting and Challenging Story." The authors reported the results of ultra-thin Descemet stripping endothelial keratoplasty performed in a 59-year-old patient with congenital aniridia who developed progressive endothelial dysfunction and aniridia-related keratopathy and was observed to have corneal decompensation after cataract surgery.

In their case report titled "Asymptomatic Unilateral Full-Thickness Macular Hole in a Patient with Bietti Crystalline Dystrophy During 13-Year Follow-up with Optical Coherence Tomography," Saatci et al. reported the longitudinal follow-up results of a patient with Bietti crystalline dystrophy who developed a unilateral full-thickness macular hole 13 years after her first examination.

The final case report, presented by Şahin et al. and titled "Sheath-Preserving Complete Optic Nerve Avulsion Following Closed-Globe Injury: A Case Report," describes a case of complete optic nerve avulsion with intact optic nerve sheath as a result of injury by a compressed air hose.

We hope that the articles selected for this issue will provide you interesting and enjoyable reading.

Respectfully on behalf of the Editorial Board,

Hakan Özdemir, MD

DOI: 10.4274/tjo.galenos.2021.66168
Turk J Ophthalmol 2022;52:157-161

Original Article

Dry Eye and Meibomian Gland Dysfunction in Neovascular Age-Related Macular Degeneration Patients Treated with Intravitreal Injections

Pelin Kıyat, Melis Palamar, Serhad Nalçacı, Cezmi Akkın

Ege University Faculty of Medicine, Department of Ophthalmology, İzmir, Turkey

Abstract

Objectives: To determine if patients treated with multiple intravitreal injections for neovascular age-related macular degeneration are more likely to suffer from dry eye and meibomian gland dysfunction.

Materials and Methods: Sixty eyes of 30 patients were enrolled. One eye of each patient was treated with multiple monthly intravitreal injections for neovascular AMD (Group 1) and the fellow healthy eye received no treatment (Group 2). The presence of dry eye was evaluated using tear film break-up time, Schirmer 1 test, the Oxford scale, and Ocular Surface Disease Index (OSDI). The loss rate of meibomian glands was evaluated by meibography and was graded and scored (meiboscore) from grade 0 (no loss of glands) to grade 3 (loss of >2/3 of total meibomian glands) for each eyelid.

Results: Group 1 had lower mean Schirmer 1 and tear film break up-time measurements and higher mean OSDI score than Group 2, but the differences were not statistically significant (p=0.257, p=0.113, and p=0.212, respectively). Mean Oxford scale scores and meiboscore of the upper eyelids showed no statistically significant difference between the groups (p=0.594, p=0.663, respectively). The meiboscore of the lower eyelids was significantly higher in Group 1 (p=0.048).

Conclusion: Multiple factors such as povidone-iodine and the preservatives in topical eye drops may cause inflammation leading to ocular surface damage in patients treated with multiple intravitreal injections. As the treatment requires repeated injections, exposure to these factors might worsen the ocular surface inflammation. The possibility of dry eye and meibomian gland dysfunction should be considered in these patients.

Keywords: Intravitreal injection, neovascular age-related macular degeneration, dry eye, meibomian gland dysfunction, meibography

Address for Correspondence: Pelin Kıyat, Ege University Faculty of Medicine, Department of Ophthalmology, İzmir, Turkey
E-mail: pelinkiyat@hotmail.com **ORCID-ID:** orcid.org/0000-0002-3581-7059
Received: 14.10.2020 **Accepted:** 26.05.2021

Cite this article as: Kıyat P, Palamar M, Nalçacı S, Akkın C. Dry Eye and Meibomian Gland Dysfunction in Neovascular Age-Related Macular Degeneration Patients Treated with Intravitreal Injections. Turk J Ophthalmol 2022;52:157-161

Introduction

Age-related macular degeneration (AMD) is an important cause of blindness in older people in developed countries,[1] and the neovascular type requires treatment with anti-vascular endothelial growth factor (anti-VEGF) inhibitors.[2] In our daily practice, we noticed that AMD patients treated with intravitreal injections often complain about dry eye symptoms and seem more prone to meibomian gland dysfunction and dry eye in ophthalmic examinations. In addition, in previous studies it has been emphasized that patients treated with intravitreal injections reported grittiness and ocular pain very frequently.[3,4]

Although different dosing regimens such as "as needed" (*pro re nata* [PRN]) or "treat and extend" are preferred to decrease injection frequency, treatment is repetitive and carries risks such as endophthalmitis.[5] Ophthalmic povidone-iodine is routinely used to prevent endophthalmitis because of its wide antimicrobial activity and cost-effectiveness.[6] Short-term topical antibiotic therapy is another option used by many ophthalmologists to prevent endophthalmitis, although some trials found ocular surface bacteria to be resistant to topical antibiotics.[7] However, repetitive usage of these agents and the preservatives they contain might have an impact on the ocular surface and meibomian glands and contribute to damage in the long term. However, to our knowledge, no study to date has evaluated the relation between intravitreal injections and meibomian gland function with meibography.

Dry eye is a multifactorial ocular surface disease which reduces patients' quality of life.[8] Meibomian gland dysfunction is one of the most important causes of dry eye syndrome.[9] Meibomian glands can be imaged using many different tools performing meibography, and gland loss can be evaluated with the scoring systems defined in previous studies.[10] In the 2017 TFOS Dry Eye Workshop, dry eye was identified as a disease in which inflammation plays a significant role.[11] Ocular surface inflammation is considered to be one of the main causative factors in aqueous deficiency and evaporative type dry eye disease, and the latter is correlated to meibomian gland dysfunction.[11,12] Exaggerated and abnormal immune stimulation or disrupted immunoregulatory mechanisms resulting in dysregulation of the ocular surface immune system may cause dry eye disease.[13]

Previous studies mentioned the relation between inflammation-related diseases and meibomian gland dysfunction.[14,15] We hypothesize that the intravitreal injection treatment procedure in AMD might lead to dry eye and have an impact on the meibomian glands.

The purpose of this study was to determine if patients treated with multiple intravitreal injections for neovascular AMD (nAMD) are more likely to suffer from dry eye and meibomian gland dysfunction in comparison to normal untreated eyes.

Materials and Methods

In the present study, 60 eyes of 30 patients were evaluated. Patients diagnosed with nAMD who had a minimum of 6 doses of monthly intravitreal ranibizumab and/or aflibercept injections to only one eye were included. Patients who were treated in both eyes, received fewer than 6 intravitreal injections, received intravitreal injections for other retinal diseases such as diabetes, or had a history of ophthalmic surgery, preexisting dry eye disease, or any autoimmune disease that may be associated with dry eye were excluded. The eyes with nAMD that had at least 6 monthly intravitreal injections were evaluated as group 1 and the healthy, untreated fellow eyes of the same patients were evaluated as group 2. To prevent endophthalmitis, povidone-iodine (10%) was applied for 3 minutes before the injection and topical antibiotic (netilmicin, 4 times daily) was provided for a week after the injection.

All subjects included in the study underwent a detailed ophthalmological examination 4 weeks after the last injection. Dry eye tests were also performed on both treated and healthy eyes, including tear film break-up time (TBUT), Schirmer 1 test, corneal and conjunctival fluorescein staining and Oxford scoring, and Ocular Surface Disease Index (OSDI) assessment.

Evaluation of the upper and lower eyelid meibomian glands were performed using the infrared filter of a slit-lamp biomicroscope (Topcon, SL-D701, IJssel, Netherlands) and the loss rate of meibomian glands was graded and scored (meiboscore) for each eye. Gland loss was classified as grade 0 if there was no loss of the meibomian glands, grade 1 if the loss rate was less than 1/3 of the total meibomian glands, grade 2 if the loss rate was between 1/3 and 2/3 of the total meibomian glands, and grade 3 if the loss rate was more than 2/3 of the total meibomian glands.[16] The meibomian gland dropout ratio was evaluated blindly by the same researcher (M.P.). Meiboscores for the upper, lower, and total (upper+lower) eyelids were determined for each eye.

Statistical Analysis

Each subject provided written informed consent. The institutional review board of Ege University Hospital approved the study, which adhered to the tenets of the Declaration of Helsinki. For statistical analyses, the Statistical Package for the Social Sciences version 11.5.0 was used. A biostatistician was consulted for the data analysis.

Results

The mean age of the patients was 73.8±9.07 years (range, 61-86) (Table 1). The mean Schirmer 1 values in groups 1 and 2 were 19.2±4.8 mm (range, 10-30) and 20.3±4.4 mm (range, 12-30), respectively (p=0.257). The groups' respective mean TBUT values were 9.6±3.8 s (range, 3-18) and 11.3±4.1 s (range, 3-19) (p=0.113), mean Oxford scale (superficial punctate staining of the cornea and conjunctiva) scores were 0.6±0.7 (range, 0-2) and 0.6±0.7 (range, 0-2) (p=0.594), and mean OSDI values were 28.9±20.7 (range, 2.1-71.5) and 22.2±18.5 (range, 2.1-71.5) (p=0.212).

In Group 1, the mean upper meiboscore was 1.4±0.9 (range, 0-3), lower meiboscore was 0.9±0.8 (range, 0-3), and total meiboscore was 1.1±0.8 (range, 0-3). In Group 2, the mean upper meiboscore was 1.3±0.9 (range, 0-3), lower meiboscore

was 0.4±0.7 (range, 0-2), and total meiboscore was 0.9±0.7 (range, 0-2.5). The upper eyelid and total meiboscores were higher in Group 1 but the differences were not statistically significant (p=0.663, p=0.211, respectively). The meiboscore for the lower eyelids was significantly higher in Group 1 (p=0.048).

Discussion

Dry eye is an ocular surface disease with multifactorial pathogenesis including an inflammatory basis. It causes hyperosmolarity and elevated inflammatory mediators in the tear film which lead to ocular surface damage such as epithelial cell apoptosis and goblet cell death, resulting in more inflammation.[17,18]

Neovascular AMD is an important cause of blindness among older people in developed countries.[19] Anti-VEGF agents such as ranibizumab or aflibercept are the gold-standard therapy for nAMD and almost all patients require repeated intravitreal injections.[20] Treatment with intravitreal anti-VEGF injections is a prolonged repetitive procedure, after which many patients complain of dry eye-related symptoms. As the treatment and the antiseptic precautions have to be repeated, the ocular surface faces more inflammation, which can trigger dry eye syndrome. In this study, Schirmer 1 measurements and TBUT measurements were found to be lower and OSDI scores were found to be higher in eyes treated with at least six intravitreal injections compared to healthy untreated eyes, but the differences were not statistically significant. However, treated eyes had a significantly higher mean lower eyelid meiboscore.

The most serious but rare complication of anti-VEGF treatment is endophthalmitis. To prevent endophthalmitis, povidone-iodine is applied before the injection and topical antibiotics are provided after the injection. Povidone-iodine is an antiseptic agent which is preferred for its effectiveness and wide spectrum.[21] However, repeated exposure to povidone-iodine can cause ocular inflammation. Jiang et al.[22] showed that higher concentration (higher than 5%) and longer treatment (more than 2 minutes) lead to corneal epithelial and endothelial cell damage. Another study by Laude et al.[23] suggested that repeated exposure to povidone-iodine may cause discomfort in patients receiving intravitreal anti-VEGF agents.

After the injections, most practitioners prefer to use short-term topical antibiotics to prevent endophthalmitis.[24] The preservatives in topical preparations can contribute to ocular surface inflammation, which might also lead to dry eye disease.[25] Single-use preservative free topical agents can be useful to prevent toxic inflammation and reduce patient discomfort.[26,27] In addition, oxybuprocaine was suggested to be responsible for epithelial corneal damage, and this damage was found to be correlated with the product's concentration.[28]

A recently published article claimed that intravitreal injections induced ocular surface damage through the use of povidone-iodine and topical anesthetics.[29] In the same article it was also reported that TBUT was lower in the injected eye when compared to the healthy fellow eye of the same patients. The authors also emphasized that this treatment procedure could cause iatrogenic and chronic dry eye, not only temporary damage.[29]

Another striking point is the anti-VEGF effect itself. A study by Pan et al.[30] showed that VEGF had a positive impact on corneal healing, suggesting that intravitreal anti-VEGF injections might have a role in delayed healing of corneal damage related to the procedure.

Ocular inflammation associated with intravitreal anti-VEGF injections is a well-documented phenomenon that can be categorized into two clinical manifestations.[31] The first presentation is "acute-onset sterile inflammation," the clinical features of which can vary widely from subclinical anterior chamber inflammation to severe inflammation that can be misdiagnosed as endophthalmitis. Subclinical anterior chamber inflammation is a fairly common sign after anti-VEGF injections, seen at rates as high as 20% of patients.[31] The second manifestation is a recently described one, 'delayed-onset inflammatory vasculitis' associated with brolucizumab.[32] As a result, inflammation can occur after intravitreal anti-VEGF injections and the clinical manifestation can range broadly. On the other hand, a study by Karti et al.[33] suggested that intravitreal anti-VEGF injections can be beneficial in treating choroidal neovascularization secondary to inflammatory diseases such as noninfectious uveitis in terms of both visual and anatomical improvement. Anti-VEGF agents exert their beneficial effect in these cases by inhibiting VEGF locally and reducing choroidal

Table 1. The dry eye test results and meiboscores of eyes treated with intravitreal injections (group 1) and healthy fellow eyes (group 2) of the same patients.

	Group 1, mean ± SD (range)	Group 2, mean ± SD (range)	p value
Schirmer-1 (mm)	19.2±4.8 (10-30)	20.3±4.4 (12-30)	0.257
TBUT (s)	9.6±3.8 (3-18)	11.3±4.1 (3-19)	0.113
Oxford scale	0.6±0.7 (0-2)	0.6±0.7 (0-2)	0.594
OSDI score	28.9±20.7 (2.1-71.5)	22.2±18.5 (2.1-71.5)	0.212
Upper meiboscore	1.4±0.9 (0-3)	1.3±0.9 (0-3)	0.663
Lower meiboscore	0.9±0.8 (0-3)	0.4±0.7 (0-2)	0.048
Total meiboscore	1.1±0.8 (0-3)	0.9±0.7 (0-2.5)	0.211

SD: Standard deviation, TBUT: Tear film break-up time, OSDI: Ocular Surface Disease Index

vascular permeability. However, as emphasized in the study, it is crucial to treat inflammation, mainly with steroids or immunosuppressive agents.

Povidone-iodine has antibacterial properties that can be protective against ocular surface damage associated with eyelid margin diseases. However, in our study patients with eyelid margin diseases did not receive any intravitreal injections in order to prevent endophthalmitis.

Dry eye disease is common in older adults. Age-related diseases or comorbid conditions such as diabetes also cause nerve damage and may increase the likelihood of dry eye. In most cases it is difficult to identify whether dry eye is caused by treatment or age-related changes. However, in the present study, the control group comprised the fellow eyes of the study group, which means that there is no variation in the age and systemic or ocular comorbid diseases between the treated and control groups. Therefore, we can effectively evaluate the effect of the treatment procedure.

Study Limitations

Evaluating meibomian gland dysfunction with meibography has become important in demonstrating the pathogenesis of dry eye disease. Previous studies showed that meibomian gland dysfunction is associated with inflammatory systemic diseases such as rosacea[34] or vitiligo[35] and ocular conditions such as pseudophakic bullous keratopathy[36] or contact lens usage.[37] However, to our knowledge, there has been no study to date evaluating meibomian gland function in patients treated with intravitreal injections. In the present study, meiboscores of the lower lids were higher in treated eyes than untreated eyes. This result might be the consequence of greater exposure of the inferior eyelid and meibomian glands to topical antibiotics and povidone-iodine.

Conclusion

In summary, AMD requires treatment with intravitreal injections. Although intravitreal anti-VEGF therapy is the gold standard, these patients may suffer from dry eye and/or meibomian gland dysfunction. In our study, we found statistically significant differences in meibomian gland dropout ratio, although treated eyes showed no significant differences in the dry eye tests. Still, we advise ophthalmologists to be vigilant for dry eye development and meibomian gland dysfunction in these patients. Due to the chronic nature of the treatment protocols, prolonged and repeated exposure to povidone-iodine, topical antibiotics, topical anesthetics, and preservatives in eye drops might predispose to ocular surface inflammation. OSDI scoring before multiple injections can help diagnose dry eye earlier. More studies with larger patient numbers are needed to understand the effect of intravitreal injection treatment procedures on the ocular surface.

Ethics

Ethics Committee Approval: The institutional review board 68 of Ege University Hospital no: 19-6.1T/45

Informed Consent: Obtained.

Peer-review: Externally and internally peer reviewed.

Authorship Contributions

Concept: P.K., M.P., S.N., C.A., Design: P.K., M.P., S.N., C.A., Data Collection or Processing: P.K., M.P., S.N., C.A., Analysis or Interpretation: P.K., M.P., S.N., C.A., Literature Search: P.K., M.P., S.N., C.A., Writing: P.K., M.P., S.N., C.A.

Conflict of Interest: No conflict of interest was declared by the authors.

Financial Disclosure: The authors declared that this study received no financial support.

References

1. Friedman DS, O'Colmain BJ, Muñoz B, Tomany SC, McCarty C, de Jong PT, Nemesure B, Mitchell P, Kempen J; Eye Diseases Prevalence Research Group. Prevalence of age-related macular degeneration in the United States. Arch Ophthalmol. 2004;122:564-572.
2. Klaver CC, Wolfs RC, Vingerling JR, Hofman A, de Jong PT. Age-specific prevalence and causes of blindness and visual impairment in an older population: the Rotterdam study. Arch Ophthalmol. 1998;116:653-658.
3. Saedon H, Nosek J, Phillips J, Narendran N, Yang YC. Ocular surface effects of repeated application of povidone iodine in patients receiving frequent intravitreal injections. Cutan Ocul Toxicol. 2017;36:343-346.
4. Oakley C, Allen P, Hooshmand J, Vote BJT. Pain and antisepsis after ocular administration of povidone-iodine versus chlorhexidine. Retina. 2018;38:2064-2066.
5. Heier JS, Brown DM, Chong V, Korobelnik JF, Kaiser PK, Nguyen QD, Kirchhof B, Ho A, Ogura Y, Yancopoulos GD, Stahl N, Vitti R, Berliner AJ, Soo Y, Anderesi M, Groetzbach G, Sommerauer B, Sandbrink R, Simader C, Schmidt-Erfurth U; VIEW 1 and VIEW 2 Study Groups. Intravitreal aflibercept (VEGF trap-eye) in wet age-related macular degeneration. Ophthalmology. 2012;119:2537-2548.
6. Grzybowski A, Kanclerz P, Myers WG. The use of povidone-iodine in ophthalmology. Curr Opin Ophthalmol. 2018;29:19-32.
7. Hsu J, Gerstenblith AT, Garg SJ, Vander JF. Conjunctival flora antibiotic resistance patterns after serial intravitreal injections without postinjection topical antibiotics. Am J Ophthalmol. 2014;157:514-518.
8. Periman LM, Perez VL, Saban DR, Lin MC, Neri P. The immunological basis of dry eye disease and current topical treatment options. J Ocul Pharmacol Ther. 2020;36:137-146.
9. Stapleton F, Alves M, Bunya VY, Jalbert I, Lekhanont K, Malet F, Na KS, Schaumberg D, Uchino M, Vehof J, Viso E, Vitale S, Jones L. TFOS DEWS II Epidemiology Report. Ocul Surf. 2017;15:334-365.
10. Nelson JD, Shimazaki J, Benitez-del-Castillo JM, Craig JP, McCulley JP, Den S, Foulks GN. The international workshop on meibomian gland dysfunction: report of the definition and classification subcommittee. Invest Ophthalmol Vis Sci. 2011;52:1930-1937.
11. Craig JP, Nichols KK, Akpek EK, Caffery B, Dua HS, Joo CK, Liu Z, Nelson JD, Nichols JJ, Tsubota K, Stapleton F. TFOS DEWS II definition and classification report. Ocul Surf. 2017;15:276-283.
12. Knop E, Knop N, Millar T, Obata H, Sullivan D. The international workshop on Meibomian gland dysfunction: report of the subcommittee on anatomy, physiology, and pathophysiology of the Meibomian gland. Invest Ophthalmol Vis Sci. 2011;52:1938-1978.
13. Gagliano C, Visalli E, Toro MD, Amato R, Panta G, Scollo D, Scandura G, Ficili S, Amato G, Benenati A, Foti R, Malaguarnera G, Gagliano G, Falsaperla R, Avitabile T, Foti R. Dry Eye in Systemic Sclerosis Patients: Novel Methods to Monitor Disease Activity. Diagnostics (Basel). 2020;10:404.
14. Kiyat P, Palamar M, Gerceker Turk B, Yagci A. Dry eye and quantitative and qualitative changes of Meibomian glands in patients with pemphigus. Cornea. 2020;39:1108-1111.
15. Adiguzel S, Palamar M, Yargucu F, Oksel F, Yagci A. Evaluation of Ocular Surface and Meibomian Glands in Patients With Scleroderma. Cornea. 2021;40:977-981.

16. Arita R, Itoh K, Inoue K, Amano S. Noncontact infrared meibography to document age-related changes of the meibomian glands in a normal population. Ophthalmology. 2008;115:911-915.
17. Calonge M, Enríquez-de-Salamanca A, Diebold Y, González-García MJ, Reinoso R, Herreras JM, Corell A. Dry eye disease as an inflammatory disorder. Ocul Immunol Inflamm. 2010;18:244-253.
18. Yeh S, Song XJ, Farley W, Li DQ, Stern ME, Pflugfelder SC. Apoptosis of ocular surface cells in experimentally induced dry eye. Invest Ophthalmol Vis Sci. 2003;44:124-129.
19. Congdon NG, Friedman DS, Lietman T. Important causes of visual impairment in the world today. JAMA. 2003;290:2057-2060.
20. Ferrara N, Damico L, Shams N, Lowman H, Kim R. Development of ranibizumab, an anti-vascular endothelial growth factor antigen binding fragment, as therapy for neovascular age-related macular degeneration. Retina. 2006;26:859-870.
21. Speaker MG, Menikoff JA. Prophylaxis of endophthalmitis with topical povidone-iodine. Ophthalmology. 1991;98:1769-1775.
22. Jiang J, Wu M, Shen T. The toxic effect of different concentrations of povidone iodine on the rabbit's cornea. Cutan Ocul Toxicol. 2009;28:119-124.
23. Laude A, Lim JW, Srinagesh V, Tong L. The effect of intravitreal injections on dry eye, and proposed management strategies. Clin Ophthalmol. 2017;11:1491-1497.
24. Garg P, Roy A, Sharma S. Endophthalmitis after cataract surgery: epidemiology, risk factors, and evidence on protection. Curr Opin Ophthalmol. 2017;28:67-72.
25. Mantelli F, Tranchina L, Lambiase A, Bonini S. Ocular surface damage by ophthalmic compounds. Curr Opin Allergy Clin Immunol. 2011;11:464-470.
26. Mencucci R, Paladini I, Pellegrini-Giampietro DE, Menchini U, Scartabelli T. In vitro comparison of the cytotoxic effects of clinically available ophthalmic solutions of fluoroquinolones on human keratocytes. Can J Ophthalmol. 2011;46:513-520.
27. Li XM, Zhao X, Hu LZ, Wang W. [Clinical observation of dry eye in patients before and after cataract surgery]. Zhonghua Yan Ke Za Zhi. 2007;43:10-13.
28. Brewitt H, Bonatz E,Honegger H. Morphological changes of the corneal epithelium after application of topical anaesthetic ointments. Ophthalmologica. 1980;180:198-206.
29. Verrecchia S, Chiambaretta F, Kodjikian L, Nakouri Y, El Chehab H, Mathis T, Badri Y, Chudzinski R, Levron A, Chaperon M, Agard E, Pradat P, Dot C. A prospective multicentre study of intravitreal injections and ocular surface in 219 patients: IVIS study. Acta Ophthalmol. 2021;99:877-884.
30. Pan Z, Fukuoka S, Karagianni N, Guaiquil VH, Rosenblatt MI. Vascular endothelial growth factor promotes anatomical and functional recovery of injured peripheral nerves in the avascular cornea. FASEB J. 2013;27:2756-2767.
31. Anderson WJ, da Cruz NFS, Lima LH, Emerson GG, Rodrigues EB, Melo GB. Mechanisms of sterile inflammation after intravitreal injection of antiangiogenic drugs: a narrative review. Int J Retina Vitreous. 2021;7:37.
32. Cox JT, Eliott D, Sobrin L. Inflammatory complications of intravitreal anti-VEGF injections. J Clin Med. 2021;10:981.
33. Karti O, Ipek SC, Ates Y, Saatci AO. Inflammatory Choroidal Neovascular Membranes in Patients With Noninfectious Uveitis: The Place of Intravitreal Anti-VEGF Therapy. Med Hypothesis Discov Innov Ophthalmol. 2020;9:118-126.
34. Palamar M, Degirmenci C, Ertam I, Yagci A. Evaluation of dry eye and meibomian gland dysfunction with meibography in patients with rosacea. Cornea. 2015;34:497-499.
35. Palamar M, Kiyat P, Ertam I, Yagci A. Evaluation of dry eye and meibomian gland dysfunction with meibography in vitiligo. Eye (Lond). 2017;31:1074-1077.
36. Palamar M, Kiyat P, Yagci A. Dry eye and meibomian gland dysfunction in pseudophakic bullous keratopathy. Int Ophthalmol. 2019;39:393-396.
37. Arita R, Fukuoka S, Morishige N. Meibomian gland dysfunction and contact lens discomfort. Eye Contact Lens. 2017;43:17-22.

DOI: 10.4274/tjo.galenos.2022.38839
Turk J Ophthalmol 2022;52:162-167

Original Article

Palliative Efficacy of Intrastromal Amniotic Membrane Procedure in Symptomatic Bullous Keratopathy Patients

Onur Furundaoturan, Melis Palamar, Özlem Barut Selver

Ege University Faculty of Medicine, Department of Ophthalmology, İzmir, Turkey

Abstract

Objectives: To evaluate the palliative efficacy of the intrastromal human amniotic membrane (hAM) surgery technique in patients with symptomatic bullous keratopathy and limited visual potential.

Materials and Methods: The study was carried out retrospectively by reviewing the medical data of 10 patients with poor visual prognosis who underwent intrastromal hAM surgery due to bullous keratopathy-related severe pain. Visual acuity, surgical indication, epithelization time, preoperative and postoperative pain scores, as well as anterior segment optical coherence tomography images and anterior segment photographs were obtained from the medical records.

Results: Ten patients (6 females/4 males) were included in the study. Nine patients underwent surgery for pseudophakic bullous keratopathy and glaucoma, and 1 patient due to graft failure and glaucoma. The mean time for corneal epithelization was 27.10±13.05 days (range, 10-50), while the mean follow-up time was 37.5±1.6 months (range, 36-39.2). Subjective pain score improved in all patients after surgery. Suture-induced keratitis occurred during follow-up in one patient and was controlled with medical treatment.

Conclusion: Intrastromal amniotic membrane surgery may be an alternative to keratoplasty for pain palliation in patients with limited visual prognosis after corneal transplantation when donor tissue is scarce. With this method, hAM remains on the ocular surface longer, and superficial stromal excision is believed to provide a more regular ocular surface and extend the asymptomatic period.

Keywords: Amniotic membrane inlay technique, bullous keratopathy, poor visual prognosis

Address for Correspondence: Özlem Barut Selver, Ege University Faculty of Medicine, Department of Ophthalmology, İzmir, Turkey
E-mail: ozlembarutselver@gmail.com **ORCID-ID:** orcid.org/0000-0003-3333-3349
Received: 06.04.2021 **Accepted:** 22.06.2021

Cite this article as: Furundaoturan O, Palamar M, Barut Selver Ö. Palliative Efficacy of Intrastromal Amniotic Membrane Procedure in Symptomatic Bullous Keratopathy Patients. Turk J Ophthalmol 2022;52:162-167

Introduction

Bullous keratopathy (BK) is characterized by chronic edema and visual impairment due to corneal endothelial insufficiency. It often occurs after Fuchs endothelial dystrophy or endothelial trauma secondary to intraocular surgery and can cause severe pain.[1,2,3] Keratoplasty is the primary treatment for eyes with visual potential.[4,5] Palliative treatment methods are important for eyes without visual potential, especially in the management of pain. These methods include noninterventional approaches such as bandage contact lens use,[6] as well as surgical options such as phototherapeutic keratectomy,[7] cross-linking,[8] stromal micropunctures,[9] and conjunctival flaps.[9]

The human amniotic membrane (hAM) is the inner layer of the placenta consisting of the epithelium, basement membrane, and connective tissue. It has been used for years as a biomaterial in ocular surface diseases, including BK. hAM is used in BK for pain palliation and the treatment of recurrent epithelial erosion. It is usually applied to the ocular surface by direct suturing with the epithelial surface facing up. The hAM remains on the ocular surface for 2-8 weeks depending on the degree of inflammation present.[2,10,11] Various modifications to the hAM transplantation procedure can be made if epithelial healing is not achieved or longer-term symptom control is needed. One of these is the inlay technique, in which the amniotic membrane is applied intra- or suprastomally.[12]

The aim of this study was to evaluate the clinical outcomes of the intrastromal hAM surgical technique performed for palliation of symptomatic BK in patients with limited visual potential.

Materials and Methods

The study was conducted by retrospectively screening the results of intrastromal amniotic membrane surgery for severe pain in 10 patients with BK and limited visual prognosis who were followed up in the Corneal Unit of the Ege University Faculty of Medicine.

The study was carried out in accordance with the principles of the Declaration of Helsinki after obtaining approval from the local medical research ethics committee and informed consent from each patient.

Visual acuity, surgical indication, epithelialization time, preoperative and postoperative pain scores (rated on scale of 0-10 with 0 being mildest and 10 most severe), anterior segment optical coherence tomography images, and anterior segment photographs were collected from the patients' records.

The intrastromal hAM surgical technique was performed as follows: After mechanical debridement of the corneal epithelium, a depth of approximately 100 µm was determined using an 8-mm trepan and superficial lamellar stromal dissection was performed in the central 8-mm area. A 360-degree peripheral corneal tunnel was then prepared using a crescent blade. Cryopreserved hAM cut using a 9-mm donor punch was obtained from the eye bank and prepared as described in the literature.[13] It was then used to cover the dissection area with the epithelial side up and its peripheral ends placed in the prepared tunnel. The hAM was fixed in place with 8 interrupted nylon sutures in the peripheral cornea (Figure 1a-h).

Statistical Analysis

IBM SPSS Statistics version 20.0 software package (IBM Corp, Armonk, NY, USA) was used for statistical data analysis.

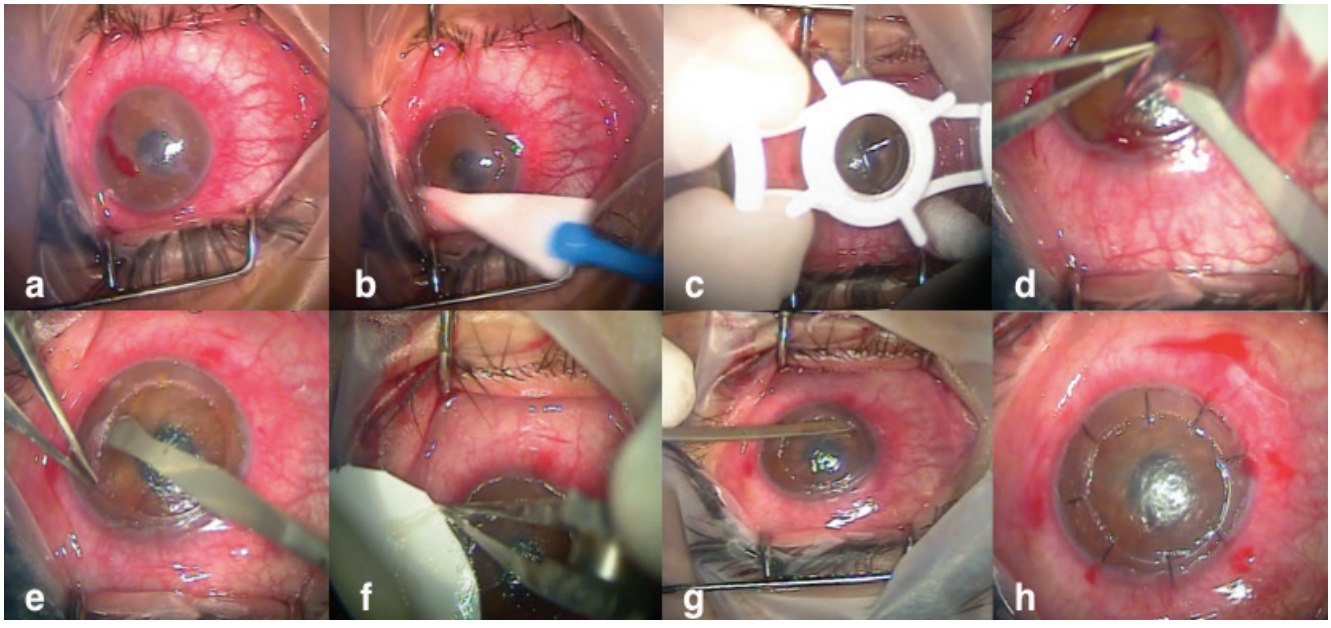

Figure 1. Steps of amniotic membrane implantation: a-b) Epithelial debridement, c) A 8-mm trepan is used to determine of a depth of approximately 100 µm, d) Superficial lamellar stromal dissection, e) A 360-degree peripheral corneal tunnel is prepared using a crescent knife, f-g) The amniotic membrane is used to cover the defect epithelial side up, with peripheral ends placed into the prepared tunnel, h) The amniotic membrane is fixed to the peripheral cornea with 8 nylon interrupted sutures

Numerical variables were presented as mean, standard deviation, and range. Dependent data were evaluated using Mann-Whitney U test, with p values less than 0.05 were considered statistically significant.

Results

The mean age of the 10 patients (6 women, 4 men) was 68.5±15.6 years (range, 34-85). Surgical indications were pseudophakic BK and glaucoma in 9 patients and graft failure and glaucoma in 1 patient (Table 1). All of the patients included were symptomatic and had not benefited from previous conservative treatments (artificial tears, bandage contact lens). The mean time required for corneal epithelialization was 27.10±13.05 days (range, 10-50) (Figure 2a-h).

Preoperative visual acuity was counting fingers at 50 centimeters in 9 patients and counting fingers at 2 meters in 1 patient. Mean follow-up time was 37.5±1.6 months (range, 36-39.2). In all patients, the hAM remained visible between the epithelium and stroma and maintained its barrier function throughout follow-up, despite peripheral areas of partial degradation (Figure 3a-d, pre- and postoperative images of patient 4). Subjective pain score improved in all patients after surgery (preoperative mean 8.7 [range, 8-10]; postoperative mean 1.1 [range, 0-2]; p=0.00018). One patient developed keratitis with hypopyon associated with loose suture at 6-month follow-up that was controlled with appropriate antibiotherapy after removing the loose suture. No growth was detected in the microbiological sample obtained (Figure 4a-f).

Discussion

BK is characterized by chronic corneal edema and subepithelial bullous changes resulting from corneal endothelial insufficiency. Despite all of the advances in surgical methods, it remains a serious complication.[14] The intrastromal hAM

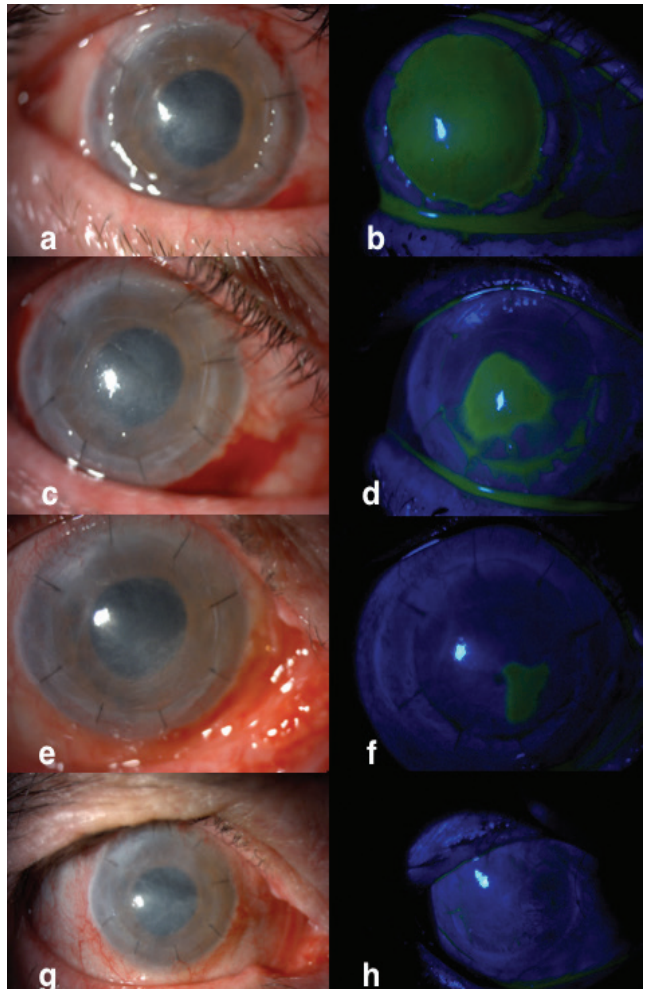

Figure 2. The corneal epithelialization process recorded using biomicroscopic photography during postoperative follow-up (a-h)

Table 1. Demographic characteristics, surgical indications, and examination findings of all patients (subjective pain scoring from a minimum of 1 to maximum of 10)

	Indication	Age (years)	Sex	Visual acuity	Follow-up time	Epithelialization time	Other characteristics	Subjective pain score	
								Before	After
Patient 1	BK	53	F	LP	39.0 months	50 days	Glaucoma	8	0
Patient 2	BK	85	F	NLP	36.0 months	18 days	Glaucoma, Keratitis	9	2
Patient 3	BK	77	F	HM	37.1 months	32 days	Glaucoma	8	1
Patient 4	Graft failure	71	F	CF 2 m	38.7 months	12 days	Glaucoma	8	1
Patient 5	BK	67	M	CF 20 cm	39.2 months	20 days	Glaucoma	9	2
Patient 6	BK	34	F	HM	38.7 months	28 days	Glaucoma	9	1
Patient 7	BK	62	M	CF 50 cm	38.2 months	23 days	Glaucoma	10	1
Patient 8	BK	85	M	HM	34.1 months	35 days	Glaucoma	9	0
Patient 9	BK	74	F	NLP	36.2 months	43 days	Glaucoma	8	2
Patient 10	BK	77	M	HM	38.2 months	10 days	Glaucoma	9	1

BK: Bullous keratopathy, M: Male, F: Female, LP: Light perception, NLP: No light perception, HM: Hand movements, CF: Counting fingers

technique is one of the treatment alternatives for symptomatic BK cases with limited visual potential.[12] With this procedure, hAM acts as a barrier for the corneal epithelium and effectively prevents corneal edema associated with endothelial failure from causing ocular surface disease.[12,15] In this technique, hAM prepared to the size of the damaged area acts as a basement membrane for corneal epithelial cell proliferation and suppresses subsequent inflammation by reducing contact with tear-induced mediators.[16]

In the literature, there are studies reporting the use of hAM in patients with persistent epithelial defects and in patients with poor visual prognosis, and the patients' symptoms were reported to resolve with no recurrence.[2,12,17] hAM is generally fixed to the ocular surface by various suturing methods. The most common is referred to as the "overlay" method, in which the graft is applied epithelial side up covering the entire epithelial defect and even the corneal surface. In this method, which protects the damaged area from external contact such as from a contact lens, the hAM is resorbed over 2-8 weeks depending on ocular surface inflammation.[2] However, this widely used method provides limited palliation in pathologies accompanied by chronic processes because of the epithelialization time, the occasional need to repeat the procedure, and the limited duration on the ocular surface.[16] Placing a defect-sized hAM graft suprastromally/intrastromally so as to trap it under the developing epithelial layer is referred to as the "inlay" technique. This method is proposed to enable the formation of an uninterrupted and smooth transition surface for epithelial cell growth. In addition, because the hAM remains under the epithelium, it is protected from enzymatic degradation and

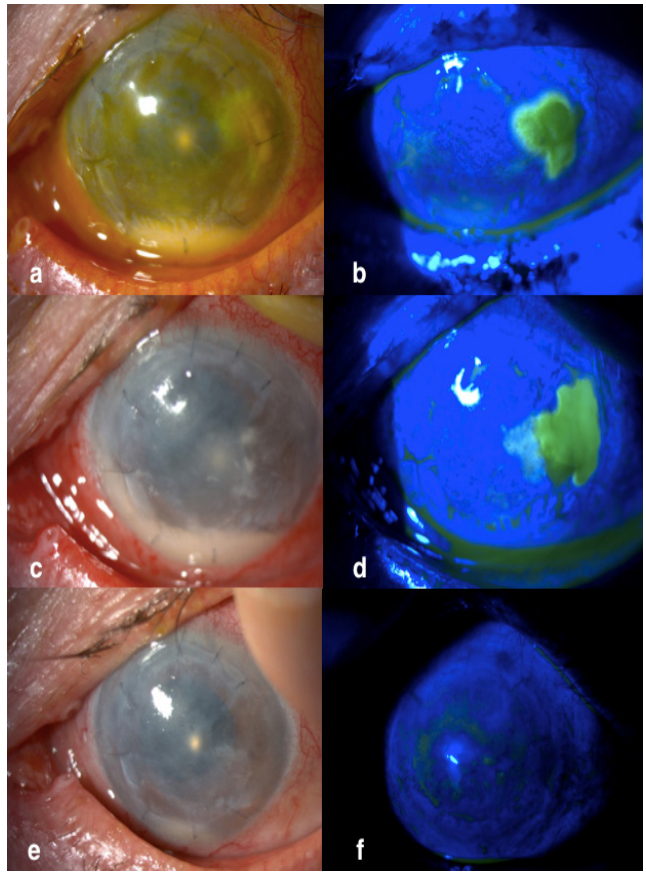

Figure 4. Anterior segment image and post-treatment status of the patient with hypopyon keratitis (a-f)

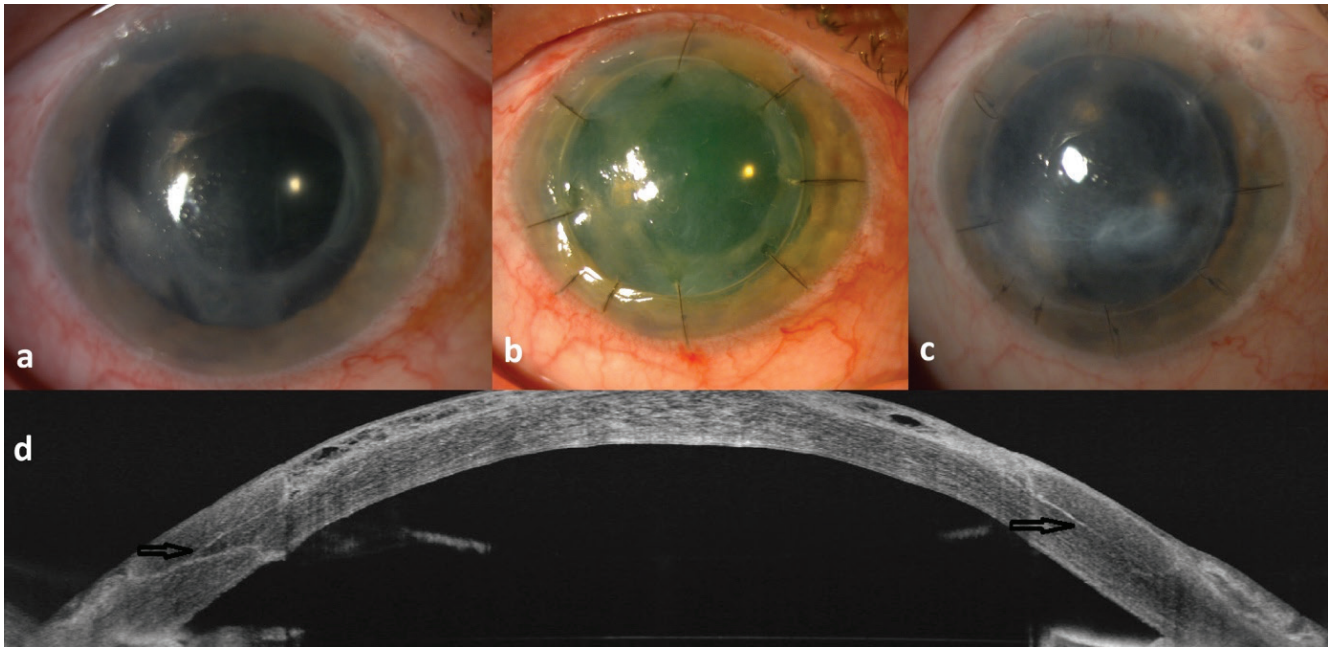

Figure 3. Images of patient 4: a) Anterior segment photograph before surgery, b) Anterior segment photograph at postoperative 3 months, c) Last follow-up photograph at postoperative 38 months, d) Anterior segment optical coherence tomography image at postoperative 36 months (amniotic membrane in the corneal peripheral tunnel is marked with black arrows)

remains in place long term. The greatest unwanted effect of this is visual impairment and unsatisfactory cosmetic appearance due to the semi-opaque nature of the amniotic membrane.[17,18]

In a study from Turkey comparing overlay hAM suturing with an inlay method involving mechanical removal of the epithelium without stromal debridement and suturing the hAM into stromal pockets, it was observed that the inlay method provided pain palliation in more patients, better pain scores during follow-up, and significantly longer duration of the hAM on the ocular surface. There was no decline in pain palliation and pain scores in the inlay group, whereas the number of symptomatic patients in the overlay group increased during follow-up.[18] In a case series by Espana et al.,[17] one of the first studies in the literature to include the inlay technique, hAM was sutured to the prepared peripheral 360° stromal tunnel after only epithelial debridement. Pain palliation and reepithelialization were achieved in nearly all patients. In this study, approximately 100 µm of anterior stroma was removed during debridement in addition to the epithelium to prepare the bed for hAM.[19] Removal of the superficial stroma by this method offers a smoother surface to receive the hAM and eliminates potential bulging caused by the thickness of hAM itself. Based on our review of the literature, we believe this modified inlay technique incorporating stromal excision is novel.

In studies in the literature reporting the use of hAM for palliation, indications have included causes such as pseudophakia, aphakia, and graft failure.[2,12,17] Similarly, in this study pseudophakia was the indication in 9 patients and graft failure in 1 patient. All patients in our study also had glaucoma as a concomitant ocular pathology, which is the biggest difference between the current series and study groups in the literature. In previous studies using hAM methods, epithelialization rates were between 55% and 100%, with an average epithelialization time of 15.4-16.8 days.[17,20,21] In the present study, reepithelialization was achieved in all patients (100%) and the mean epithelialization time was 27.10±13.05 days (range, 10-50), which is long compared to previous studies. As all patients in this study had a history of using antiglaucoma drops with epithelial toxicity, a relative delay in epithelial healing was considered an expected outcome.

Study Limitations

In the literature, pain palliation after hAM surgery has been reported at rates varying between 22% and 90%.[17,20,21] In our study, the rate of successful pain palliation was 100%, with statistically significant pain control in all patients. Here again, we believe that stromal excision to a depth corresponding to the thickness of the amniotic membrane graft may result in more effective pain palliation by providing a more regular ocular surface.

In the few studies in the literature reporting inlay surgical techniques, the mean follow-up period was 7 months. The follow-up time in the current study was 37.5±1.6 months (range, 36-39.2), which is quite long compared to the literature. Consistent with the literature, our study showed that hAM placed between the corneal stroma and newly forming epithelium could remain on the ocular surface longer.[17,18]

Conclusion

In conclusion, the intrastromal amniotic membrane inlay technique should be kept in mind as an alternative to corneal transplantation and an auxiliary method for pain palliation in BK patients with poor visual prognosis and little cosmetic concern. Moreover, the method of removing the superficial stroma creates a more regular ocular surface and may provide stability over long-term follow-up.

Ethics

Ethics Committee Approval: Ege University Medical Research Ethics Committee (decision no: 21-3.1T/54, 18.03.21).

Informed Consent: Obtained.

Peer-review: Externally peer reviewed.

Authorship Contributions

Surgical and Medical Practices: Ö.B.S., M.P., Concept: Ö.B.S., M.P., Design: Ö.B.S., M.P., Data Collection or Processing: O.F., Ö.B.S., Analysis or Interpretation: O.F., Ö.B.S., M.P., Literature Search: O.F., Ö.B.S., Writing: O.F., Ö.B.S.

Conflict of Interest: No conflict of interest was declared by the authors.

Financial Disclosure: The authors declared that this study received no financial support.

References

1. Aquavella JV. Chronic corneal edema. Am J Ophthalmol. 1973;76:201-207.
2. Pires RT, Tseng SC, Prabhasawat P, Puangsricharern V, Maskin SL, Kim JC, Tan DT. Amniotic membrane transplantation for symptomatic bullous keratopathy. Arch Ophthalmol. 1999;117:1291-1297.
3. Palamar M, Kiyat P, Yagci A. Dry eye and meibomian gland dysfunction in pseudophakic bullous keratopathy. Int Ophthalmol. 2019;39:393-396.
4. Brady SE, Rapuano CJ, Arentsen JJ, Cohen EJ, Laibson PR. Clinical indications for and procedures associated with penetrating keratoplasty, 1983-1988. Am J Ophthalmol. 1989;108:118-122.
5. Barut Selver O, Karaca I, Palamar M, Egrilmez S, Yagci A. Graft Failure and Repeat Penetrating Keratoplasty. Exp Clin Transplant. 2021;19:72-76.
6. Gasset AR, Kaufman HE. Bandage Lenses in the Treatment of Bullous Keratopathy. Am J Ophthalmol. 1971;72:376-380.
7. Maini R, Sullivan L, Snibson GR, Taylor HR, Loughnan MS. A comparison of different depth ablations in the treatment of painful bullous keratopathy with phototherapeutic keratectomy. Br J Ophthalmol. 2001;85:912-915.
8. Kaya E, Eğrilmez S, Palamar M. Effect of Corneal Collagen Cross-Linking on Quality of Life in Patients with Bullous Keratopathy. Turkiye Klinikleri J Ophthalmol. 2015;24:95-101.
9. Cormier G, Brunette I, Boisjoly HM, LeFrançois M, Shi ZH, Guertin MC. Anterior stromal punctures for bullous keratopathy. Arch Ophthalmol. 1996;114:654-658.
10. Palamar M, Kaya E, Egrilmez S, Akalin T, Yagci A. Amniotic membrane transplantation in surgical management of ocular surface squamous neoplasias: long-term results. Eye (Lond). 2014;28:1131-1135.
11. Palamar Onay M, Yaman B, Akalın T, Yağcı A. Amniotic Membrane Transplantation in Surgical Treatment of Conjunctival Melanoma: Long-term Results. Turk J Ophthalmol. 2017;48:15-18.
12. Siu GD, Young AL, Cheng LL. Long-term symptomatic relief of bullous keratopathy with amniotic membrane transplant. Int Ophthalmol. 2015;35:777-783.

13. Kim JC, Tseng SC. Transplantation of preserved human amniotic membrane for surface reconstruction in severely damaged rabbit corneas. Cornea. 1995;14:473-484.
14. Pricopie S, Istrate S, Voinea L, Leasu C, Paun V, Radu C. Pseudophakic bullous keratopathy. Rom J Ophthalmol. 2017;61:90-94.
15. Koizumi N, Fullwood NJ, Bairaktaris G, Inatomi T, Kinoshita S, Quantock AJ. Cultivation of Corneal Epithelial Cells on Intact and Denuded Human Amniotic Membrane. Invest Ophthalmol Vis Sci. 2000;41:2506-2513.
16. Letko E, Stechschulte SU, Kenyon KR, Sadeq N, Romero TR, Samson CM, Nguyen QD, Harper SL, Primack JD, Azar DT, Gruterich M, Dohlman CH, Baltatzis S, Foster CS. Amniotic membrane inlay and overlay grafting for corneal epithelial defects and stromal ulcers. Arch Ophthalmol. 2001;119:659-663.
17. Espana EM, Grueterich M, Sandoval H, Solomon A, Alfonso E, Karp CL, Fantes F, Tseng SC. Amniotic membrane transplantation for bullous keratopathy in eyes with poor visual potential. J Cataract Refract Surg. 2003;29:279-284.
18. Altiparmak UE, Oflu Y, Yildiz EH, Budak K, Aslan BS, Nurozler A, Onat M, Kasim R, Duman S. Prospective comparison of two suturing techniques of amniotic membrane transplantation for symptomatic bullous keratopathy. Am J Ophthalmol. 2009;147:442-446.
19. Tanaka TS, Demirci H. Cryopreserved Ultra-Thick Human Amniotic Membrane for Conjunctival Surface Reconstruction After Excision of Conjunctival Tumors. Cornea. 2016;35:445-450.
20. Mejía LF, Santamaría JP, Acosta C. Symptomatic management of postoperative bullous keratopathy with nonpreserved human amniotic membrane. Cornea. 2002;21:342-345.
21. Georgiadis NS, Ziakas NG, Boboridis KG, Terzidou C, Mikropoulos DG. Cryopreserved amniotic membrane transplantation for the management of symptomatic bullous keratopathy. Clin Exp Ophthalmol. 2008;36:130-135.

DOI: 10.4274/tjo.galenos.2021.48275
Turk J Ophthalmol 2022;52:168-173

Original Article

Evaluation of Choroidal Vascular Index in Amblyopic Patients

Onur Furundaoturan, Cumali Değirmenci, Cezmi Akkın, Elif Demirkılınç Biler, Önder Üretmen, Serhad Nalçacı, Filiz Afrashi

Ege University Faculty of Medicine, Department of Ophthalmology, İzmir, Turkey

Abstract

Objectives: To compare subfoveal choroidal thickness (SFCT) and choroidal vascular index (CVI) in patients with hyperopic refractive and strabismic amblyopia and healthy subjects.

Materials and Methods: The study included 17 patients with strabismic amblyopia (Group 1), 29 patients with hyperopic refractive amblyopia (Group 2), and 16 eyes of 16 healthy volunteers (Group 3). Best corrected visual acuity was noted in all patients and volunteers. In addition to detailed anterior and posterior segment examinations, macular images were obtained by enhanced-depth imaging mode of optical coherence tomography (OCT). SFCT measurements were made from these images and CVI was calculated using the Image J program.

Results: No significant difference was found between the groups in terms of age, gender, and intraocular pressure (p=0.27, 0.64, and 0.85, respectively). Mean BCVAs in Group 1 were 0.57±0.16 (0.3-0.8) in the amblyopic eyes, 0.94±0.08 (0.8-1.0) in the fellow eyes, and in Group 2 were 0.61±0.17 (0.2-0.8) in amblyopic eyes, 0.92±0.1 (0.8-1.0) in fellow eyes. BCVA in Group 3 was 1.0±0 (1.0-1.0). Mean SFCT of the amblyopic eyes in Groups 1 and 2 was 341.50±60.4 (277-481) and 370.06±65.3 (247-462), respectively, and in the healthy eyes of Groups 1 and 2 and Group 3 was 321.92±68.26 (251-440), 330.35±74.00 (194-502), and 327.62±40.79 (238-385), respectively. SFCT was significantly greater in the amblyopic eyes of Group 2 compared to Group 3 (p=0.01). Mean CVI was 0.681±0.032 (0.642-0.736) in the amblyopic eyes and 0.685±0.054 (0.587-0.788) in the fellow eyes of Group 1 patients; 0.664±0.033 (0.592-0.719) in the amblyopic eye and 0.707±0.039 (0.625-0.779) in the fellow eye in Group 2 patients; and 0.689±0.031 (0.612-0.748) in Group 3 patients. CVI was significantly lower in the amblyopic eyes of Group 2 compared with fellow eyes (p=0.02) and Group 3 (p=0.025).

Conclusion: Morphological changes may be seen in the choroid in amblyopic eyes. We observed that the choroidal stromal component is increased in hyperopic amblyopic patients especially.

Keywords: Amblyopia, choroidal thickness, choroidal vascularity index

Address for Correspondence: Onur Furundaoturan, Ege University Faculty of Medicine, Department of Ophthalmology, İzmir, Turkey
E-mail: onurfurundaoturan@hotmail.com **ORCID-ID:** orcid.org/0000-0001-6929-6645
Received: 25.12.2020 **Accepted:** 26.05.2021

Cite this article as: Furundaoturan O, Değirmenci C, Akkın C, Demirkılınç Biler E, Üretmen Ö, Nalçacı S, Afrashi F. Evaluation of Choroidal Vascular Index in Amblyopic Patients. Turk J Ophthalmol 2022;52:168-173

Introduction

Amblyopia is a pathology caused by abnormal binocular image or visual deprivation that manifests clinically with unilateral or bilateral reduction in best corrected visual acuity (BCVA).[1,2] Its global prevalence varies between 2% and 4%.[2,3] It is considered the most important cause of unilateral visual impairment, especially in children, and can be prevented with treatment if detected at an early age.[2,4]

The two most common subtypes of amblyopia are strabismus and anisometropia, which also constitute its main causes. Amblyopia may occur as a result of strabismus and anisometropia alone or the coexistence of these two pathologies.[1,3,4,5]

Various defects in the visual cortex and cell degradation in the lateral geniculate nucleus are thought to play a role in the development of amblyopia, and it is suggested that inhibition by the fellow eye occurs at various stages of visual development.[6] In addition, structural anomalies of the optic radiation axons and extrastriate areas have been detected in amblyopic patients; however, studies on this subject are ongoing.[7,8]

The choroid, which has important roles in ocular physiology and homeostasis such as temperature control, nutrition, and waste removal, may also play a role in the pathophysiology of amblyopia. It is believed that the choroid influences the formation of a clear retinal image through its ability to change in thickness and volume.[9] Recent studies have shown that changes in subfoveal choroidal thickness (SFCT), which can help adjust retinal image clarity, can also occur over short periods of time.[10] SFCT is determined using optical coherence tomography (OCT) and its enhanced-depth imaging (EDI) mode. In many studies using EDI-OCT, retinal thickness and SFCT were reported to be higher in amblyopic eyes than in both the patients' fellow eyes and normal control groups.[11,12]

The choroidal vascular index (CVI), a parameter recently used in the evaluation of the choroidal vasculature, is the ratio of the vascular lumen to the entire choroidal area. It can provide information about the pathophysiological changes that occur the choroid, which almost certainly has a role in amblyopia.[13,14]

This study aimed to compare the SFCT and CVI values of patients with hypermetropic refractive and strabismic amblyopia with those of healthy eyes.

Materials and Methods

This study was designed as a prospective, case-control study and included amblyopic patients seen in the strabismus unit of the Ege University Faculty of Medicine Hospital and healthy volunteers examined in the outpatient clinic. Approval was obtained from the medical research ethics committee of the university in which the study was conducted, and an informed consent form was signed by the parent or legal guardian of each participant.

The study included 17 eyes of 17 patients with strabismic amblyopia who were currently receiving occlusion therapy (Group 1), 29 eyes of 29 patients with hyperopic anisometropic amblyopia (Group 2), and 16 eyes of 16 age- and gender-matched healthy volunteers (Group 3, control group). All patients and controls underwent detailed ophthalmological examination including BCVA measurement, anterior and posterior segment examinations, intraocular pressure measurement (Tono-Pen, Avia), and cycloplegic refraction (Topcon KR-7000P, Topcon Europe BV, Capelle a/d IJssel, Netherlands). Spherical equivalent was derived from cycloplegic refraction values. In addition, a single subfoveal EDI-OCT (Heidelberg Engineering, Heidelberg, Germany) scan was obtained. As previous studies have shown that the choroid shows diurnal variations, scans were performed between 9:00 AM and 12:00 PM in all patients and by the same researcher.[15,16] SFCT and CVI were evaluated from EDI-OCT images. From these images, CVI was measured with the binarization method using the Image J program (National Institutes of Health, Bethesda, MD, USA). To calculate CVI, lines were drawn at the RPE-choroidal junction 750 µm nasal and temporal of the foveal center, after which the area up to the chorioscleral junction was selected using the program's polygon drawing tool. As described in the literature, the index was calculated as the proportion of the luminal area to the total choroidal area (Figure 1).[13,14,17] Measurements based on EDI-OCT were performed by two different researchers and the average of the two measurements was included in the analysis.

Amblyopia was diagnosed as one eye with BCVA lower than 8/10 and at least 2 Snellen lines difference from the fellow eye with normal BCVA. The patients were included in the appropriate group according to the cause of amblyopia. Only patients with hyperopic refractive errors and anisometropic patients with refractive error difference of +2 diopters or greater between the eyes were included in the refractive amblyopia group. Patients with meridial amblyopia and astigmatic amblyopia were excluded.

We also excluded patients who had amblyopia associated with organic causes, a history of ocular surgery, autoimmune-inflammatory diseases that may cause retinal or choroidal involvement or thickness changes, any drug use, high coffee intake or heavy smoking, systemic comorbidity, or inability to cooperate with OCT.[18,19]

The control group was selected from among patients presenting for routine outpatient visits who had no significant refractive error or manifest deviation, had uncorrected BCVA of 20/20 bilaterally, and were able to cooperate with OCT scans.

Only their right eyes were included in the study to ensure data diversity.

IBM SPSS Statistics version 20.0 (IBM Corp, Armonk, NY, USA) software package was used for statistical analyses. Numerical variables were expressed as mean and standard deviation (minimum-maximum). Mann-Whitney U test was used for intergroup comparisons and chi-square test was used for comparisons of demographic data. P values lower than 0.05 were considered statistically significant.

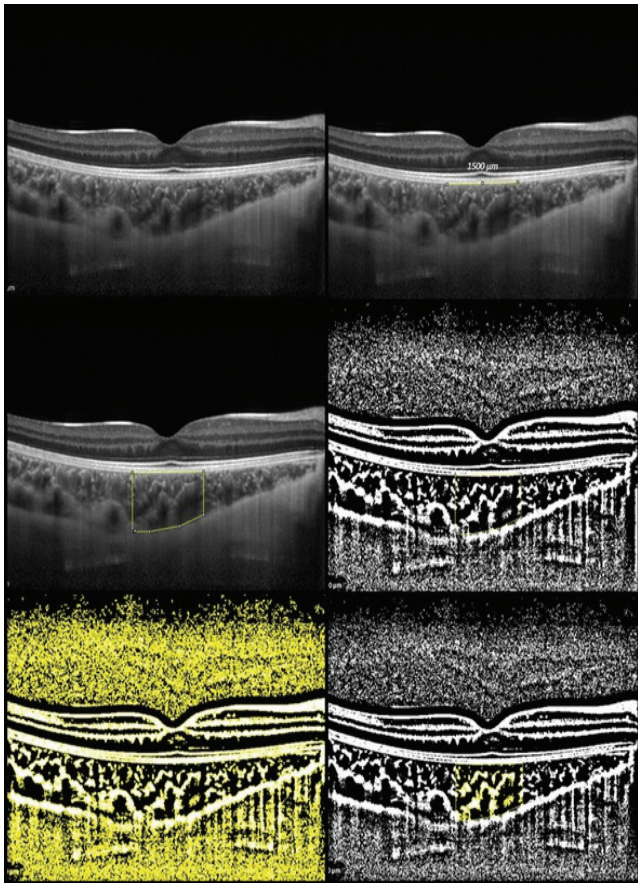

Figure 1. Calculating the choroidal vascular index at 750 µm nasal and temporal of the foveal center by binarization method using Image J software

Results

The study included 46 patients with amblyopia and 16 healthy volunteers. There was no significant difference in age, sex, or intraocular pressure measurements between the groups (p=0.271, p=0.647, and p=0.853, respectively) (Table 1).

Mean BCVA was 0.57±0.16 (range: 0.30-0.80) in Group 1 amblyopic eyes and 0.94±0.07 (range: 0.80-1.00) in Group 1 fellow eyes. In Group 2, mean BCVA was 0.61±0.17 (range: 0.20-0.70) in amblyopic eyes and 0.92±0.10 (range: 0.80-1.00) in fellow eyes. Mean BCVA was 1.00 in Group 3 controls. SFCT was significantly higher and CVI was significantly lower in the amblyopic eyes of Group 2 when compared with these patients' fellow eyes (p=0.05 and p=0.02, respectively) and Group 3 (p=0.01 and p=0.025, respectively) (Table 2).

Discussion

Although the cause of amblyopia has not been fully determined, various mechanisms have been suggested as being involved in its pathophysiology, such as cell destruction in the lateral geniculate body and visual stimuli reaching different projections.[7] Recent advances in imaging technologies have led to a differing view of the pathophysiology of diseases. Thickness changes in the choroid are observed in many diseases, including amblyopia. This study examined the choroidal vasculature in addition to SFCT and showed that CVI was significantly lower in amblyopia, especially cases of hyperopic anisometropic etiology, while the luminal area corresponding to the choroidal vessels did not differ significantly.

With OCT and EDI mode becoming indispensable in ophthalmology practice, detailed examination of the choroid and its layers has become more accessible. The relationship between the choroid and amblyopia, which remains an important problem with still unclear pathophysiology, has also been a subject of research.[12,17,20,21,22] In a meta-analysis evaluating 17 studies including 768 eyes, SFCT was found to be significantly higher in eyes with refractive amblyopia compared to fellow eyes and the control group, consistent with our study (p<0.01).[12] Aygit et al.[23] analyzed SFCT in 120 eyes with both strabismic and anisometropic amblyopia and determined that SFCT was

Table 1. Demographic data of the patient and control groups

	Group 1 mean ± SD (range)	Group 2 mean ± SD (range)	Control mean ± SD (range)	p value
Number	17	29	16	
Age (years)	9.75±4.24 (4-17)	8.20±1.32 (6-10)	11.35±3.05 (6-17)	0.271
Gender (M/F)	9/8	17/15	10/6	0.647

SD: Standard deviation, M: Male, F: Female

significantly greater in both groups compared to control and fellow eyes. Findings from these studies reveal a relationship between choroidal thickness and strabismic and hyperopic refractive amblyopia. Consistent with the literature, in the present study SFCT values were significantly higher in eyes with hyperopic anisometropic amblyopia. However, there was no significant difference in patients with strabismic amblyopia.

Choroidal thickness is known to be significantly affected by axial length. Choroidal thickness was found to be lower in myopic patients and higher in hyperopic patients compared to healthy volunteers.[19] Since axial length could not be examined in this study, we could not evaluate this.

An important component of the retinal blood supply, the choroid is a dense vascular tissue supported by a loose stroma and has the highest blood flow per unit of tissue in the body.[9] Therefore, in diseases in which the choroid is involved in the pathophysiology, such as amblyopia, it may be more important to evaluate the subcomponent of the tissue responsible for the increase/decrease rather than simply evaluating a change in thickness. CVI is presented here as data that may be more meaningful and detailed than thickness.[13,14]

CVI, a new parameter first described by Sonoda et al.,[17] is based on binarization and provides information about the vascular/luminal and stromal components of the choroid.[24,25] In another study, it was reported that with aging, the luminal-vascular area decreased while the stromal area remained stable, resulting in a decrease in the ratio of vascular area to total area.[26]

In a study evaluating the choroidal structure in hyperopic amblyopic eyes, CVI was found to be higher in amblyopic eyes compared to fellow eyes and was positively correlated with SFCT.[24] In the present study, CVI was significantly lower in eyes with hyperopic anisometropic amblyopia compared to fellow eyes and healthy controls. To our knowledge, there is no study in the literature specifically comparing strabismic amblyopia groups, and this study is the first to evaluate CVI according to the type of amblyopia. No significant differences in CVI were detected between the strabismic amblyopia group and the subgroups. This suggests that the choroidal thickening associated with hyperopic refractive error may not be due to amblyopia and may be caused by high hyperopia. However, previous studies have shown that in hyperopic patients, choroidal thickness increases and vascular structures enlarge in association with the degree of hyperopia.[25] In the present study, the stromal component increased more significantly.

In a study of anisometropic amblyopia patients receiving one-year refractive correction and/or occlusion therapy, it was observed that the choroidal vascular component decreased and the stromal component increased in amblyopic eyes after treatment, while no significant change was detected in non-amblyopic eyes.[25] This shows that the choroid plays an important role in the pathophysiology and treatment of the disease, especially in eyes with refractive amblyopia. This is supported by the fact that the morphology of the amblyopic eyes after treatment resembled that of the fellow eyes. In the present study, the fact that the stromal component in relation to the luminal area is significantly different in patients receiving treatment compared to the control group may suggest an effect of treatment on choroidal pathophysiology. We believe that post-treatment follow-up of the same patient group and comparison with initial data would support these findings.

Study Limitations

This case-control study has various limitations. The data were calculated manually based on EDI-OCT images. To prevent potential errors arising due to this, the average of data calculated by two experienced researchers was analyzed. The

Table 2. Visual acuity, refraction, and choroidal parameters of the patients

	Group 1		Group 2		Control Mean ± SD (range)
	Amblyopic eye mean ± SD (range)	Fellow eye mean ± SD (range)	Amblyopic eye mean ± SD (range)	Fellow eye mean ± SD (range)	
BCVA	0.57±0.16 (0.30-0.80)	0.94±0.08 (0.80-1.00)	0.61±0.17 (0.20-0.80)	0.92±0.10 (0.80-1.00)	1.00±0 (1.00-1.00)
SE	3.07±2.85 (0.50-5.00)	2.61±3.46 (0.75-6.00)	4.88±2.83 (2.00-8.00)	2.99±2.51 (0.25-5.50)	0.25±0.50 (0.25-0.50)
SFCT	341.50±60.4 (277-481)	321.92±68.26 (251-440)	370.06±65.36 (247-462)	330.35±74.0 (194-502)	327.62±40.79 (238-385)
CVI	0.681±0.032 (0.641-0.736)	0.685±0.054 (0.587-0.788)	0.664±0.033 (0.592-0.719)	0.707±0.039 (0.625-0.779)	0.688±0.031 (0.612-0.748)
LA	1.011±0.187 (0.690-1.310)	0.964±0.230 (0.560-1.270)	1.106±0.165 (0.770-1.400)	1.012±0.174 (0.570-1.300)	1.105±0.135 (0.830-1.310)

SD: Standard deviation, BCVA: Best corrected visual acuity, SE: Spherical equivalent, SFCT: Subfoveal choroidal thickness, CVI: Choroidal vascular index, LA: Luminal area

amblyopia patients in the study are those being followed up and treated in the pediatric ophthalmology department of our center. We hope to confirm our data in larger scale studies with a sufficient number of treatment-naive patients. In addition, since AL measurements could not be taken, it was not possible to compare the refraction values obtained after cycloplegic drops and other parameters according to AL. The strabismic amblyopia group in our study was also small compared to the other groups. The majority of patients with strabismic amblyopia also have refractive errors, which limited the number of patients in this group. Although there was no statistically significant difference in the mean, the number of patients in the study groups and their heterogeneity in terms of age distribution constituted a significant limitation of the study. Therefore, studies with larger samples of all groups are needed.

Conclusion

Whether amblyopia is of strabismic or refractive etiology, morphological changes can be seen in the choroid. However, CVI values showed that the stromal component of the choroid was increased in patients with refractive amblyopia.

Ethics

Ethics Committee Approval: Ege University Medical Research Ethics Committee, decision no: 20-4.2T/33, 29.04.2020.

Informed Consent: Approval was obtained from the medical research ethics committee of the university in which the study was conducted, and an informed consent form was signed by the parent or legal guardian of each participant.

Peer-review: Externally peer reviewed.

Authorship Contributions

Surgical and Medical Practices: C.D., O.F., Concept: O.F., E.D.B., F.A., C.A., S.N., Design: O.F., E.D.B., F.A., C.A., S.N., Ö.Ü., Data Collection or Processing: C.D., O.F., Analysis or Interpretation: C.D., O.F., Literature Search: C.D., O.F., Writing: C.D., O.F.

Conflict of Interest: No conflict of interest was declared by the authors.

Financial Disclosure: The authors declared that this study received no financial support.

References

1. Tailor V, Bossi M, Greenwood JA, Dahlmann-Noor A. Childhood amblyopia: current management and new trends. Br Med Bull. 2016;119:75-86.
2. Wallace DK, Repka MX, Lee KA, Melia M, Christiansen SP, Morse CL, Sprunger DT; American Academy of Pediatric Ophthalmology/Strabismus Preferred Practice Pattern Pediatric Ophthalmology Panel. Amblyopia Preferred Practice Pattern®. Ophthalmology. 2018;125:105-142.
3. Maurer D, McKEE SP. Classification and diversity of amblyopia. Vis Neurosci. 2018;35:E012.
4. Webber AL. Amblyopia treatment: an evidence-based approach to maximising treatment outcome. Clin Exp Optom. 2007;90:250-257.
5. von Noorden GK. Amblyopia: a multidisciplinary approach. Proctor lecture. Invest Ophthalmol Vis Sci. 1985;26:1704-1716.
6. Weinacht S, Kind C, Mönting JS, Gottlob I. Visual development in preterm and full-term infants: a prospective masked study. Invest Ophthalmol Vis Sci. 1999;40:346-353.
7. Daw NW. Critical periods and amblyopia. Arch Ophthalmol. 1998;116:502-505.
8. Vagge A, Nelson LB. Amblyopia update: new treatments. Curr Opin Ophthalmol. 2016;27:380-386.
9. Nickla DL, Wallman J. The multifunctional choroid. Prog Retin Eye Res. 2010;29:144-168.
10. Chiang ST, Phillips JR, Backhouse S. Effect of retinal image defocus on the thickness of the human choroid. Ophthalmic Physiol Opt. 2015;35:405-413.
11. Li J, Ji P, Yu M. Meta-analysis of retinal changes in unilateral amblyopia using optical coherence tomography. Eur J Ophthalmol. 2015;25:400-409.
12. Liu Y, Dong Y, Zhao K. A Meta-Analysis of Choroidal Thickness Changes in Unilateral Amblyopia. J Ophthalmol. 2017;2017:2915261.
13. Agrawal R, Gupta P, Tan KA, Cheung CM, Wong TY, Cheng CY. Choroidal vascularity index as a measure of vascular status of the choroid: Measurements in healthy eyes from a population-based study. Sci Rep. 2016;6:21090.
14. Agrawal R, Salman M, Tan KA, Karampelas M, Sim DA, Keane PA, Pavesio C. Choroidal Vascularity Index (CVI) - A Novel Optical Coherence Tomography Parameter for Monitoring Patients with Panuveitis? PLos One. 2016;11:e0146344.
15. Ostrin LA, Jnawali A, Carkeet A, Patel NB. Twenty-four hour ocular and systemic diurnal rhythms in children. Ophthalmic Physiol Opt. 2019;39:358-369.
16. Burfield HJ, Patel NB, Ostrin LA. Ocular Biometric Diurnal Rhythms in Emmetropic and Myopic Adults. Invest Ophthalmol Vis Sci. 2018;59:5176-5187.
17. Sonoda S, Sakamoto T, Yamashita T, Shirasawa M, Uchino E, Terasaki H, Tomita M. Choroidal structure in normal eyes and after photodynamic therapy determined by binarization of optical coherence tomographic images. Invest Ophthalmol Vis Sci. 2014;55:3893-3899.
18. Steiner M, Esteban-Ortega MDM, Muñoz-Fernández S. Choroidal and retinal thickness in systemic autoimmune and inflammatory diseases: A review. Surv Ophthalmol. 2019;64:757-769.
19. Jin P, Zou H, Zhu J, Xu X, Jin J, Chang TC, Lu L, Yuan H, Sun S, Yan B, He J, Wang M, He X. Choroidal and Retinal Thickness in Children With Different Refractive Status Measured by Swept-Source Optical Coherence Tomography. Am J Ophthalmol. 2016;168:164-176.
20. Araki S, Miki A, Goto K, Yamashita T, Takizawa G, Haruishi K, Ieki Y, Kiryu J, Yaoeda K. Macular retinal and choroidal thickness in unilateral amblyopia using swept-source optical coherence tomography. BMC Ophthalmol. 2017;17:167.
21. Kara O, Altintas O, Karaman S, Emre E, Caglar Y. Analysis of Choroidal Thickness Using Spectral-Domain OCT in Children With Unilateral Amblyopia. J Pediatr Ophthalmol Strabismus. 2015;52:159-166.
22. Celik E, Çakır B, Turkoglu EB, Doğan E, Alagoz G. Evaluation of the retinal ganglion cell and choroidal thickness in young Turkish adults with hyperopic anisometropic amblyopia. Int Ophthalmol. 2016;36:515-520.
23. Aygit ED, Yilmaz I, Ozkaya A, Alkin Z, Gokyigit B, Yazici AT, Demirok A. Choroidal thickness of children's eyes with anisometropic and strabismic amblyopia. J AAPOS. 2015;19:237-241.

24. Baek J, Lee A, Chu M, Kang NY. Analysis of Choroidal Vascularity in Children with Unilateral Hyperopic Amblyopia. Sci Rep. 2019;9:12143.
25. Nishi T, Ueda T, Mizusawa Y, Semba K, Shinomiya K, Mitamura Y, Sonoda S, Uchino E, Sakamoto T, Ogata N. Effect of optical correction on choroidal structure in children with anisohypermetropic amblyopia. PLos One. 2020;15:e0231903.
26. Ruiz-Medrano J, Ruiz-Moreno JM, Goud A, Vupparaboina KK, Jana S, Chhablani J. Age-Related Changes In Choroıdal Vascular Densıty Of Healthy Subjects Based On Image Bınarızatıon Of Swept-Source Optıcal Coherence Tomography. Retina. 2018;38:508-515.

DOI: 10.4274/tjo.galenos.2021.72929
Turk J Ophthalmol 2022;52:174-178

Original Article

Hedgehog Signal Defect Leading to Familial Exudative Vitreoretinopathy-Like Disease and Gastrointestinal Malformation

Nedime Şahinoğlu Keşkek*, İmren Akkoyun**, Abdülkerim Temiz***, Özgür Kütük****

*Başkent University Faculty of Medicine, Adana Research and Training Center, Department of Ophthalmology, Adana, Turkey
**Başkent University Faculty of Medicine, Department of Ophthalmology, Ankara, Turkey
***Başkent University Faculty of Medicine, Adana Research and Training Center, Department of Pediatric Surgery, Adana, Turkey
****Başkent University Faculty of Medicine, Adana Research and Training Center, Department of Medical Genetics, Adana, Turkey

Abstract

Objectives: The aim of the study was to present a new genetic association presenting with gastrointestinal tract malformations (GTMs) and familial exudative vitreoretinopathy (FEVR)-like disease and review the genetics of Hedgehog signaling.

Materials and Methods: Three neonates were diagnosed with FEVR-like retinal vascular disease upon routine ophthalmological examination during hospitalization in the neonatal surgical intensive care unit for GTMs. Genetic analysis of the neonates was performed.

Results: Gestational age of the neonates was 39, 38, and 39 weeks and birth weights were 3,500, 3,600, and 3,300 grams, respectively. All six eyes of the three infants were treated by laser photocoagulation. Recurrence was not seen in any of the eyes. Genetical analysis of all the neonates diagnosed with FEVR-like disease revealed defects in the Hedgehog pathway.

Conclusion: FEVR is a genetically well-defined retinal vascular disease. The current study is the first to show an association between FEVR-like retinal vascular disease and GTMs. This study demonstrates the importance of the Hedgehog pathway in retinal vascular and gut development.

Keywords: Familial exudative vitreoretinopathy, gastrointestinal tract malformations, genetic, hedgehog pathway, retinal vascular disease

Address for Correspondence: Nedime Şahinoğlu Keşkek, Başkent University Faculty of Medicine, Adana Research and Training Center, Department of Ophthalmology, Adana, Turkey
E-mail: nedime_sahin@yahoo.com **ORCID-ID:** orcid.org/0000-0001-8544-103X
Received: 07.01.2021 **Accepted:** 22.06.2021

Cite this article as: Şahinoğlu Keşkek N, Akkoyun İ, Temiz A, Kütük Ö. Hedgehog Signal Defect Leading to Familial Exudative Vitreoretinopathy-Like Disease and Gastrointestinal Malformation. Turk J Ophthalmol 2022;52:174-178

Introduction

Familial exudative vitreoretinopathy (FEVR) is a congenital retinal vascular disease characterized by retinal nonperfusion, proliferative retinopathy, and retinal detachment.[1] Clinically, FEVR displays remarkably varying phenotypes, from barely detectable retinal vascular anomaly to retinal detachment.[2] Classical clinical findings consist of peripheral avascular retina, neovascularization, exudation, dragging of vascular elements, and retinal detachment.[1] Mutations of the Wnt/Norrin signaling pathway underlie the molecular mechanisms leading to FEVR.[3] Particularly, four genes are well documented to be related to FEVR: *FZD4, LRP5, TSPAN12*, and *NDP*.[3,4,5,6]

Hedgehog (Hh) signals are considered to play an important role in embryonic gut development. Abnormal Hh signaling had been identified in the molecular etiology of the common gastrointestinal tract malformations (GTMs).[7] The family of Hh signaling proteins includes three members: sonic (Shh), Indian (Ihh), and desert (Dhh) hedgehogs. Shh signaling forms the key molecules in gut morphogenesis. These molecules are expressed in the endoderm throughout early embryogenesis and have an important role in gut formation.[8]

In addition to gut development, the Shh signaling pathway is important in neuronal differentiation, axon guidance, and angiogenesis.[9] Astrocytes secrete Shh to promote formation of the blood-brain barrier.[10] A recent study with an in vitro model of retinal vascular endothelial cells demonstrated that the Shh pathway regulates endothelial permeability.[11] A mutation in the Shh pathway may cause a disorder consisting of GTMs and retinal vascular disease.

The aim of this study was to report three unrelated sporadic patients with GTMs exhibiting the FEVR phenotype. Genetic analyses revealed defects in the Shh pathway. This association may necessitate the referral of patients with GTMs to retina specialists.

Materials and Methods

This was a case series including six eyes of three neonates who underwent routine ophthalmological examination during their hospitalization in the neonatal surgical intensive care unit for GTMs between September 2016 and September 2019. All three of the neonates were male, having gestational ages of 39, 38, and 39 weeks and birth weight of 3500, 3600, and 3300 grams, respectively (Table 1). All were examined by the same ophthalmologist (N.S.K.) using a binocular indirect ophthalmoscope and diagnosed as having FEVR. FEVR was classified based on ophthalmoscopic findings: stage 1, avascular periphery; stage 2, avascular periphery with neovascularization; stage 3, macula-sparing retinal detachment; stage 4, macula-involving retinal detachment; and stage 5, complete retinal detachment.[12]

Diode laser photocoagulation was performed to 360° presumed avascular areas of retina (0.15 seconds and 160 mW power) in a near confluent pattern, under general anesthesia, in the operating room.

The research was conducted at our tertiary care facility after receiving approval from the local ethics committee (KA19/306). The study complied with the principles of the Declaration of Helsinki. Informed consent form was obtained from the parents of the patients.

Statistical Analysis

Patient DNA was isolated from whole blood (3 mL) using the QIA amp DNA blood kit (QIAGEN, Hilden, Germany). Three micrograms of high-molecular-weight DNA was sheared using a Covarias ultrasonicator and the genomic DNA library was prepared with an Agilent SureSelect Target Enrichment System. Following enrichment with Agilent SureSelect Human All Exon V7, sequencing was performed on an IlluminaHiSeq 2500 System (Illumina, San Diego, USA). Data interpretation and variant calling were performed on SOPHiA DDM® version 5.4.2 (Sophia Genetics, Switzerland).

Results

Fundus examination revealed flat neovascularizations and brush-paint-like retinal hemorrhages in all 6 eyes. Figure 1a shows a macular image from patient 1 and Figure 1b shows a presumed avascular area and hemorrhage in the same patient. Fundus images of patient 2 before and after treatment are shown in Figure 1c and 1d. Patient 3 also had hemorrhages as a result of neovascularizations on the border of the vascular zone and presumed avascular retinal regions (Figure 1e,f). All eyes were diagnosed as having stage 2 FEVR without exudation (stage 2A). Presumed avascular areas were treated successfully with laser photocoagulation and no additional treatment was needed. Recurrence was not seen in any case.

Two of the neonates had anal atresia and one had Hirschsprung disease (HSCR). Next, we explored the putative causative mutations associated with the patients' phenotypes. We identified a heterozygous *LRP5* (low-density lipoprotein receptor-related protein 5) mutation (rs80358313, NP_002326.2:p.Gly610Arg, NM_002335.4:c.1828G>A) in patient 1 and a heterozygous

Table 1. Characteristics of the patients

Patient no, sex	GA (weeks)	BW (g)	LP time (weeks)	Follow-up time (months)	FEVR stage	GTMs
1, male	39	3500	41	56	2A	Anal atresia
2, male	38	3600	40	42	2A	Anal atresia
3, male	39	3300	40	30	2A	Hirschsprung disease

FEVR: Familial exudative vitreoretinopathy, GTMs: Gastrointestinal tract malformations, GA: Gestational age, BW: Birth weight, LP: Laser photocoagulation

KIF7 (kinesin-like protein KIF7) mutation (rs143877028, NP_940927.2:p.Ser1281Ile, NM_198525.3:c.3842G>T) in patient 2, who both presented with anal atresia. In patient 3, who had HSCR, we detected a heterozygous *GLI2* (zincfinger protein GLI2) mutation (rs751513015, NP_005261.2:p.Asp705Asn, NM_005270.4:c.2113G>A). Altogether, our findings demonstrated mutations of different genes in the Shh pathway.

Discussion

Familial exudative vitreoretinopathy was first defined by Criswick and Schepens[1] in 1969. FEVR presents with varying clinical manifestations but is limited to abnormalities in ocular development.[13] Four genes were found to be associated with FEVR. Autosomal dominant FEVR appears from mutations in *FZD4, LRP5, and TSPAN12;* the autosomal recessive form occurs in homozygous *LRP5* mutations, and X-linked FEVR arises from mutations in *NDP.*[6] Norrie disease is another hereditary disorder occurring mainly in full-term infants, defined by abnormal retinal vascularization causing retinal detachment. Norrie disease causes blindness soon after birth and most patients have systemic disorders such as mental retardation and deafness.[13] Mutations in the Norrie disease protein *(NDP)* gene leads to Norrie disease.[14] At birth, NDP is markedly increased in the retina in order to enhance levels of norrin, which is involved in progenitor proliferation in the postnatal period.[15] McNeill et al.[16] showed that Hh signaling regulates NDP expression and concluded that NDP is essential downstream of Hh activation to trigger retinal progenitor proliferation in the retina. In addition, Wang et al.[17] showed that Hh signaling is mandatory to support retinal precursor cell proliferation.

Surace et al.[18] investigated the association between the Hh pathway and retinopathy of prematurity (ROP) in murine models and found upregulation of Hh expression similar to vascular endothelial growth factor (VEGF). To support the results, the investigators systemically administered the selective Hh inhibitor cyclopamine in ROP models and revealed that neovascularization was inhibited. Their results proved that Hh pathway activation has an important role in hypoxia-induced retinal neovascularization.

Liu et al.[19] investigated the association between VEGF, retinal neovascularization, and the Hh signaling pathway in murine ROP models. Their results demonstrated that under normal oxygen concentrations, VEGF had low transcription and expression, high oxygen levels stimulated VEGF expression significantly, and cyclopamine inhibited VEGF expression by Hh blockade. The authors hypothesized that the Hh pathway participated in regulating VEGF levels in ROP and that blocking the Hh signaling pathway may be useful in the treatment of ROP.

The *FZD4, LRP5, TSPAN12,* and *NDP* genes are parts of the Wnt/b-catenin signaling pathway and have roles in cell survival, proliferation, and migration throughout the body. In the current study, an *LRP5* mutation expected in FEVR was found in one patient. However, to our knowledge, this is the first reported case accompanied by anal atresia. Mutations in the *LRP5, FZD4,* and *NDP* gene have also been found in patients with ROP at varying frequencies.[20-22] In the current study, we diagnosed the patients as having FEVR based on the clinical presentation and medical data of the neonates, such as gestational age and birth weight. It is difficult to differentiate ROP and FEVR in premature infants. In our cases, the clinical findings mimicked ROP. However, there was no ridge appearance. Instead, all patients had flat

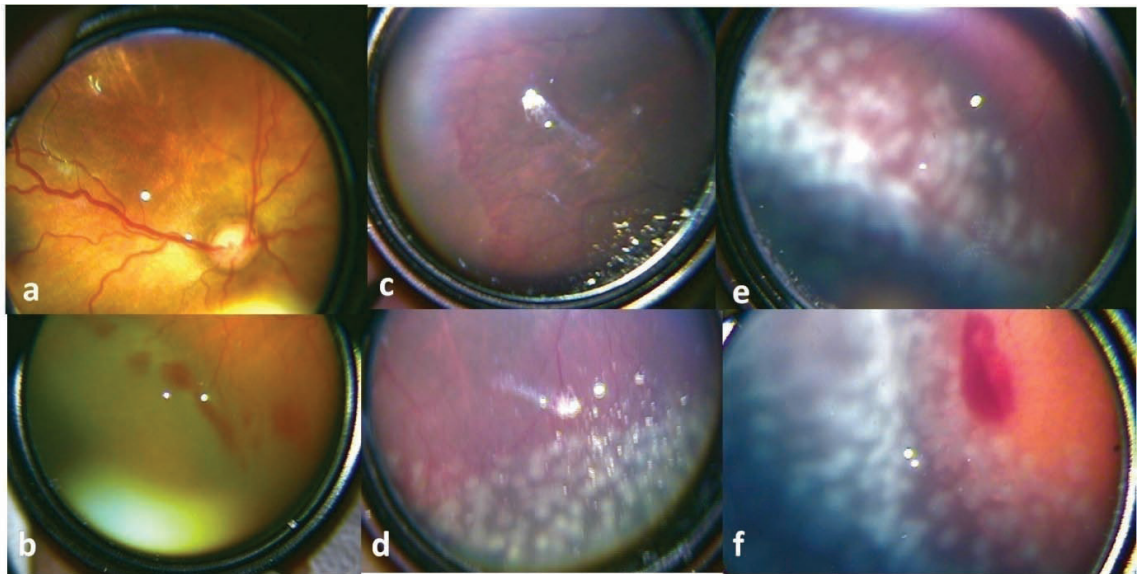

Figure 1. Fundus photographs of the patients. **a)** Patient 1, a plus-like appearance is seen in the macular region of the right eye. **b)** Patient 1, retinal hemorrhages and neovascularizations are seen at the border of vascularized and avascular retinal regions of the right eye. **c)** Patient 2, flat neovascularizations are seen in the temporal periphery of the right eye. **d)** Patient 2, fundus appearance after laser photocoagulation in the right eye. **e)** Patient 3, flat neovascularizations and laser spots after treatment in the left eye. **f)** Patient 3, retinal hemorrhage and laser spots after treatment in the left eye

neovascularizations in zone 2 and brush-paint-like hemorrhages. A new classification named ROPER (ROP vs. FEVR) was recently introduced due to the clinical resemblance of these two disorders.[23] John et al.[23] described ROPER in premature infants demonstrating retinal findings more typical of FEVR than ROP. They reported the differentiating fluorescein angiography features of ROPER as irregular buds of vascularization at the vascular/avascular junction, definite pruning of vessels, pinpoint hyperfluorescent areas, and segmental vascular leakage areas. Our patients did not undergo fluorescein angiography, but their retinal findings mimicked ROP. One patient had neovascularization on the iris. The differential diagnosis of these vascular disorders is important, because ROPER may have an unpredictable and long-term course.

In the course of organogenesis, cell numbers are regulated by balancing proliferation and cell death. During development, the Hh signaling pathway controls cell proliferation and survival.[24] Shh is a crucial survival factor for the neural stem cells, midbrain, forebrain, retina, and neural crest.[25,26] Furthermore, a recent study proved that Shh signaling functions in the maintenance of retinal endothelial tight junctions.[11]

Retinal vessels have a high number of pericytes covering the endothelial cells. Signals from pericytes are essential for the formation and maintenance of the blood-retinal barrier.[27] Neovascular vessels are generally associated with disturbance of the blood-retinal barrier. The relationship between Shh signaling and vessel growth and barrier formation demonstrates the role of Shh in angiogenesis and barrier formation. A defect in the Shh pathway is likely to disrupt the blood-retinal barrier, impair oxygen supply to the retina, and cause retinal neovascularization.

HSCR is characterized by functional intestinal obstruction of a genetic etiology.[28] It involves abnormal development of the enteric nervous system resulting in intestinal dysfunction. Congenital anorectal malformations including anal atresia are common manifestations, with an incidence of 1 in 1,000-5,000 neonates.[29] The Hh family proteins (Shh, Ihh, Dhh) are secreted signaling molecules that manage the development and balancing of tissues.[30] Shh, Ihh, and Dhh are all expressed in the gut tube.[30] Gao et al.[31] found that genetic polymorphisms in the Hh gene were associated with HSCR and anorectal malformations. Two of our patients were diagnosed with anal atresia and one was diagnosed with HSCR.

Study Limitations

The current study emphasizes the role of the Hh pathway in both retinal vascular and gut development and describes a new syndrome involving FEVR and GTMs. Pediatric surgeons should be aware of this association and refer neonates with GTMs to retina specialists.

Conclusion

In future investigations, analysis of clinical findings, retinal imaging with fluorescein angiography, and family genetic analysis may further our understanding of the genetics of neonatal vascular disease.

Ethics

Ethics Committee Approval: Obtained from the local ethics committee (KA19/306).

Informed Consent: Obtained from the parents of all patients.

Peer-review: Externally and internally peer reviewed.

Authorship Contributions

Concept: N.Ş.K., İ.A., A.T., Ö.K., Design: N.Ş.K., İ.A., A.T., Ö.K., Data Collection or Processing: N.Ş.K., İ.A., A.T., Ö.K., Analysis or Interpretation: N.Ş.K., İ.A., A.T., Ö.K., Literature Search: N.Ş.K., İ.A., A.T., Ö.K., Writing: N.Ş.K., İ.A., A.T., Ö.K.

Conflict of Interest: No conflict of interest was declared by the authors.

Financial Disclosure: The authors declared that this study received no financial support.

References

1. Criswick VG, Schepens CL. Familial exudative vitreoretinopathy. Am J Ophthalmol. 1969;68:578-594.
2. Tang M, Sun L, Hu A, Yuan M, Yang Y, Peng X, Ding X. Mutation spectrum of the LRP5, NDP, and TSPAN12 genes in Chinese patients with familial exudative vitreoretinopathy. Invest Ophthalmol Vis Sci. 2017;58:5949-5957.
3. Warden SM, Andreoli CM, Mukai S. The Wnt signaling pathway in familial exudative vitreoretinopathy and Norrie disease. Semin Ophthalmol. 2007;22:211-217.
4. Gong Y, Slee RB, Fukai N, Rawadi G, Roman-Roman S, Reginato AM, Wang H, Cundy T, Glorieux FH, Lev D, Zacharin M, Oexle K, Marcelino J, Suwairi W, Heeger S, Sabatakos G, Apte S, Adkins WN, Allgrove J, Arslan-Kirchner M, Batch JA, Beighton P, Black GC, Boles RG, Boon LM, Borrone C, Brunner HG, Carle GF, Dallapiccola B, De Paepe A, Floege B, Halfhide ML, Hall B, Hennekam RC, Hirose T, Jans A, Jüppner H, Kim CA, Keppler-Noreuil K, Kohlschuetter A, LaCombe D, Lambert M, Lemyre E, Letteboer T, Peltonen L, Ramesar RS, Romanengo M, Somer H, Steichen-Gersdorf E, Steinmann B, Sullivan B, Superti-Furga A, Swoboda W, van den Boogaard MJ, Van Hul W, Vikkula M, Votruba M, Zabel B, Garcia T, Baron R, Olsen BR, Warman ML; Osteoporosis-Pseudoglioma Syndrome Collaborative Group. LDL receptor-related protein 5 (LRP5) affects bone accrual and eye development. Cell. 2001;107:513-523.
5. Toomes C, Downey L. Familial exudative vitreoretinopathy, autosomal dominant. 2005 Mar 21 [Updated 2011Sep 22]. In: Pagon RA, Adam MP, Ardinger HH, editors. GeneReviews[Internet] Seattle (WA): University of Washington, Seattle; 1993-2014 Accessed August 8, 2014.
6. Sims KB. NDP-related retinopathies. 1999 Jul 30 [Updated 2009 Jul 23]. In: Pagon RA, Adam MP, Ardinger HH, editors. GeneReviews[Internet] Seattle (WA): University of Washington, Seattle; 1993-2014. Accessed August 8, 2014.
7. de Santa Barbara P, van den Brink GR, Roberts DJ. Molecular etiology of gut malformations and diseases. Am J Med Genet. 2002;115:221-230.
8. Roberts DJ. Molecular mechanisms of development of the gastrointestinal tract. Dev Dyn. 2000;219:109-120.
9. Nagase T, Nagase M, Machida M, Fujita T. Hedgehog signalling in vascular development. Angiogenesis. 2008;11:71-77.
10. Alvarez JI, Dodelet-Devillers A, Kebir H, Ifergan I, Fabre PJ, Terouz S, Sabbagh M, Wosik K, Bourbonnière L, Bernard M, van Horssen J, de Vries HE, Charron F, Prat A. The Hedgehog pathway promotes blood-brain barrier integrity and CNS immune quiescence. Science. 2011;334:1727-1731.
11. Díaz-Coránguez M, Chao DL, Salero EL, Goldberg JL, Antonetti DA. Cell autonomous sonic hedgehog signaling contributes to maintenance of retinal endothelial tight junctions. Exp Eye Res. 2017;164:82-89.

12. Ranchod TM, Ho LY, Drenser KA, Capone A Jr, Trese MT. Clinical presentation of familial exudative vitreoretinopathy. Ophthalmology. 2011;118:2070-2075.
13. Shastry B, Hiraoka M, Trese D, Trese M. Norrie disease and exudative vitreoretinopathy in families with affected female carriers. Eur J Ophthalmol 1999;9:238-242.
14. Chen ZY, Battinelli EM, Fielder A, Bundey S, Sims K, Breakefield XO, Craig IW. A mutation in the Norrie disease gene (NDP) associated with X-linked familial exudative vitreoretinopathy. Nat Genet. 1993;5:180-183.
15. Ye X, Smallwood P, Nathans J. Expression of the Norrie disease gene (Ndp) in developing and adult mouse eye, ear, and brain. Gene Expr. Patterns. 2011;11:151-155.
16. McNeill B, Mazerolle C, Bassett EA, Mears AJ, Ringuette R, Lagali P, Picketts DJ, Paes K, Rice D, Wallace VA. Hedgehog regulates Norrie disease protein to drive neural progenitor self-renewal. Hum Mol Genet. 2013;22:1005-1016.
17. Wang Y, Dakubo GD, Thurig S, Mazerolle CJ, Wallace VA. Retinal ganglion cell-derived sonic hedgehog locally controls proliferation and the timing of RGC development in the embryonic mouse retina. Development. 2005;132: 5103-5113.
18. Surace EM, Balaggan KS, Tessitore A, Mussolino C, Cotugno G, Bonetti C, Vitale A, Ali RR, Auricchio A. Inhibition of ocular neovascularization by hedgehog blockade. Mol Ther. 2006;13:573-579.
19. Liu M, Chen X, Liu H, Di Y. Expression and significance of the Hedgehog signal transduction pathway in oxygen-induced retinal neovascularization in mice. Drug Des Devel Ther. 2018;12:1337-1346.
20. Kondo H, Kusaka S, Yoshinaga A, Uchio E, Tawara A, Tahira T. Genetic variants of FZD4 and LRP5 genes in patients with advanced retinopathy of prematurity. Mol Vis. 2013;19:476-485.
21. Dailey WA, Gryc W, Garg PG,Drenser KA. Frizzled-4 variations associated with retinopathy and intrauterine growth retardation: a potential marker for prematurity and retinopathy. Ophthalmology. 2015;122:1917-1923.
22. Hutcheson KA, Paluru PC, Bernstein SL, Koh J, Rappaport EF, Leach RA, Young TL. Norrie disease gene sequence variants in an ethnically diverse population with retinopathy of prematurity. Mol Vis. 2005;11:501-508.
23. John VJ, McClintic JI, Hess DJ, Berrocal AM. Retinopathy of prematurity versus familial exudative vitreoretinopathy: report on clinical and angiographic findings. Ophthalmic Surg Lasers Imaging Retina. 2016;47:14-19
24. Varjosalo M, Taipale J. Hedgehog: functions and mechanisms. Genes Dev. 2008;22:2454-2472.
25. Cai C, Thorne J, Grabel L. Hedgehog serves as a mitogen and survival factor during embryonic stem cell neurogenesis. Stem Cells. 2008;26:1097-1108.
26. Stenkamp DL, Frey RA, Mallory DE, Shupe EE. Embryonic retinal gene expression in sonic-you mutant zebrafish. Dev Dyn. 2002;225:344-350.
27. Shen W, Fruttiger M, Zhu L, Chung SH, Barnett NL, Kirk JK, Lee S, Coorey NJ, Killingsworth M, Sherman LS, Gillies MC. Conditional Müllercell ablation causes independent neuronal and vascular pathologies in a novel transgenic model. J Neurosci. 2012;32:15715-15727.
28. Amiel J, Sproat-Emison E, Garcia-Barcelo M, Lantieri F, Burzynski G, Borrego S, Pelet A, Arnold S, Miao X, Griseri P, Brooks AS, Antinolo G, de Pontual L, Clement-Ziza M, Munnich A, Kashuk C, West K, Wong KK, Lyonnet S, Chakravarti A, Tam PK, Ceccherini I, Hofstra RM, Fernandez R; Hirschsprung Disease Consortium. Hirschsprung disease, associated syndromes and genetics: a review. J Med Genet. 2008;45:1-14.
29. Rintala RJ. Congenital anorectal malformations: Anything new? J Pediatr Gastroenterol Nutr. 2009;48:7982.
30. McMahon AP, Ingham PW, Tabin CJ. Developmental roles and clinical significance of hedgehog signaling. Curr Top Dev Biol. 2003;53:1114.
31. Gao H, Wang D, Bai Y, Zhang J, Wu M, Mi J, Jia H, Wang W. Hedgehog gene polymorphisms are associated with the risk of Hirschsprung's disease and anorectal malformation in a Chinese population. Mol Med Rep. 2016;13:4759-4766.

DOI: 10.4274/tjo.galenos.2021.37075
Turk J Ophthalmol 2022;52:179-185

Original Article

Survey of Intravitreal Injection Preferences for the Treatment of Age-Related Macular Degeneration and Macular Edema Among Members of the Turkish Ophthalmological Association

V. Levent Karabaş*, Ecem Önder Tokuç**, Figen Şermet***

*Kocaeli University Faculty of Medicine, Department of Ophthalmology, Kocaeli, Turkey
**University of Health Sciences Turkey, Derince Training and Research Hospital, Clinic of Ophthalmology, Kocaeli, Turkey
***Ankara University Faculty of Medicine, Department of Ophthalmology, Ankara, Turkey

Abstract

Objectives: To analyze the current preferences of ophthalmologists for the treatment of macular edema and age-related macular degeneration (AMD) and to evaluate off-label use of bevacizumab in Turkey.

Materials and Methods: All members of the Turkish Ophthalmological Association were contacted by e-mail to complete an anonymous, 47-question internet-based survey. The second part of the survey (questions 36-47) was evaluated.

Results: When current legal regulations were considered, ophthalmologists used bevacizumab as the first-line agent in patients with diabetic macular edema (DME), AMD, and retinal vein occlusion (RVO) (58.25%, 55.89%, and 52.29%, respectively). When economic and legal constraints were disregarded, the participants' preference for bevacizumab in the treatment of DME, AMD, and RVO decreased (11.64%, 10.58%, and 10.93%, respectively). Approximately three-quarters (75.75%) of ophthalmologists stated that dispensing multiple syringes from a single bevacizumab bottle could increase the risk of endophthalmitis. Most participants (93.68%) did not feel legally safe from harm caused by off-label bevacizumab use. However, 66.43% of ophthalmologists stated that bevacizumab is as effective as other anti-vascular endothelial growth factor (anti-VEGF) drugs.

Conclusion: Bevacizumab is widely used as a first-line treatment for all indications of anti-VEGF use in the current reimbursement conditions, which preclude the right of ophthalmologists to treat according to their own preferences.

Keywords: Anti-VEGF, bevacizumab, aflibercept, ranibizumab, off-label, diabetic macular edema, age-related macular degeneration, retinal vein occlusion

Address for Correspondence: V. Levent Karabaş, Kocaeli University Faculty of Medicine, Department of Ophthalmology, Kocaeli, Turkey
E-mail: karabas@superonline.com **ORCID-ID:** orcid.org/0000-0001-7860-4603
Received: 16.04.2021 **Accepted:** 17.08.2021

Cite this article as: Karabaş VL, Önder Tokuç E, Şermet F. Survey of Intravitreal Injection Preferences for the Treatment of Age-Related Macular Degeneration and Macular Edema Among Members of the Turkish Ophthalmological Association. Turk J Ophthalmol 2022;52:179-185

Introduction

The treatment of neovascular age-related macular degeneration (AMD), diabetic macular edema (DME), and retinal vein occlusion (RVO) is evolving as new research results become available. Ophthalmologists widely use intravitreal injection of anti-vascular endothelial growth factor (anti-VEGF) agents such as ranibizumab, aflibercept, and bevacizumab in the treatment of these conditions.[1,2,3,4] Aflibercept and ranibizumab were approved by the United States Food and Drug Administration (FDA) for the treatment of AMD, RVO, and DME. However, bevacizumab does not have FDA approval for ophthalmic use and is thus "off-label," despite being widely used.[5] Bevacizumab is also not approved for ophthalmologic use in Turkey. The ophthalmic off-label use of bevacizumab has caused great controversy due to the ethical, legal, economic, and political issues surrounding its use.[6]

As a global health issue, the substantial cost variation, the risk of endophthalmitis, the legal restriction of off-label use, the cost of obtaining medications, and reimbursements contribute to a controversial health policy and an ethical dilemma in regard to anti-VEGF agents. In Turkey, reimbursement regulations suggest three consecutive monthly injections of bevacizumab for the treatment of DME, AMD, and RVO. The aim of this study was to describe the preferences of ophthalmologists regarding anti-VEGF drugs and evaluate the off-label use of bevacizumab.

Materials and Methods

All members of the Turkish Ophthalmological Association were contacted via e-mail in May 2020 to complete a 47-question online survey conducted using SurveyMonkey (www.surveymonkey.com; SurveyMonkey, San Mateo, CA). Three reminder e-mails were sent to participants who had not completed the survey yet. Data collection was concluded on June 4, 2020. Results from the first part of the survey (questions 1-35) evaluating intravitreal injection techniques were published previously.[7] The second part of the survey (questions 36-47) evaluated ophthalmologists' approaches to bevacizumab and other FDA-approved anti-VEGF drugs for patients with DME, AMD, and RVO. The participants were divided into subgroups as representatives of private hospitals, private offices, public hospitals, city hospitals, university hospitals, training and research hospitals, and foundation universities. The research protocol was approved by the Institutional Ethics Committee and Review Board of Kocaeli University (number: KAEK 2020/219).

Results

In total, 892 ophthalmologists answered the questionnaire, and 660 participants who were actively performing intravitreal injections were included in the study. The institutions of the participants are presented in Table 1.

Considering the current reimbursement restrictions, 58.3% (332/570) of the participants used bevacizumab as a first-line agent in patients with DME (Figure 1). The participants' preference for bevacizumab varied between institutions (Table 2). Participants working in private offices were more likely to use aflibercept than bevacizumab (51.9%, 14/27 vs. 22.2%, 6/27).

Of the participants, 49.4% stated that they would prefer aflibercept as a first-line agent in patients with DME if there were no economic and reimbursement restrictions (Figure 2). Preferences for aflibercept were similar among institutions except in public hospitals (Table 3). Participants working in public hospitals preferred ranibizumab for patients with DME (43.8%, 21/48).

Considering the current reimbursement restrictions, over half of the participants (55.9%, 318/569) used bevacizumab as a first-line agent in patients with AMD (Figure 3). Bevacizumab was used in most institutions (Table 4). However, participants from private offices and foundation universities reported greater use of aflibercept for patients with AMD (51.9%, 14/27 and 59.4%, 19/32, respectively).

Most of the participants (61.7%, 350/567) stated that they would prefer aflibercept as first-line treatment for AMD if there were no economic and reimbursement restrictions (Figure 4).

Table 1. Demographics of the participants

Institutions	Number*	Percent
Private hospital	219/890	24.61
Private office	42/890	4.72
Public hospital	147/890	16.52
City hospital	48/890	5.39
University hospital	239/890	26.85
Training and research hospital	194/890	21.80
Foundation university	46/890	5.17

*Participants could choose more than one option

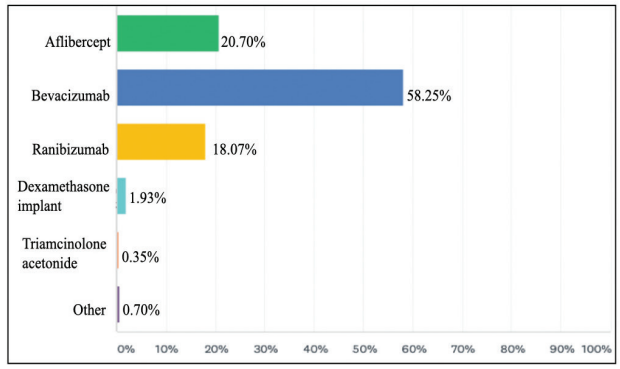

Figure 1. Ophthalmologists' preferences for anti-vascular endothelial growth factors and other agents in patients with diabetic macular edema under the current reimbursement restrictions

Under these circumstances, aflibercept was preferred for patients with AMD in all institutions (Table 5).

Over half the participants (52.3%, 297/568) used bevacizumab initially for patients with RVO under the current reimbursement restrictions. Participants in city hospitals (73.1%, 19/26), university hospitals (53.1%, 94/177), training and research hospitals (61.8%, 81/131), and private hospitals (53.2%, 84/158) mostly used bevacizumab, while the participants at foundation universities (31.3%, 10/32) and private offices (37.0%, 10/27) used aflibercept. However, participants in public hospitals preferred ranibizumab.

Overall, 35.5% of participants would prefer aflibercept as first-line therapy in patients with RVO if there were no economic and reimbursement restrictions. Participants in private hospitals (44.9%, 71/158), private offices (40.7%, 11/27), foundation universities (43.8%, 14/32), and training and research hospitals (38.9%, 51/131) mostly preferred aflibercept as a first-line agent. Participants in public hospitals mostly preferred ranibizumab (40.4%, 19/47), while dexamethasone implants were preferred as first-line treatment by those in city hospitals (53.9%, 14/26) and university hospitals (33.0%, 58/176).

Table 2. Preference for bevacizumab in patients with diabetic macular edema under the current reimbursement restrictions

Institutions	Number	Percent
Private hospital	90/159	56.60
Private office	6/27	22.22
Public hospital	22/48	45.83
City hospital	20/27	74.07
University hospital	103/178	57.87
Training and research hospital	91/131	69.47
Foundation university	13/32	40.63

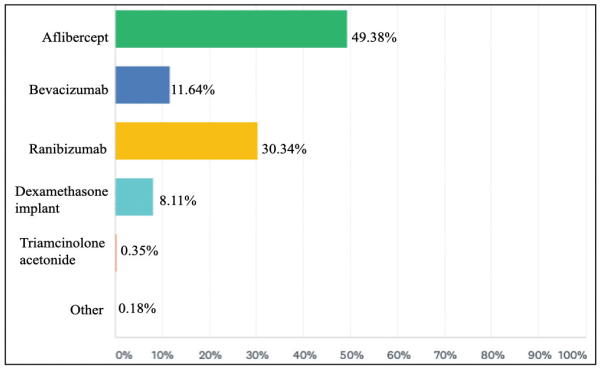

Figure 2. Ophthalmologists' preferences for anti-vascular endothelial growth factors and other agents in patients with diabetic macular edema if there were no economic and reimbursement restrictions

Table 3. Preference for aflibercept in patients with diabetic macular edema if there were no economic and reimbursement restrictions

Institutions	Number	Percent
Private hospital	**80/158**	**50.63**
Private office	17/27	62.96
Public hospital	14/48	29.17
City hospital	16/27	59.26
University hospital	82/176	46.59
Training and research hospital	73/131	55.73
Foundation university	17/31	54.84

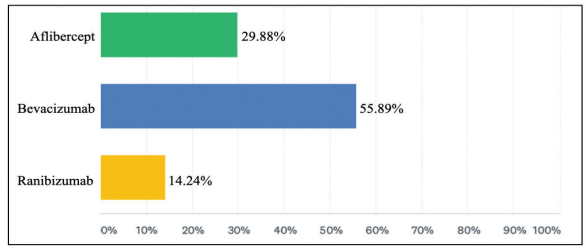

Figure 3. Ophthalmologists' use of anti-vascular endothelial growth factor agents in patients with age-related macular degeneration under the current reimbursement restrictions

Table 4. Preference for bevacizumab in patients with age-related macular degeneration under the current reimbursement restrictions

Institutions	Number	Percent
Private hospital	87/158	55.06
Private office	7/27	25.93
Public hospital	21/48	43.75
City hospital	19/27	70.37
University hospital	93/177	52.54
Training and research hospital	92/131	70.23
Foundation university	9/32	28.13

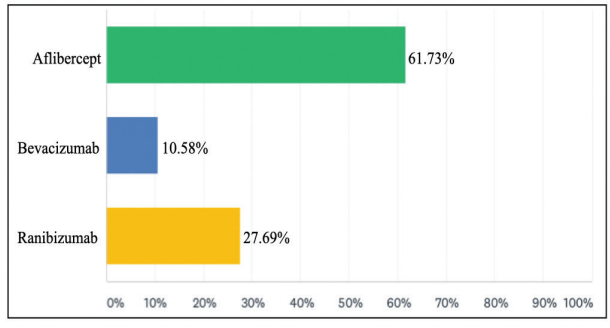

Figure 4. Ophthalmologists' preferences for anti-vascular endothelial growth factor agents in patients with age-related macular degeneration if there were no economic and reimbursement restrictions

Most of the participants (75.8%, 431/569) stated that dispensing multiple syringes from a single bevacizumab bottle could increase the risk of endophthalmitis (private hospitals: 59.5% [94/158]; private offices: 73.1% [19/26], public hospitals: 80.9% [38/47], city hospitals: 80.8% [21/26], university hospitals: 81.5% [145/178], training and research hospitals: 84.1% [111/132], and foundation universities: 78.1% [25/32]). However, 47.1% of the participants reported that they dispense multiple syringes from a single bevacizumab bottle (Table 6).

In addition, less than half (48.2%) of the participants stated that they did not feel under pressure to use a single bevacizumab bottle for more than one patient. The percentages of participants who felt pressure to use a single bevacizumab bottle on several patients are presented in Table 7. Unlike participants in other institutions, those in training and research hospitals were under greater pressure to use a single bevacizumab bottle for more than one patient (47.7%, 63/132). However, 16.2% of the participants did not use bevacizumab.

Some participants (25.6%) noted that they did not use bevacizumab while an approved anti-VEGF drug was available for that indication. Most of the participants (93.7%, 534/570) stated that they did not feel legally safe from harm caused by off-label bevacizumab use.

Overall, 66.4% (376/566) of participants stated that bevacizumab is as effective as other anti-VEGF drugs. In contrast, 60.6% of the participants stated that they think aflibercept is more effective and safer than other anti-VEGF agents (bevacizumab and ranibizumab) in patients with AMD, RVO, and DME (Table 8). However, participants in public hospitals stated that they think ranibizumab is more effective and safer than other anti-VEGFs (38.3%, 18/47).

Table 5. Preference for aflibercept in patients with age-related macular degeneration if there were no economic and reimbursement restrictions

Institutions	Number	Percent
Private hospital	95/157	60.51
Private office	16/27	59.26
Public hospital	23/48	47.92
City hospital	18/27	66.67
University hospital	100/176	56.82
Training and research hospital	90/131	68.70
Foundation university	26/32	81.25

Table 6. Participants who dispense multiple syringes from a single bevacizumab bottle

Institutions	Number	Percent
Private hospital	90/157	57.32
Private office	6/27	22.22
Public hospital	23/47	48.94
City hospital	8/26	30.77
University hospital	72/177	40.68
Training and research hospital	66/130	50.77
Foundation university	11/32	34.38

Discussion

Due to the necessity of using bevacizumab for the first three loading doses under the current reimbursement restrictions in our country, most ophthalmologists prefer bevacizumab as first-line therapy in patients with DME, RVO, and AMD. However, when reimbursement restrictions were not considered, ophthalmologists' drug preferences differed. Many participants working in private offices and foundation universities did not prefer bevacizumab as first-line therapy.

Diabetic Macular Edema

In Turkey, ophthalmologists utilize anti-VEGF injections as first-line therapy to treat DME. Due to the current reimbursement restrictions, 58.3% of ophthalmologists stated that they use bevacizumab as a first-line therapy in DME. However, participants working in private offices preferred aflibercept (51.9%). This may be related to the better socioeconomic level of the patients who receive service from private offices and the higher compliance of ophthalmologists with their drug preference. Nearly half (49.8%) of all the participants would prefer aflibercept if there was no reimbursement limitation.

Table 7. Participants who feel pressure to use a single bevacizumab bottle for several patients

Institutions	Number	Percent
Private hospital	36/156	23.08
Private office	3/27	11.11
Public hospital	18/47	38.30
City hospital	11/26	42.31
University hospital	73/178	41.01
Training and research hospital	63/132	47.73
Foundation university	7/32	21.88

Table 8. Participants who consider aflibercept more effective and safer in patients with age-related macular degeneration, retinal vein occlusion, and diabetic macular edema than other anti-vascular endothelial growth factor agents (bevacizumab and ranibizumab)

Institutions	Number	Percent
Private hospital	106/157	67.52
Private office	15/25	60.00
Public hospital	19/47	40.43
City hospital	17/26	65.38
University hospital	94/175	57.71
Training and research hospital	84/132	63.63
Foundation university	24/31	77.42

In the 2019 American Society of Retina Specialists (ASRS) global trends survey, most of the participants (Africa/Middle East: 74.0%; Asia/Pacific: 33.7%; and United States: 65.8%) used bevacizumab for initial treatment of DME based on the Diabetic Retinopathy Clinical Research Network (DRCR.net) Protocol T 2-year results.[8] However, in the same survey, European participants (39.8%) and Central and South American participants (33.6%) preferred aflibercept for patients with DME. The use of off-label drugs, cost effectiveness, and changing reimbursement policies of states may be the reasons for this difference. In the United States, 65.8% of ASRS participants preferred bevacizumab as a first-line agent for patients with DME. However, in the 2020 ASRS global trends survey, 57.8% of retina specialists in the United States chose aflibercept (pre-filled syringe [PFS]) for their own center-involving DME.[9] Similarly, in Europe, the preference of aflibercept increased from 39.8% for patients with DME in 2019 to 47.6%+20.7% (PFS+vial) for retina specialists' own center-involving DME in 2020.

In addition, 49.4% of the ophthalmologists in our study preferred aflibercept for the treatment of DME when reimbursement restrictions are not considered. This may be due to the doctors' desire to reduce the treatment burden (number of injections) with aflibercept. However, unlike in other institutions, participants in public hospitals (43.8%) preferred ranibizumab for the treatment of DME. The higher preference for ranibizumab may be due to the use of PFSs to reduce the risk of endophthalmitis. The use of a PFS eliminates most of the steps in injection preparation (aseptic), thereby reducing the risk of contamination.[10,11] The participants in public hospitals may prefer to use PFSs due to the lack of equipment and the lack of retina specialists to manage endophthalmitis complications that may occur after intravitreal injection.

Age-related Macular Degeneration

Anti-VEGF therapy is the current treatment for AMD. Under current reimbursement policies, bevacizumab was preferred for AMD treatment in all institutions except private offices and foundation universities. When restrictions were not considered, 61.7% of the participants stated that they would use aflibercept as the first-line therapy for AMD. In the 2020 ASRS global trends survey, 60.6% of American retina specialists stated that aflibercept delivers the most effective fluid resolution in wet AMD.[9] The participants may have thought that aflibercept is more effective for the treatment of standard AMD patients. The eight-week dosing regimen of aflibercept represents reduced treatment requirements in comparison with monthly dosing regimens and thus has the potential to reduce the treatment burden and risks associated with frequent injections.

In European countries, the usage of off-label bevacizumab for the treatment of AMD and associated cost vary from country to country.[12] The intravitreal administration of bevacizumab has also been a matter of legal dispute in European countries. Moreover, the specific factors influencing medication choice appear to go beyond clinical considerations. The controversy over the ophthalmic off-label use of bevacizumab remains remarkably unresolved within the world's largest single market. In the United States, 70.2% of American retina specialists use bevacizumab as the first-line anti-VEGF.[13]

Retinal Vein Occlusion

In this survey, no consensus among ophthalmologists was observed for the treatment of RVO when economic and reimbursement restrictions were ignored. According to the 2019 Euretina RVO guideline, intravitreal anti-VEGF therapy has become the standard of care for treating this disease.[14] According to the guideline, corticosteroids are important in the armamentarium of drugs for treating patients with RVO, but largely as a second choice. In the 2015 ASRS global trends survey, retina specialists primarily used anti-VEGF agents for the treatment of RVO.[15]

Use of Bevacizumab

Of the total participants, 93.7% stated that they did not feel that it was legally safe to use off-label bevacizumab. The legal safety of off-label bevacizumab use is also unclear in European countries.[12] Considering the current reimbursement restrictions in Turkey, it can be understood why the participants do not feel that it is safe. According to the Off-Label Drug Use guideline, "In our country, off-label drug use is not allowed for diseases that can be treated with medication within an approved indication. However, if there are treatment options that provide significant advantages according to scientific data, the request for off-label drug use is evaluated by the Institution."[16] However, the requirement of three doses of bevacizumab for reimbursement before the use of approved anti-VEGF drugs leaves ophthalmologists in a dilemma.

No large-scale prospective randomized clinical trial has been conducted showing that bevacizumab is superior to the approved anti-VEGF drugs (aflibercept and ranibizumab). The Protocol T study was the only randomized controlled clinical trial that compared bevacizumab with other approved anti-VEGFs for the treatment of DME. In the Protocol T study, aflibercept had superior 2-year visual acuity outcomes compared with bevacizumab among eyes with baseline visual acuity of 20/50 to 20/320, and bevacizumab was not superior to aflibercept and ranibizumab under any circumstances.[17] The superiority of aflibercept over ranibizumab has also not been verified.

Moreover, 75.8% of participants believed that dispensing multiple syringes from a single bevacizumab vial could increase the risk of endophthalmitis and 35.6% felt pressured to use a single bevacizumab bottle for more than one patient, although the reimbursement restrictions are not clear regarding dispensing multiple syringes from a single bevacizumab bottle. The multiple use of bevacizumab from a single bottle remains

a matter of debate. Ng et al.[18] reused vials for a maximum of 10 consecutive injections in their trial and concluded that as long as proper sterile techniques are implemented, using the same vial does not increase the risk of endophthalmitis from intravitreal injections. Das et al.[19] stated that bevacizumab does not lose stability when stored at 4°C and may be used for a week by direct withdrawal from the vial without fear of infection or inflammation if all standard precautions related to intravitreal injection are adhered to. Ornek et al.[20] stated that the storage and reuse of bevacizumab do not seem to result in microbial contamination, and multiple doses of bevacizumab from a single-use vial could be used within 2 weeks. However, an endophthalmitis outbreak in a university hospital was caused by dividing the same single-use bevacizumab into multiple doses. In fact, several endophthalmitis cases have been reported in association with splitting bevacizumab from a single bottle.[21]

Conclusion

Bevacizumab is widely used as a first-line treatment for all indications of anti-VEGF, and reimbursement conditions preclude ophthalmologists' right to treat patients according to their own preferences. Given the current reimbursement situation, it is not possible for doctors to freely choose a patient-specific treatment.

Acknowledgements: The authors express their appreciation to the Turkish Ophthalmological Association for their support. The authors would like to thank Dr. İzzet Can for his support.

Ethics

Ethics Committee Approval: The research protocol was approved by the Institutional Ethics Committee and Review Board of Kocaeli University (number: KAEK 2020/219).

Informed Consent: Obtained.

Peer-review: Externally peer reviewed.

Authorship Contributions

Surgical and Medical Practices: V.L.K., E.Ö.T., Concept: V.L.K., E.Ö.T., Design: V.L.K., E.Ö.T., Data Collection or Processing: V.L.K., E.Ö.T., Analysis or Interpretation: V.L.K., E.Ö.T., F.Ş., Literature Search: V.L.K., E.Ö.T., Writing: V.L.K., E.Ö.T., F.Ş.

Conflict of Interest: No conflict of interest was declared by the authors.

Financial Disclosure: The authors declared that this study received no financial support.

References

1. Nguyen QD, Brown DM, Marcus DM, Boyer DS, Patel S, Feiner L, Gibson A, Sy J, Rundle AC, Hopkins JJ, Rubio RG, Ehrlich JS; RISE and RIDE Research Group. Ranibizumab for diabetic macular edema: results from 2 phase III randomized trials: RISE and RIDE. Ophthalmology. 2012;119:789-801.
2. Scott IU, VanVeldhuisen PC, Ip MS, Blodi BA, Oden NL, Awh CC, Kunimoto DY, Marcus DM, Wroblewski JJ, King J; SCORE2 Investigator Group. Effect of Bevacizumab vs Aflibercept on Visual Acuity Among Patients With Macular Edema Due to Central Retinal Vein Occlusion: The SCORE2 Randomized Clinical Trial. JAMA. 2017;317:2072-2087.
3. Diabetic Retinopathy Clinical Research Network, Elman MJ, Aiello LP, Beck RW, Bressler NM, Bressler SB, Edwards AR, Ferris FL 3rd, Friedman SM, Glassman AR, Miller KM, Scott IU, Stockdale CR, Sun JK. Randomized trial evaluating ranibizumab plus prompt or deferred laser or triamcinolone plus prompt laser for diabetic macular edema. Ophthalmology. 2010;117:1064-1077.
4. Brown DM, Kaiser PK, Michels M, Soubrane G, Heier JS, Kim RY, Sy JP, Schneider S; ANCHOR Study Group. Ranibizumab versus verteporfin for neovascular age-related macular degeneration. N Engl J Med. 2006;355:1432-1444.
5. Highlights of Prescribing Information: Avastin 2017 [cited 2021 March 20] Available at: https://www.accessdata.fda.gov/scripts/cder/daf/index.cfm?event=overview.process&ApplNo=125085.
6. Cohen D. Why have UK doctors been deterred from prescribing Avastin? BMJ. 2015;350:h1654.
7. Önder Tokuç E, Karabaş VL, Şermet F. Survey of Intravitreal Injection Techniques and Treatment Protocols Among Members of the Turkish Ophthalmological Association. Turk J Ophthalmol. 2021;51:373-380.
8. Singh RP. 2019 Global Trends in Retina Survey, Available at: https://www.asrs.org/content/documents/2019-global-trends-survey-for-website.pdf [cited 2021 March 20].
9. Eliot D. 2020 Global Trends in Retina Survey, Available at: https://www.asrs.org/content/documents/2020-global-trends-in-retina-survey-highlights-for-website.pdf [cited 2021 March 20].
10. Subhi Y, Kjer B, Munch IC. Prefilled syringes for intravitreal injection reduce preparation time. Dan Med J. 2016;63:A5214.
11. Michaud JE, Sigg J, Boado L, Momm J, Weber C, Alete D, Peregi E, Picci M. Ranibizumab pre-filled syringe approved in the European union: innovation to improve dose accuracy, reduce potential infection risk, and offer more efficient treatment administration. Invest Ophthalmol Vis Sci. 2014;55:1949.
12. Bro T, Derebecka M, Jørstad ØK, Grzybowski A. Off-label use of bevacizumab for wet age-related macular degeneration in Europe. Graefes Arch Clin Exp Ophthalmol. 2020;258:503-511.
13. Singh RP. 2018 Global Trends in Retina Survey, Available at: https://www.asrs.org/content/documents/2018-global-trends-in-retina-survey-highlights-website.pdf [cited 2021 March 20].
14. Schmidt-Erfurth U, Garcia-Arumi J, Gerendas BS, Midena E, Sivaprasad S, Tadayoni R, Wolf S, Loewenstein A. Guidelines for the Management of Retinal Vein Occlusion by the European Society of Retina Specialists (EURETINA). Ophthalmologica. 2019;242:123-162.
15. Rezaei KA. 2015 Global Trends in Retina Survey 2015, Available at: https://www.asrs.org/content/documents/2015_global_trends_in_retina_survey_-_for_website.pdf [cited 2021 March 20].
16. Republic of Turkey Ministry of Health. Turkish Medicines and Medical Devices Agency. Available at: https://www.titck.gov.tr/mevzuat/endikasyon-disi-ilac-kullanimi-kilavuzu-27122018172948
17. Wells JA, Glassman AR, Ayala AR, Jampol LM, Bressler NM, Bressler SB, Brucker AJ, Ferris FL, Hampton GR, Jhaveri C, Melia M, Beck RW; Diabetic Retinopathy Clinical Research Network. Aflibercept, Bevacizumab, or Ranibizumab for Diabetic Macular Edema: Two-Year Results from a Comparative Effectiveness Randomized Clinical Trial. Ophthalmology. 2016;123:1351-1359.
18. Ng DS, Kwok AK, Chan CW, Li WW. Intravitreal bevacizumab: safety of multiple doses from a single vial for consecutive patients. Hong Kong Med J. 2012;18:488-495.

19. Das T, Volety S, Ahsan SM, Thakur AK, Sharma S, Padhi TR, Basu S, Rao ChM. Safety, sterility and stability of direct-from-vial multiple dosing intravitreal injection of bevacizumab. Clin Exp Ophthalmol. 2015;43:466-473.
20. Ornek K, Karahan ZC, Ergin A, Tekeli A, Tekeli O. Bevacizumab sterility in multiple doses from a single-use vial. Ann Pharmacother. 2008;42:1425-1428.
21. Khan P, Khan L, Mondal P. Cluster endophthalmitis following multiple intravitreal bevacizumab injections from a single use vial. Indian J Ophthalmol. 2016;64:694-696.

DOI: 10.4274/tjo.galenos.2021.33581
Turk J Ophthalmol 2022;52:186-192

Original Article

Comparison of Reading Test Parameters from the Print and Tablet Application Forms of the Minnesota Low Vision Reading Test

Deniz Altınbay*,**,***, Esra Şahlı**,***, Şefay Aysun İdil**

*Private NivEye Center, Adana, Turkey
**Ankara University Faculty of Medicine, Department of Ophthalmology, Vision Studies and Low Vision Rehabilitation Unit, Ankara, Turkey
***Ankara University Graduate School of Health Sciences, Ankara, Turkey

Abstract

Objectives: To compare reading parameters measured with the Turkish version of the Minnesota Low Vision Reading Test (MNREAD-TR) printed acuity chart and the tablet application version of the same test for both normally sighted and low-vision individuals.

Materials and Methods: A total of 116 individuals (92 normally sighted and 24 low-vision) were included in the study. All participants were tested with both the print version of the MNREAD-TR chart (method 1) and the tablet application version (method 2). Reading acuity (RA), critical print size (CPS), maximum reading speed (MRS), and reading accessibility index (ACC) were compared statistically.

Results: No statistically significant difference was found in RA and CPS between the two methods for the normally sighted individuals ($p=0.083$ and $p=0.075$, respectively). There was no statistically significant difference in RA and ACC between the two methods for the patients with low vision ($p=0.159$ and $p=0.103$, respectively). The mean MRS was 233.1±34.7 words per minute (wpm) with method 1 and 169.3±23.4 wpm with method 2 in the normally sighted group ($p<0.001$) and 93.2±50.2 wpm with method 1 and 68.2±34.7 wpm with method 2 in the low-vision group ($p<0.001$).

Conclusion: In our study, it was found that the parameters RA and CPS in the normally sighted individuals and RA and ACC in the low vision individuals provided similar results in both forms of the MNREAD. The tablet application method can be preferred to eliminate evaluators' bias of scoring the printed chart. In addition, applications have other advantages such as being faster and more practical and providing automatic analysis of parameters, especially in low-vision rehabilitation.

Keywords: Low vision rehabilitation, MNREAD, near vision examination, reading acuity, reading speed

Address for Correspondence: Deniz Altınbay, Private NivEye Center, Adana, Turkey
E-mail: denizaltinbay01@gmail.com **ORCID-ID:** orcid.org/0000-0002-3976-4361
Received: 25.02.2021 **Accepted:** 22.06.2021

Cite this article as: Altınbay D, Şahlı E, İdil ŞA. Comparison of Reading Test Parameters from the Print and Tablet Application Forms of the Minnesota Low Vision Reading Test. Turk J Ophthalmol 2022;52:186-192

Introduction

Reading ability is a strong determinant of quality of life.[1,2,3] According to the results of the Wilmer Eye Institute Vision Rehabilitation Department, the chief complaint in 64% of all low-vision patients is reading difficulty.[4] Therefore, it is crucial to measure reading performance in low-vision individuals. Minnesota Low Vision Reading (MNREAD) acuity charts are text-based charts used to assess near vision and reading speed in individuals with normally sight and low vision.[5]

Several versions of the MNREAD acuity charts have been prepared in various languages.[6] The Turkish version (MNREAD-TR) was created by Idil et al.[7] MNREAD acuity charts are widely used in evaluating reading ability.[8] However, the examiner is responsible for counting errors, calculating MNREAD parameters, and timing reading speed, leading to potential scoring subjectivity and detection bias. Standardization is necessary to achieve objective and repeatable measurements, especially for individuals with low vision.[9,10,11] Technological developments have provided promising opportunities to solve such problems. For instance, the use of tablets for medical screening tests has drawn interest to digital reading.[12,13] The ease of access to tablets created an opportunity to perform MNREAD tests with an iPad application. An MNREAD iPad application has been introduced for clinical use to standardize the measurement of reading parameters and make the test more practical.[9,14] Calabrèse et al.[14] created a digital version of the MNREAD charts to be used with the MNREAD iPad App ©2017. They compared MNREAD parameters from the printed acuity chart and the iPad application and reported similar results for both methods in normally sighted and low-vision individuals. They concluded that the MNREAD application would be useful for the standardization of the results.

In this study, we aimed to evaluate whether the consistency between the MNREAD chart and MNREAD iPad application previously reported for the original form also exists in different language versions. For this purpose, we planned to conduct a similar study for the MNREAD-TR in normally sighted and low-vision individuals. The findings of this evaluation will help us determine whether we can use the tablet application, which seems to be a more practical method, instead of the conventional printed method for the assessment of reading parameters in patients presenting to low vision rehabilitation centers.

Materials and Methods

The study included a total of 116 participants, 92 normally sighted and 24 low-vision individuals, and was carried out in the Ankara University Faculty of Medicine Vision Research and Low Vision Rehabilitation Center. All participants were tested with both the printed form of the MNREAD-TR chart and the tablet application form (MNREAD iPad App ©2017) and the MNREAD parameter results obtained with the two methods were compared. Participants in the normally sighted group had visual acuity of 0.00 logMAR with or without refractive correction and had no reported cognitive or reading impairment. Participants in the low-vision group had various diagnoses and visual acuity levels but no cognitive impairment or reading deficit diagnosis reported in previous examinations. The native language of all participants was Turkish. Ethics committee approval was received before study initiation and participant enrollment. An informed consent form was obtained from all participants. The study was conducted in accordance with the Helsinki Declaration.

In the printed form of MNREAD, there are 19 sentences with print sizes ranging from 8 M to 0.12 M (according to the M unit, 1 M=8 points), corresponding to a largest print size of 1.3 logMAR and smallest print size of -0.5 logMAR. Each sentence consists of 60 characters and the print size decreases by 0.1 logMAR with each consecutive sentence. The values on the chart are adjusted for a viewing distance of 40 cm. However, for those with low vision, there is a correction table that enables testing at varying distances. The cards have white-on-black and black-on-white polarities. This study used the MNREAD-TR, and four parameters of reading performance were assessed. The first three parameters were reading acuity (RA; the smallest print size that can be read without making a significant mistake), critical print size (CPS; the smallest print size that can be read with maximum reading speed), and maximum reading speed (MRS; reading speed irrespective of print size).[5] Reading accessibility index (ACC) is a new parameter defined in 2016.[15] ACC is calculated by dividing the reading speed obtained in the first 10 sentences of the MNREAD chart by 200. These sentences represent the most frequently used print sizes in daily life. As normal reading speed corresponds to 200 wpm, the normal ACC value is 1. This parameter represents the visual accessibility of commonly encountered printed material, where 0 means no accessible print and 1 means average normal accessibility.[15,16,17] With the printed form, the practitioner records reading time, number of errors, and reading distance. Therefore, the examiner is responsible for calculating the four MNREAD parameters.

The MNREAD tablet application developed for the iPad by the University of Minnesota also includes a Turkish version. For the print and tablet application forms, different sentences meeting the standard guidelines were chosen from a previously prepared sentence pool. This application can be run on third-generation or later iPads and requires a minimum of iOS 7.0 operating system (http://www.precision-vision.com/product/mnreadchart1). For now, the tablet form of MNREAD is only available on iOS operating systems while the MNREAD Android application is still in development.

To assess the performance of the MNREAD iPad application in routine clinical practice, two questions need to be answered: Are automatic results obtained from the MNREAD iPad application consistent with those obtained from the printed MNREAD chart? What can be done for problems caused by screen size and screen resolution? For the second question,

Calabrèse et al.[14] suggested changing the reading distance and reducing the number of sentences in the test to solve these limitations with the iPad app. Due to screen size and resolution limitations in the tablet method, the first sentence and the last 4 sentences were removed and a total of 14 sentences were used.[14] Print sizes are between 1.2 and -0.1 logMAR (6.3M-0.32M). For each presentation, a sentence from the pool prepared for MNREAD is selected and displayed centered on the screen in Times New Roman font (Figure 1).

With normally sighted participants, the printed MNREAD chart was tested at a distance of 40 cm. For the tablet application method, the test distance was extended to 80 cm to compensate for the smaller print size range.[14] The individuals with low vision were tested at their preferred distance for both methods and the reading distance was recorded. In both groups, the preferred distance was adjusted according to the 4th largest print size.[14] The test was done with black-on-white polarity for both methods. All participants underwent a near vision examination before the test. Different sentence sets were used for the chart and the application to eliminate the bias of participants' remembering the sentences read in the previous method.

During the test with the printed MNREAD chart, an additional light source was directed at the paper (using a 200 cd/m² table lamp) in addition to the ceiling light.[18] The room lighting was 300 lux, while the MNREAD iPad application was set to a brightness of 200 cd/m^2. Sentences were displayed once in both methods and the participants were asked to read the sentences out loud as quickly and accurate as possible until they reached a print size at which no words could be read. The practitioner measured the reading time with a stopwatch and recorded the number of incorrect/missing words for each sentence of the printed MNREAD chart test. MNREAD parameter calculation was performed by the same examiner (D.A.).

The tablet application method was implemented using the MNREAD iPad App (©2017) on an iPad with Retina display (MP2F2TU/A, 32 GB, 9.7 inches, 5th generation, 264 pixels/inch or 104 pixels/cm resolution, LED, backlit) held horizontally. The overhead light was kept on, with no additional lighting and the iPad set to 200 cd/m^2. This light level was not strong enough to disturb low-vision patients with albinism and cone dystrophy. None of the participants with these diagnoses stated that they were uncomfortable with the light level or needed to reduce the light to see better. Incorrect/missing words were recorded by the practitioner and the graphs of the parameters were generated automatically by the application. The reading speed curve for normally sighted individuals is similar in general (Figure 2). However, that standard curve cannot be drawn when measuring reading speed in individuals with low vision (Figure 3).[9]

In this experimental study, the paired samples t-test/Wilcoxon signed-rank test was used to compare the two testing methods. Bland-Altman plots were used for comparative analysis of MNREAD chart/application performance. IBM SPSS Statistics Version 20.0 (IBM Corp, Armonk, NY, USA) statistical software package was used for all statistical analyses. Statistical significance was accepted as $p<0.05$ for all tests.

Results

The normally sighted group consisted of 92 people (37 males and 55 females) with a mean age of 26.24±5.97 years (median, 25). The low-vision group consisted of 24 people (12 males and 12 females) with a mean age of 50.92±29.45 years (median, 57). Of the low-vision individuals, 13 (54%) had age-related macular degeneration (AMD), 7 (29%) had albinism, and 4 (17%) had cone dystrophy. The mean distance visual acuity in this group was 0.73±0.20 logMAR (0.21±0.09 decimal).

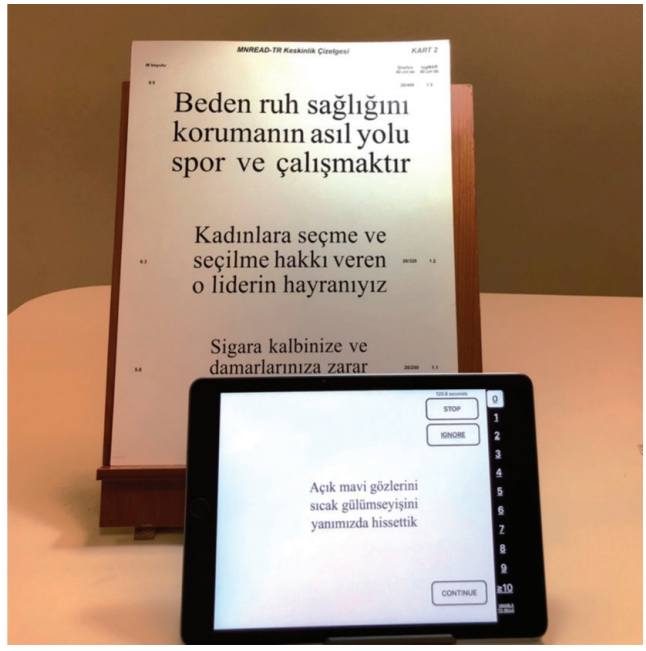

Figure 1. The printed and the tablet application forms of the Turkish version of the Minnesota Low Vision Reading (MNREAD) charts (with the permission of Aysun İdil)

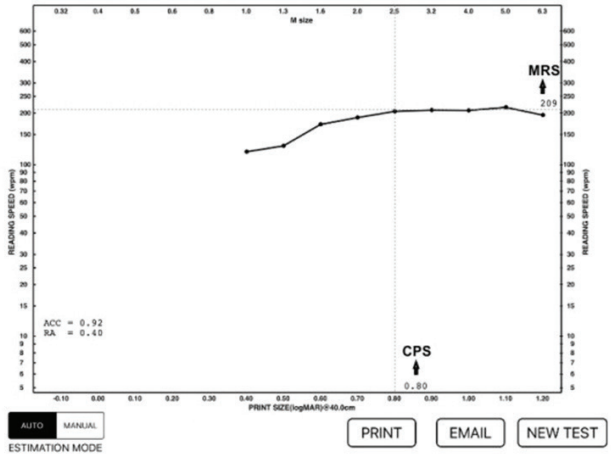

Figure 2. An example of the MNREAD curve of a normally sighted participant with RA = 0.40 logMAR CPS = 0.80 logMAR, ACC = 0.92, and MRS = 209 wpm. Reading speed shows a plateau
RA: Reading acuity, CPS: Critical print size, ACC: Reading accessibility index, MRS: Maximum reading speed

The reading parameter values of individuals with normal vision obtained by printed chart and tablet application are shown in Table 1. No statistically significant difference was found in RA and CPS between the methods (p=0.083 and p=0.075, respectively). However, MRS and ACC differed significantly between the methods (p<0.001 for both) (Table 1). The mean MRS was signiŞcantly faster in the chart method (2.36 logWPM, 95% confidence interval [CI]: 2.35-2.38) than in the tablet application method (2.22 logWPM, 95% CI: 2.21-2.24) (Figure 4). The mean ACC was significantly higher with the chart (1.19, 95% CI: 1.16-1.23) than the application (0.86, 95% CI: 0.83-0.88) in normally sighted individuals (p<0.001 for both).

The reading parameter values obtained with the two methods in individuals with low vision are shown in Table 2. There was no statistically significant difference in RA and ACC between the methods (p=0.159 and p=0.103, respectively), while MRS and CPS differed significantly (p<0.001 and p=0.015, respectively) (Table 2). The mean MRS was significantly faster with the printed chart method (1.89 logWPM, 95% CI: 1.78-2.01) than with the tablet application (1.77 logWPM, 95% CI: 1.68-1.87) (Figure 5). The mean CPS was found to be statistically higher with the chart (1.19, 95% CI: 1.16-1.23) than the application (0.86, 95% CI: 0.83-0.88) in low-vision individuals (p<0.001 for both).

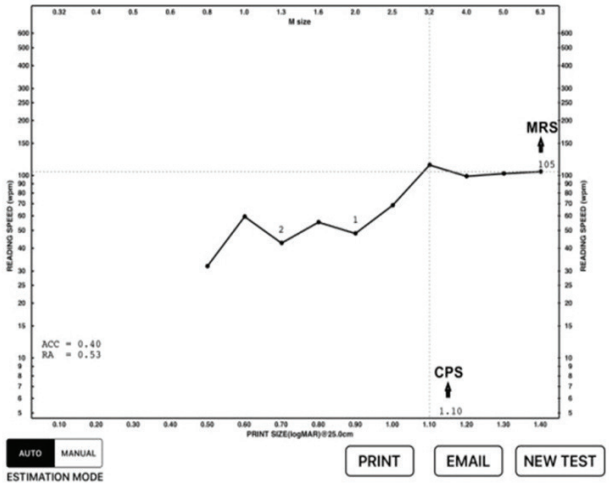

Figure 3. An example of the MNREAD curve of a low vision participant with RA = 0.53 logMAR, CPS = 1.10 logMAR, ACC = 0.40, and MRS = 105 wpm. Reading speed does not plateau
RA: Reading acuity, CPS: Critical print size, ACC: Reading accessibility index, MRS: Maximum reading speed

Discussion

Assessment of reading performance in low-vision rehabilitation is important for determining reading aids and rehabilitation strategies and monitoring the rehabilitation process.[19] Calabrèse et al.[14] compared the results obtained from the printed MNREAD chart and tablet application and found them to be consistent. Our study is a similar study using the Turkish version of MNREAD. In this study, RA results were similar with both methods in individuals with normal vision and low vision. RA and ACC results, which are important for near visual rehabilitation, were similar in individuals with low vision. This suggests that the MNREAD tablet application may be especially useful in the low-vision rehabilitation setting. The MNREAD

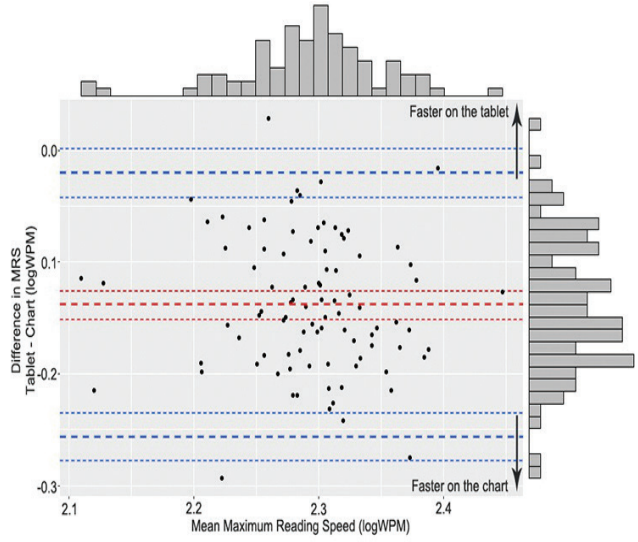

Figure 4. Comparison of the maximum reading speed (MRS) in the MNREAD tablet application and printed forms in the normally sighted group. Bland-Altman plots show the difference between measured MRS plotted against the mean MRS in normally sighted individuals. The red dashed lines show the average difference and the blue dashed lines show the limits of agreement (±1.96 SD). The dotted lines represent the 95% confidence interval

Table 1. Comparison of MNREAD parameters in the printed and the tablet application form in the normally sighted group

	MRS (WPM)	MRS (logWPM)	ACC	RA (logMAR)	CPS (logMAR)
Printed form	233.1±34.7	2.36±0.07	1.19±0.17	-0.04±0.10	0.06±0.10
Tablet form	169.3±23.4	2.22±0.06	0.86±0.11	-0.01±0.20	0.11±0.30
p-value	<0.001	<0.001	<0.001	0.083	0.075

WPM: Words per minute, MRS: Maximum reading speed, ACC: Reading accessibility index, RA: Reading acuity, CPS: Critical print size

Table 2. Comparison of MNREAD parameters in the printed and the tablet application form of MNREAD in the low-vision group					
	MRS (WPM)	**MRS (logWPM)**	**ACC**	**RA (logMAR)**	**CPS (logMAR)**
Printed form	93.2±50.2	1.89±0.29	0.39±0.29	0.77±0.27	0.88±0.21
Tablet form	68.2±34.7	1.77±0.24	0.33±0.16	0.70±0.27	0.71±0.31
p-value	<0.001	<0.001	**0.103**	**0.159**	0.015
WPM: Words per minute, MRS: Maximum reading speed, ACC: Reading accessibility index, RA: Reading acuity, CPS: Critical print size					

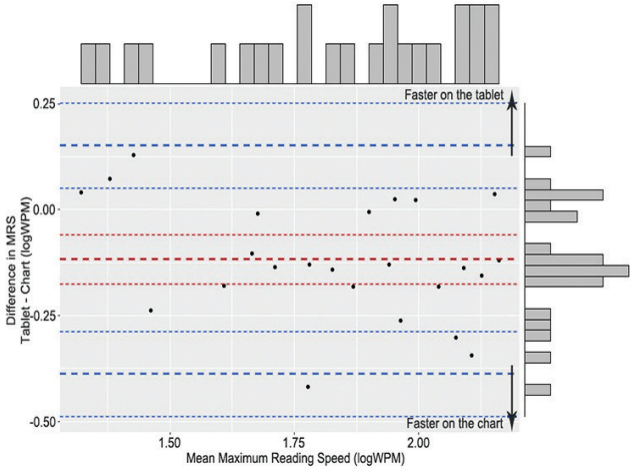

Figure 5. Comparison of the maximum reading speed (MRS) in the low vision group in the printed and the tablet application forms of MNREAD. Bland-Altman plots show the difference between measured MRS plotted against the mean MRS in low-vision individuals. The red dashed lines show the average difference and the blue dashed lines show the limits of agreement (±1.96 SD). The dotted lines represent the 95% confidence interval

iPad application has advantages such as being practical and fast, offering two polarities and different language options, recording reading speed, displaying graphical results, estimating the MNREAD curve, providing MNREAD parameter calculations, and saving and sharing the data.[20] These advantages increase the possibility of using the MNREAD application.[14]

There are limited studies in the literature regarding the use of tablets in near vision examinations. Varadaraj et al.[21] compared the results of tablet-based tests and MNREAD acuity chart test in near visual acuity test and found that the RA values were consistent. Although the results of their study are valuable, parameters other than RA were not considered. Calabrèse et al.[14] evaluated all parameters of the MNREAD reading test. Reading speed is generally considered the primary parameter in the studies investigating reading performance.[22,23] Calabrèse et al.[14] found higher MRS values with the printed charts than with the tablet application in the normally sighted group, and the difference was greater in those with high MRS. They attributed the difference in MRS values between printed and application methods to the difference in timing methods and suggested that a coefficient could be used to make the MRS results equivalent in two forms.[14] In their study, they determined this equivalence coefficient to be 1.1 for MRS results in the normally sighted group. In our study, we found that the MRS values were also higher with the printed chart compared to the application in both the normal-sighted and low-vision groups, with an equivalence coefficient of 1.37 in both groups. It was seen that this coefficient can also be used for ACC in the group with normal vision.

In the study by Calabrèse et al.,[14] there was no significant difference between RA estimated with the printed chart and with the application in the normally sighted group. In our study, the RA values were similar with both methods in both groups. Xiong et al.[24] reported that RA is a more important criterion for reading performance than measuring near visual acuity. Therefore, finding similar RA with both methods is important in terms of reading performance evaluation in near vision examination.

Calabrèse et al.[14] reported that CPS, MRS, and ACC values were similar but RA values were better with the tablet application in the low-vision group. In our study, we found that RA and ACC values were similar in the low-vision group. Contrary to previous results, in our study, CPS in the low-vision group was smaller in the tablet application method. We believe displaying the sentences one after the other may have prevented confusion.

The differences between studies may be associated with the fact that we used the Turkish version of MNREAD. Differences in reading speeds in various languages have been demonstrated using the International Reading Speed Test (IReST). In this study, the reading speed for the 18-35 age group was determined as 166 wpm for Turkish and 228 wpm for English.[25] The difference between the results may also be related to the different age ranges in the studies. In a study investigating the effect of age, education, and gender on reading speed, the average number of syllables read by participants aged 20-35 was found to be higher than the average number of syllables read by participants aged 46-55.[26] The age ranges in our study were 18-49 years in normally sighted individuals and 18-89 years in low-vision individuals, while those in the study by Calabrèse et al.[14] were 8-72 years in normal-sighted individuals and 22-93 years in low-vision individuals. Although the groups in our study differed in age, there was no between-group comparison. Each group was tested by two methods separately and the results obtained from the methods were compared.

It was reported that ACC is an important indicator of reading performance in daily life in people with low vision.[15,16,17] In our study, the similarity of ACC results with both methods among low-vision participants was particularly promising for the use of MNREAD tablet application in this group. Consistency in important parameters of reading performance (RA and ACC) between the tablet-based and chart-based forms of the MNREAD-TR version in individuals with low vision is critical in terms of increasing the use of MNREAD iPad application.

The main difference between the iPad application and the printed chart was reported to be related to the digital image of the text. However, through the design of the iPad application on the Retina display, reading speed was suggested to be largely equivalent to the printed chart. The disadvantage of a reduced range of print sizes in the application form has also been overcome by increasing the viewing distance.[14]

Measurement of visual performance is necessary at various stages, such as evaluating the patient's functional vision, disease progression, and evaluating the success of treatment or rehabilitation. We would like to emphasize the importance of using continuous text-based methods in measuring a person's visual performance. With its many advantages, the MNREAD tablet application also seems to be a good option for clinical practice.

Study Limitations

Some of the limitations of our study include the heterogenic distribution of diagnoses of low-vision patients, the small number of patients in the low-vision group, and the dissimilarity of patients in the low-vision group and the normal-vision group in terms of age and gender. However, we do not consider these limitations critical as the groups in the study were not compared to each other, but each group was evaluated within itself in terms of MNREAD parameters.

Conclusion

Our study contributes to the literature by expanding the evaluation of the MNREAD tablet application in a language other than English. According to our results, the MNREAD tablet application can be preferred especially in the low-vision group for RA and ACC results, which are the most important determinants of reading performance. The reading speed difference and coefficient of equivalence between the two methods should be investigated in further studies. Similar studies need to be planned for different languages, with more participants in specific groups with the same diagnosis and similar age range and visual acuity.

Ethics

Ethics Committee Approval: Ankara University Faculty of Medicine Clinical Research Ethics Committee /24.09.2018/ decision no: 15-1023-18.

Informed Consent: Obtained.

Peer-review: Externally peer reviewed.

Authorship Contributions

Surgical and Medical Practices: D.A., E.Ş., A.İ., Concept: D.A., E.Ş., A.İ.,

Design: D.A., Data Collection or Processing: D.A., E.Ş., Analysis or Interpretation: D.A., E.Ş., A.İ., Literature Search: D.A., E.Ş., Writing: D.A., E.Ş.

Conflict of Interest: No conflict of interest was declared by the authors.

Financial Disclosure: The authors declared that this study received no financial support.

References

1. Murro V, Sodi A, Giacomelli G, Mucciolo DP, Pennino M, Virgili G, Rizzo S. Reading Ability and Quality of Life in Stargardt Disease. Eur J Ophthalmol. 2017;27:740-745.
2. Kaltenegger K, Kuester S, Altpeter-Ott E, Eschweiler GW, Cordey A, Ivanov IV, Martus P, Knipp C, Trauzettel-Klosinski S. Effects of home reading training on reading and quality of life in AMD-a randomized and controlled study. Graefes Arch Clin Exp Ophthalmol. 2019;257:1499-1512.
3. Orr P, Rentz AM, Margolis MK, Revicki DA, Dolan CM, Colman S, Fine JT, Bressler NM. Validation of the National Eye Institute Visual Function Questionnaire-25 (NEI VFQ-25) in age-related macular degeneration. Invest Ophthalmol Vis Sci. 2011;52:3354-3359.
4. Rubin GS. Vision rehabilitation for patients with age-related macular degeneration. Eye (Lond). 2001;15:430-435.
5. Mansfield JS, Ahn S, Legge GE, Luebker A. A new reading-acuity chart for normal and low vision. Ophthalmic and Visual Optics/Noninvasive Assessment of the Visual System Technical Digest. 1993;3:232-235.
6. Virgili G, Cordaro C, Bigoni A, Crovato S, Cecchini P, Menchini U. Reading acuity in children: evaluation and reliability using MNREAD charts. Invest Ophthalmol Vis Sci. 2004;45:3349-3354.
7. İdil ŞA, Çalışkan D, İdil NB. The development and validation of MNREAD acuity charts in Turkish. Turk J Ophthalmol. 2009;39:84-90.
8. Subramanian A, Pardhan S. Repeatability of reading ability indices in subjects with impaired vision. Invest Ophthalmol Vis Sci. 2009;50:3643-3647.
9. Baskaran K, Macedo AF, He Y, Hernandez-Moreno L, Queirós T, Mansfield JS, Calabrèse A. Scoring reading parameters: An inter-rater reliability study using the MNREAD chart. PLoS One. 2019;14:e0216775.
10. Macedo AF, Nascimento SM, Gomes AO, Puga AT. Fixation in patients with juvenile macular disease. Optom Vis Sci. 2007;84:852-858.
11. Rubin GS. Measuring reading performance. Vision Res. 2013;90:43-51.
12. Berger E. The iPad: gadget or medical godsend? Ann Emerg Med. 2010;56:A21-A22.
13. Xu R, Bradley A. IURead: a new computer-based reading test. Ophthalmic Physiol Opt. 2015;35:500-513.
14. Calabrèse A, To L, He Y, Berkholtz E, Rafian P, Legge GE. Comparing performance on the MNREAD iPad application with the MNREAD acuity chart. J Vis. 2018;18:8.
15. Calabrèse A, Owsley C, McGwin G, Legge GE. Development of a Reading Accessibility Index Using the MNREAD Acuity Chart. JAMA Ophthalmol. 2016;134:398-405.
16. Tarita-Nistor L, González EG, Mandelcorn MS, Brent MH, Markowitz SN, Steinbach MJ. The reading accessibility index and quality of reading grid of patients with central vision loss. Ophthalmic Physiol Opt. 2018;38:88-97.
17. Latham K. Benefits of low vision aids to reading accessibility. Vision Res. 2018;153:47-52.
18. Black JM, Jacobs RJ, Phillips G, Chen L, Tan E, Tran A, Thompson B. An assessment of the iPad as a testing platform for distance visual acuity in adults. BMJ Open. 2013;3:e002730.
19. Erbezci M. Central Scotoma and Reading. Turkiye Klinikleri J Ophthalmol-Special Topics. 2015;8:136-142.

20. Patel PJ, Chen FK, Da Cruz L, Rubin GS, Tufail A. Test-retest variability of reading performance metrics using MNREAD in patients with age-related macular degeneration. Invest Ophthalmol Vis Sci. 2011;52:3854-3859.
21. Varadaraj V, Assi L, Gajwani P, Wahl M, David J, Swenor BK, Ehrlich JR. Evaluation of Tablet-Based Tests of Visual Acuity and Contrast Sensitivity in Older Adults. Ophthalmic Epidemiol. 2021;28:293-300.
22. Hamade N, Hodge WG, Rakibuz-Zaman M, Malvankar-Mehta MS. The Effects of Low-Vision Rehabilitation on Reading Speed and Depression in Age Related Macular Degeneration: A Meta-Analysis. PLoS One. 2016;11:e0159254.
23. Markowitz SN. Principles of modern low vision rehabilitation. Can J Ophthalmol. 2006;41:289-312.
24. Xiong YZ, Calabrèse A, Cheong AMY, Legge GE. Reading Acuity as a Predictor of Low-Vision Reading Performance. Invest Ophthalmol Vis Sci. 2018;59:4798-4803.
25. Trauzettel-Klosinski S, Dietz K; IReST Study Group. Standardized Assessment of Reading Performance: The New International Reading Speed Texts IReST. Invest Ophthalmol Vis Sci. 2012;53:5452-5461.
26. İyigün E, Bekircan M, Maviş İ. Effects of Age, Education and Gender on Reading Speed of Adults. Journal of Language, Speech and Swallowing Research (DKYAD). 2018;1:162-178.

DOI: 10.4274/tjo.galenos.2021.29726
Turk J Ophthalmol 2022;52:193-200

Original Article

Investigation of the Role of Convolutional Neural Network Architectures in the Diagnosis of Glaucoma using Color Fundus Photography

Eray Atalay*, Onur Özalp*, Özer Can Devecioğlu**, Hakika Erdoğan***, Türker İnce**, Nilgün Yıldırım*

*Eskişehir Osmangazi University Faculty of Medicine, Department of Ophthalmology, Eskişehir, Turkey
**İzmir University of Economics Faculty of Engineering, Department of Electrical and Electronics Engineering, İzmir, Turkey
***Maltepe University Faculty of Medicine, Department of Ophthalmology, İstanbul, Turkey

Abstract

Objectives: To evaluate the performance of convolutional neural network (CNN) architectures to distinguish eyes with glaucoma from normal eyes.

Materials and Methods: A total of 9,950 fundus photographs of 5,388 patients from the database of Eskişehir Osmangazi University Faculty of Medicine Ophthalmology Clinic were labelled as glaucoma, glaucoma suspect, or normal by three different experienced ophthalmologists. The categorized fundus photographs were evaluated using a state-of-the-art two-dimensional CNN and compared with deep residual networks (ResNet) and very deep neural networks (VGG). The accuracy, sensitivity, and specificity of glaucoma detection with the different algorithms were evaluated using a dataset of 238 normal and 320 glaucomatous fundus photographs. For the detection of suspected glaucoma, ResNet-101 architectures were tested with a data set of 170 normal, 170 glaucoma, and 167 glaucoma-suspect fundus photographs.

Results: Accuracy, sensitivity, and specificity in detecting glaucoma were 96.2%, 99.5%, and 93.7% with ResNet-50; 97.4%, 97.8%, and 97.1% with ResNet-101; 98.9%, 100%, and 98.1% with VGG-19, and 99.4%, 100%, and 99% with the 2D CNN, respectively. Accuracy, sensitivity, and specificity values in distinguishing glaucoma suspects from normal eyes were 62%, 68%, and 56% and those for differentiating glaucoma from suspected glaucoma were 92%, 81%, and 97%, respectively. While 55 photographs could be evaluated in 2 seconds with CNN, a clinician spent an average of 24.2 seconds to evaluate a single photograph.

Conclusion: An appropriately designed and trained CNN was able to distinguish glaucoma with high accuracy even with a small number of fundus photographs.

Keywords: Glaucoma, convolutional neural network, artificial intelligence, telemedicine

Address for Correspondence: Nilgün Yıldırım, Eskişehir Osmangazi University Faculty of Medicine, Department of Ophthalmology, Eskişehir, Turkey
E-mail: nyyildirim@yahoo.com **ORCID-ID:** orcid.org/0000-0001-6266-4951
Received: 10.09.2020 **Accepted:** 22.06.2021

Cite this article as: Atalay E, Özalp O, Devecioğlu ÖC, Erdoğan H, İnce T, Yıldırım N. Investigation of the Role of Convolutional Neural Network Architectures in the Diagnosis of Glaucoma using Color Fundus Photography.. Turk J Ophthalmol 2022;52:193-200

Introduction

Glaucoma is the most common cause of irreversible blindness.[1] Globally, glaucoma affected 60 million people in 2010 and was projected to affect 80 million people by 2020 and approximately 112 million people in 2040.[2,3] Its average prevalence among people aged 40-80 years is 3.54% worldwide (confidence interval: 2.09%-5.82%), while the prevalence in Turkey has been reported as 1.29% and 2% in different studies (Yıldırım, N., Başmak, H., Kalyoncu, C., Özer, A., Aslantaş, D. Metintaş, S. 2008: Glaucoma prevalence in the population over 40 years of age in the Eskişehir region, 42nd National Congress of the Turkish Ophthalmological Association, Antalya).[3,4] Although glaucoma diagnosis has become more effective with advances in diagnostic technologies, it has been reported that 50-90% of patients do not know that they have glaucoma.[2,5,6,7,8]

Numerous methods such as intraocular pressure (IOP) measurement, optic nerve examination, visual field examination, and retinal nerve fiber analysis are used in the diagnosis of glaucoma. Fundus imaging is often preferred because digital fundus imaging is a noninvasive, cost-effective, and rapid method that is less affected by optic media opacities and is also a practical approach for telemedicine applications. The growing popularity of artificial intelligence applications in recent years further expanded the use of fundus imaging, and fundus photographs have become widely used in the artificial intelligence-assisted diagnosis of many eye diseases.

This study evaluated the performance of convolutional neural networks (CNNs) in differentiating the fundus photographs of eyes with glaucoma from those of normal eyes.

Materials and Methods

The study used 9,950 optic nerve photographs of 5,388 patients obtained as a result of glaucoma prevalence research and stored in the archive of the Eskişehir Osmangazi University Faculty of Medicine Ophthalmology Clinic. The study protocol was planned in accordance with the Declaration of Helsinki and approved by the Eskişehir Osmangazi University Ethics Committee. The photographs to be evaluated in the algorithm were obtained from the hard disk of the nonmydriatic fundus camera (Kowa nonmyd alpha-DIII, Kowa Company Ltd., Tokyo, Japan) in our clinic. All 20° posterior segment photographs in the device archive were anonymized and transferred.

The quality of the photographs was classified and recorded in the database by the relevant physicians (E.A., H.A., O.Ö.) according to the guidelines.[9] Images were considered low quality if more than 50% of the optic disc margins were not visible or haze obscured the optic disc and/or cup margins, medium quality if 0-50% of the optic disc boundaries were not clearly discernible but the cup and its margins were visible and haze did not obscure the optic disc margins or cup; and high quality if all optic disc and cup margins were visible, with or without visibility of the retinal nerve fibers.

Of the total 9,950 photographs, 2,587 medium-quality and 5,970 high-quality photographs comprised the dataset pool, while the 1,393 low-quality photographs were not included. All datasets used in the study were composed of medium- and high-quality photographs.

The clinicians blindly and randomly labeled the fundus photographs as normal, glaucoma suspect, or glaucoma using a computer program (Figure 1). This classification was made according to criteria used in previous studies.[9,10,11,12,13] Glaucoma was diagnosed in the presence of any of the following: vertical cup-to-disc ratio ≥0.9; rim width-to-disc diameter ratio ≤0.05 or presence of localized notching; and any retinal nerve fiber defect corresponding to an area of neuroretinal rim thinning or localized notching. Suspected glaucoma was classified in the presence of any of the following: vertical cup-to-disc ratio of ≥0.7 to <0.9; rim width-to-disc diameter ratio of ≤0.1 to >0.05; retinal nerve fiber defect; and disc hemorrhage. Eyes not exhibiting these characteristics were classified as normal.

Labeling was performed in two stages. In the first stage, the diagnostic codes assigned by two glaucoma specialists (E.A. and H.A.) were entered into the database as the final verdict if there was consensus between them. Disputed photographs were marked for the second stage. In the second stage, these photographs were shown to the third, more senior and experienced expert (N.Y.) and a final verdict was reached by majority vote. In the absence of a majority (e.g., E.A.: suspect, H.A.: normal, N.Y.: glaucoma), the opinion of the third expert was recorded as the final verdict. In addition, the time from the photo being opened in the program to the expert marking an option was automatically calculated by the software. After all fundus photographs were labelled, the CNN stage started.

In this study, we used an adaptive two-dimensional (2D) CNN to combine feature extraction and classification in a single learning body. CNNs are feed-forward artificial neural networks that are inspired by the brain structure and regarded as simple computational models of the mammalian visual cortex.[14,15,16] Therefore, CNNs are mostly used for 2D signals such as pictures and videos. They are generally used by the machine and visual communities as the de facto standard for both understanding and solving many image and video recognition problems. To understand a convolution in the simplest way, it can be thought of as a sliding window function applied in 2D in a matrix. CNNs acquire the basic idea through limited connectivity among multilayer sensors and restricted weight sharing. CNNs are a "restricted" version of multilayer perceptrons, only with subsampling layers added. The fully connected hidden and output layers of CNNs are exactly the same as the layers of multilayer perceptrons. Therefore, a CNN has the characteristic limitations of multilayer perceptrons when learning a complex task. Multilayer perceptrons are truly universal approaches; however, a "better" universal approach is needed for learning tasks with compact configurations.

A conventional CNN architecture uses the convolutional layers for automatic feature learning and extraction from raw or preprocessed data. It then includes multilayer perceptron layers for classification, and a one-dimensional (1D) feature map output is fed to a multilayer perceptron. These two different layers combine to automatically learn optimal features for advanced classification performance. Input data is processed using convolution layers and alternating subsampling layers that produce feature maps that have been filtered and subsampled by the processors (neurons) of the previous layers. The 2D filter cores of the CNN are optimized and trained using an error feedback algorithm (back-propagation). In this study, a 2D CNN classifier was designed and applied to detect glaucoma. The proposed system is shown in Figure 2.

The proposed 2D CNN classifier is run on Python using the Keras library, which was developed for researchers and developers to make applications of deep learning models as quickly and easily as possible (Keras Deep Learning Library Web Site: https://keras.io/). The architecture of the proposed 2D CNN classifier consists of 5 convolutional and two scalar multilayer classifier layers in all experiments to achieve high computational efficiency with competitive performance. The 2D CNN classifier, which is designed with a relatively shallow structure, can be used for real-time glaucoma diagnosis. The number of neurons in the convolutional layers was set to [64 64 32 32 16] and the filter sizes were determined as (15,15), (11,11), (7,7), (3,3), and (3,3). The fully connected multilayer perceptron layer has 512 neurons and the output layer has two neurons for detecting glaucoma. The architecture of the 2D classifier is shown in Figure 3. ReLU was used as a nonlinear activation function in all CNN layers and applied to the subsampling layers with maximum sampling. To train the 2D CNN classifier, a 10-fold cross-validation technique was implemented to improve generalization, thereby preventing over-training of the architecture. The Dropout technique (removing some connections with a certain possibility) was also implemented in the ResNet architecture for the same purpose. The RMSprop algorithm was used in training to optimize the parameters of the designed architecture.

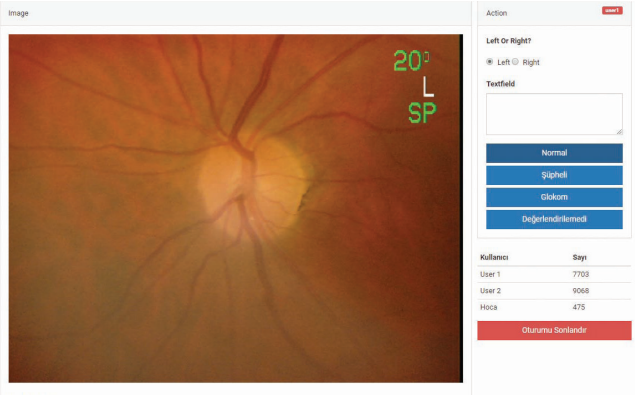

Figure 1. Fundus photograph labeling program

After classification, subdata clusters were created with digital fundus photographs labeled as healthy (n=238)/glaucoma (n=320) and healthy (n=170)/glaucoma (n=170)/glaucoma suspect (n=167). Image size was reduced to 512x512 pixels for 10-fold cross-validation training and testing. To compare the performance of a CNN model with a relatively shallow structure (5 convolutional and 1 hidden scalar layer) that was designed and trained in the most appropriate way using our own data, we also selected the ResNet-50, ResNet-101, and VGG-19 deep structures, which are frequently used in the literature, and trained them using transfer learning with the same data.[17,18,19] Our aim here is to show that in situations where big data is not available (as in most studies in the literature), the glaucoma diagnostic performance of the relatively shallow CNN model that we designed and trained may be similar or better than the performances of the deep structures trained with the transfer learning method proposed in other studies. The deep

Figure 2. Proposed glaucoma diagnosis system

structures, whose last 3 layers were trained with transfer learning methods using our own data, were previously trained using the ImageNet database, which contains approximately 14 million images.[20] While training the designed architectures, all data were randomly divided into 10 separate clusters for training/validation/generalization. This aimed to train the structure correctly and optimize the generalization performance. Standard performance measurement criteria (accuracy, sensitivity, and specificity) were calculated to compare the performance of the architectures. Heat maps were obtained by upsampling the outputs of the last convolutional layer to the image size.

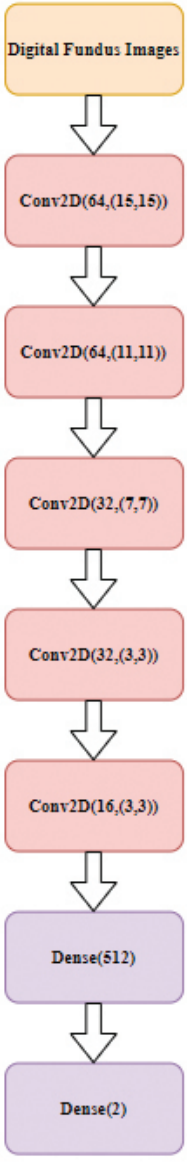

Figure 3. Proposed two-dimensional convolutional neural network architecture (Conv2D [neuron number, filter size) and Dense (neuron number])

To detect suspected glaucoma, two separate datasets (glaucoma suspect/normal and glaucoma suspect/glaucoma) consisting of 170 normal, 170 glaucoma, and 167 glaucoma-suspect fundus photographs were created. The created dataset was divided into 90% and 10% for training and testing, respectively. The transfer learning method was applied with 101-layer ResNet architectures previously trained with the ImageNet dataset.[20]

All experiments reported in this article were run on a 2.2 GHz Intel Core i7-8750H with 8 GB RAM and NVIDIA GeForce GTX 1050Ti graphics card. Both training and test datasets were processed in parallel by a total of 768 CUDA cores.

Results

Of the 5388 patients included in the study, 3825 were women (71%) and 1563 were men (29%). The mean age of the women was 54.88±10.31 years and that of the men was 58.35±10.82 years. There was no difference between the two groups in terms of age ($p>0.05$). Of the participants, 643 (11.9%) had diabetes mellitus, 1734 (32.2%) had hypertension, and 505 (9.4%) had coronary heart disease.

Of all the medium- and high-quality photographs labeled by the glaucoma specialists, 416 photos were classified as glaucoma and 342 photos as suspected glaucoma. Diagnostic agreement between E.A. and H.A. was 92%.

Accuracy, sensitivity, and specificity in glaucoma detection were 96.2%, 99.5%, and 93.7% with ResNet-50; 97.4%, 97.8%, and 97.1% with ResNet-101; 98.9%, 100%, and 98.1% with VGG-19, and 99.4%, 100%, and 99% with the 2D CNN. Figure 4 shows sample data of the 2D CNN classifier, while Figure 5 shows heat maps of selected outputs.

ResNet-101 differentiated the fundus photographs of glaucoma-suspect eyes from normal eyes with 62% accuracy, 68% sensitivity, and 56% specificity and from glaucoma eyes with 92% accuracy, 81% sensitivity, and 97% specificity.

In systems trained in diagnosis glaucoma with 10 epochs, the time per epoch was 23.6 s for the 2D CNN, 23.2 s for VGG-19, 35 s for ResNet-50, and 57 s for ResNet-101. While the mean test duration was 2 s per 55 photographs with the CNNs, we determined that clinicians evaluated one photograph in a mean of 24.2 s.

Discussion

In our study, the accuracy rate, sensitivity, and specificity in glaucoma detection were 96.2%, 99.5%, and 93.7% with ResNet-50; 97.4%, 97.8%, and 97.1% with ResNet-101; 98.9%, 100%, and 98.1% with VGG-19; and 99.4%, 100%, and 99% with the 2D CNN, respectively. With ResNet-101, glaucoma suspects were differentiated from normal eyes with an accuracy rate of 62%, sensitivity of 68%, and specificity of 56% and were differentiated from glaucomatous eyes with an

accuracy rate of 92%, sensitivity of 81%, and specificity of 97%. In glaucoma diagnosis, the CNNs tested 55 fundus photographs in 2 seconds, whereas clinicians took approximately 24 seconds on average to evaluate a single fundus photograph.

Imaging with fundus photography is the least costly method for structural evaluation of the optic nerve, but its sensitivity and specificity in detecting glaucoma or suspected glaucoma are not comparable to advanced methods such as optic coherence tomography (OCT). Large numbers of fundus images collected from diabetic retinopathy screening programs have formed a resource for evaluating glaucomatous optic disc changes with deep learning algorithms. Two different studies in which deep learning algorithms were created for glaucoma detection using fundus photographs obtained for diabetic retinopathy screening yielded high rates of 95.6% and 96.4% for sensitivity and 92% and 87.2% for specificity (area under the curve [AUC]: 0.986 and 0.942).[9,21] In another study that evaluated glaucoma from fundus photographs using the ResNet architecture, the AUC value was found to be 0.965.[22] In a study comparing five different ImageNet models used for glaucoma diagnosis, sensitivity and specificity values were found to be 90.6% and 88.2% (AUC: 0.96) with VGG-16, 92.4% and 88.5% (AUC: 0.97) with VGG-19, 92.2% and 87.5% (AUC: 0.97) with InceptionV3, 91.1% and 89.4% (AUC: 0.96) with ResNet50, and 93.5% and 85.8% (AUC: 0.96) with Xception, respectively.[18] The literature data and the results of our study indicate that CNN algorithms

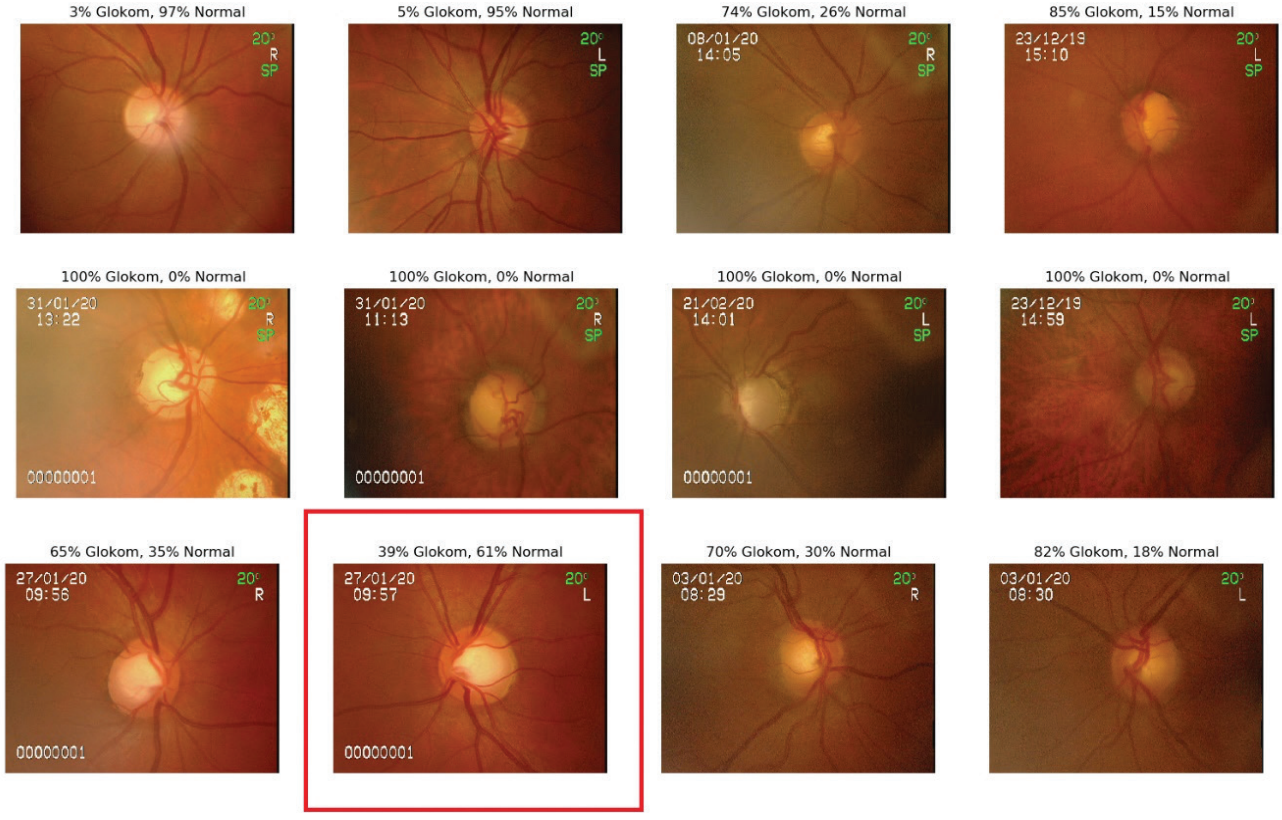

Figure 4. Sample data of the two-dimensional convolutional neural networks classifier (an incorrect result is marked in red)

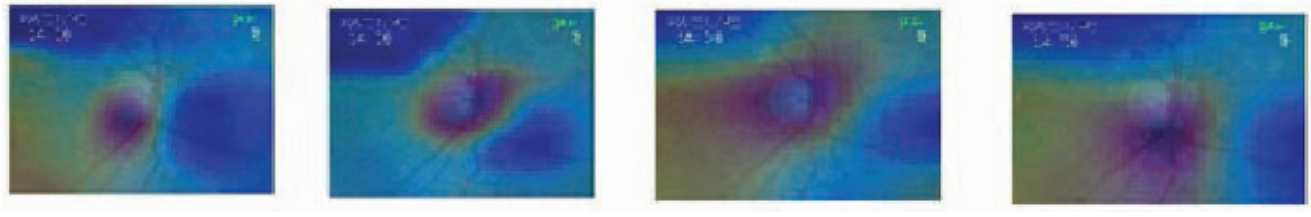

Figure 5. Heat maps of selected outputs

created with fundus photographs are effective in the detection of glaucoma. Although the study comparing different CNN models showed similar sensitivity and specificity in glaucoma detection, in our study we observed higher sensitivity and specificity rates with VGG-19 and the 2D CNN.[18]

The use of OCT and ultra-wide scanning laser ophthalmoscopy images has gained popularity in the evaluation of glaucoma with deep learning. In a study of glaucoma detection using 1399 Optos fundus photographs, it was reported that sensitivity was 81.3% and specificity was 80.2% (AUC: 0.872), with higher values in the detection of patients with advanced glaucoma.[23] In a deep learning study with 2132 OCT images, the sensitivity and specificity for early glaucoma detection were 82.5% and 93.9%, respectively (AUC: 0.937).[24] AUC values ranging from 0.877 to 0.981 were also determined in other studies using different OCT parameters.[25,26,27,28] Confocal scanning laser ophthalmoscopy (CSLO) parameters and scanning laser polarimetry (SLP) parameters have also been used in various artificial intelligence studies conducted with structural evaluations for glaucoma diagnosis. In screens performed with CSLO parameters, the sensitivity ranged from 83% to 92% and the specificity ranged from 80% to 91%,[29,30,31,32,33] while in screenings performed with SLP parameters, the sensitivity was 74% to 77% and specificity was 90% to 92%.[29,34] In the detection of glaucoma by machine learning, there are various data sources for the structural evaluation of the optic disc, such as fundus photograph, OCT, CSLO, and SLP parameters. However, fundus photographs may be preferrable since the use of fundus photographs is the cheapest and easiest method and yields high sensitivity and specificity.

There are also studies in the literature evaluating structural tests together. In an artificial intelligence study using fundus photographs and retinal nerve fiber thickness data obtained from spectral domain OCT, it was reported that glaucoma was diagnosed with 80% specificity and 90% sensitivity.[35] In addition, studies have been conducted to increase the effectiveness of artificial intelligence algorithms by using a combination of structural and functional test data for glaucoma diagnosis. It was reported that fundus photographs and visual field results evaluated together provided greater accuracy (88%) in glaucoma diagnosis than when evaluated separately.[36]

Heat maps, which are formed by upsampling the outputs of the last convolutional layer to the image sizes, can help to understand which regions of an input image affect the output prediction of a CNN. These activation maps are overlayed on the input image to highlight the areas of greatest CNN interaction. Example heat maps from the glaucoma category are shown in Figure 5. They show that alterations around the optic disc, which are also examined in the medical diagnosis of glaucoma, are the areas with which the CNN interacts the most. This suggests that physicians may be able to use machine learning outputs as an aid in the diagnosis of glaucoma or other diseases.

Study Limitations

The deep learning method was able to distinguish glaucomatous eyes from normal eyes with high accuracy, even with a small number of fundus photographs. We predict that more photographs and different optimized learning algorithms will provide even higher sensitivity and specificity values, and that a multi-modelling method combining fundus photographs and OCT or visual field data will increase the effectiveness of artificial intelligence in glaucoma diagnosis. The fundus photographs used in our study were images in the Eskişehir Osmangazi University Faculty of Medicine Eye Clinic archive obtained through glaucoma prevalence research and were not labeled with a diagnosis. For this reason, the artificial intelligence algorithm may not show the same accuracy when used in different races and ethnic groups. An additional limitation of the study was not evaluating false-negative and false-positive rates in the diagnosis of glaucoma.

Conclusion

Glaucoma leads to irreversible blindness, and its early diagnosis and treatment are important. It can be asymptomatic in the early stages, and visual field is not affected until there is between 20% and 50% retinal ganglion cell loss. Therefore, structural evaluation is more important than functional tests. Early glaucoma detection can be achieved by evaluating optical disc images with machine learning algorithms. The development of these methods will allow the creation of telemedicine glaucoma screening programs in primary health care centers and enable effective triage. Artificial intelligence-based algorithms should not be regarded as a system that can replace physicians, but as a tool that aids physicians in diagnosis and follow-up.

Ethics

Ethics Committee Approval: The study protocol was prepared in accordance with the Declaration of Helsinki and ethics committee approval was obtained from the Eskişehir Osmangazi University Ethics Committee.

Informed Consent: Obtained.

Peer-review: Externally and internally peer reviewed.

Authorship Contributions

Concept: N.Y., E.A., T.İ., Design: N.Y., E.A., T.İ., Data Collection or Processing: H.E., E.A., O.Ö.,

Analysis or Interpretation: E.A., N.Y., T.İ., Ö.D., Literature Search: E.A., O.Ö., Ö.D., Writing: E.A., N.Y., O.Ö., T.İ., Ö.D.

Conflict of Interest: No conflict of interest was declared by the authors.

Financial Disclosure: This study was created with the results obtained from the research project numbered 218E066 and coded 1002, supported by TUBITAK.

References

1. Bourne RR, Stevens GA, White RA, Smith JL, Flaxman SR, Price H, Jonas JB, Keeffe J, Leasher J, Naidoo K, Pesudovs K, Resnikoff S, Taylor HR; Vision Loss Expert Group. Causes of vision loss worldwide, 1990-2010: a systematic analysis. Lancet Glob Health. 2013;1:e339-e349.
2. Quigley HA, Broman AT. The number of people with glaucoma worldwide in 2010 and 2020. Br J Ophthalmol. 2006;90:262-267.
3. Tham YC, Li X, Wong TY, Quigley HA, Aung T, Cheng CY. Global prevalence of glaucoma and projections of glaucoma burden through 2040: a systematic review and meta-analysis. Ophthalmology. 2014;121:2081-2090.
4. Yavaş GF, Küsbeci T, Şanlı M, Toprak D, Ermiş SS, İnan ÜÜ, Öztürk F. Risk Factors for Primary Open-Angle Glaucoma in Western Turkey. Turk J Ophthalmol. 2013;43:87-90.
5. Bourne RR, Jonas JB, Flaxman SR, Keeffe J, Leasher J, Naidoo K, Parodi MB, Pesudovs K, Price H, White RA, Wong TY, Resnikoff S, Taylor HR; Vision Loss Expert Group of the Global Burden of Disease Study. Prevalence and causes of vision loss in high-income countries and in Eastern and Central Europe: 1990-2010. Br J Ophthalmol. 2014;98:629-638.
6. Varma R, Ying-Lai M, Francis BA, Nguyen BB, Deneen J, Wilson MR, Azen SP; Los Angeles Latino Eye Study Group. Prevalence of open-angle glaucoma and ocular hypertension in Latinos: the Los Angeles Latino Eye Study. Ophthalmology. 2004;111:1439-1448.
7. Baskaran M, Foo RC, Cheng CY, Narayanaswamy AK, Zheng YF, Wu R, Saw SM, Foster PJ, Wong TY, Aung T. The Prevalence and Types of Glaucoma in an Urban Chinese Population: The Singapore Chinese Eye Study. JAMA Ophthalmol. 2015;133:874-880.
8. Gupta P, Zhao D, Guallar E, Ko F, Boland MV, Friedman DS. Prevalence of Glaucoma in the United States: The 2005-2008 National Health and Nutrition Examination Survey. Invest Ophthalmol Vis Sci. 2016;57:2905-2913.
9. Li Z, He Y, Keel S, Meng W, Chang RT, He M. Efficacy of a Deep Learning System for Detecting Glaucomatous Optic Neuropathy Based on Color Fundus Photographs. Ophthalmology. 2018;125:1199-1206.
10. Foster PJ, Buhrmann R, Quigley HA, Johnson GJ. The definition and classification of glaucoma in prevalence surveys. Br J Ophthalmol. 2002;86:238-242.
11. Iwase A, Suzuki Y, Araie M, Yamamoto T, Abe H, Shirato S, Kuwayama Y, Mishima HK, Shimizu H, Tomita G, Inoue Y, Kitazawa Y; Tajimi Study Group, Japan Glaucoma Society. The prevalence of primary open-angle glaucoma in Japanese: the Tajimi Study. Ophthalmology. 2004;111:1641-1648.
12. He M, Foster PJ, Ge J, Huang W, Zheng Y, Friedman DS, Lee PS, Khaw PT. Prevalence and clinical characteristics of glaucoma in adult Chinese: a population-based study in Liwan District, Guangzhou. Invest Ophthalmol Vis Sci. 2006;47(7):2782-2788.
13. Topouzis F, Wilson MR, Harris A, Anastasopoulos E, Yu F, Mavroudis L, Pappas T, Koskosas A, Coleman AL. Prevalence of open-angle glaucoma in Greece: the Thessaloniki Eye Study. Am J Ophthalmol. 2007;144:511-519.
14. Cireşan DC, Meier U, Gambardella LM, Schmidhuber J. Deep, big, simple neural nets for handwritten digit recognition. Neural Comput. 2010;22:3207-3220.
15. Scherer D, Müller A, Behnke S. Evaluation of pooling operations in convolutional architectures for object recognition. International conference on artificial neural networks: Springer, 2010.
16. Krizhevsky A, Sutskever I, Hinton GE. Imagenet classification with deep convolutional neural networks. Communications of the ACM. 2017;60:84-90.
17. Gómez-Valverde JJ, Antón A, Fatti G, Liefers B, Herranz A, Santos A, Sánchez CI, Ledesma-Carbayo MJ. Automatic glaucoma classification using color fundus images based on convolutional neural networks and transfer learning. Biomed Opt Express. 2019;10:892-913.
18. Diaz-Pinto A, Morales S, Naranjo V, Köhler T, Mossi JM, Navea A. CNNs for automatic glaucoma assessment using fundus images: an extensive validation. Biomed Eng Online. 2019;18:29.
19. Serener A, Serte S. Transfer learning for early and advanced glaucoma detection with convolutional neural networks. 2019 Medical Technologies Congress (TIPTEKNO): IEEE, 2019.
20. Deng J, Dong W, Socher R, Li L-J, Li K, Fei-Fei L. Imagenet: A large-scale hierarchical image database. 2009 IEEE conference on computer vision and pattern recognition: Ieee, 2009.
21. Ting DSW, Cheung CY, Lim G, Tan GSW, Quang ND, Gan A, Hamzah H, Garcia-Franco R, San Yeo IY, Lee SY, Wong EYM, Sabanayagam C, Baskaran M, Ibrahim F, Tan NC, Finkelstein EA, Lamoureux EL, Wong IY, Bressler NM, Sivaprasad S, Varma R, Jonas JB, He MG, Cheng CY, Cheung GCM, Aung T, Hsu W, Lee ML, Wong TY. Development and Validation of a Deep Learning System for Diabetic Retinopathy and Related Eye Diseases Using Retinal Images From Multiethnic Populations With Diabetes. JAMA. 2017;318:2211-2223.
22. Shibata N, Tanito M, Mitsuhashi K, Fujino Y, Matsuura M, Murata H, Asaoka R. Development of a deep residual learning algorithm to screen for glaucoma from fundus photography. Sci Rep. 2018;8:14665.
23. Masumoto H, Tabuchi H, Nakakura S, Ishitobi N, Miki M, Enno H. Deep-learning Classifier With an Ultrawide-field Scanning Laser Ophthalmoscope Detects Glaucoma Visual Field Severity. J Glaucoma. 2018;27:647-652.
24. Asaoka R, Murata H, Hirasawa K, Fujino Y, Matsuura M, Miki A, Kanamoto T, Ikeda Y, Mori K, Iwase A, Shoji N, Inoue K, Yamagami J, Araie M. Using Deep Learning and Transfer Learning to Accurately Diagnose Early-Onset Glaucoma From Macular Optical Coherence Tomography Images. Am J Ophthalmol. 2019;198:136-145.
25. Burgansky-Eliash Z, Wollstein G, Chu T, Ramsey JD, Glymour C, Noecker RJ, Ishikawa H, Schuman JS. Optical coherence tomography machine learning classifiers for glaucoma detection: a preliminary study. Invest Ophthalmol Vis Sci. 2005;46:4147-4152.
26. Kim SJ, Cho KJ, Oh S. Development of machine learning models for diagnosis of glaucoma. PLoS One. 2017;12:e0177726.
27. Barella KA, Costa VP, Gonçalves Vidotti V, Silva FR, Dias M, Gomi ES. Glaucoma Diagnostic Accuracy of Machine Learning Classifiers Using Retinal Nerve Fiber Layer and Optic Nerve Data from SD-OCT. J Ophthalmol. 2013;2013:789129.
28. Christopher M, Belghith A, Weinreb RN, Bowd C, Goldbaum MH, Saunders LJ, Medeiros FA, Zangwill LM. Retinal Nerve Fiber Layer Features Identified by Unsupervised Machine Learning on Optical Coherence Tomography Scans Predict Glaucoma Progression. Invest Ophthalmol Vis Sci. 2018;59:2748-2756.
29. Bowd C, Zangwill LM, Medeiros FA, Hao J, Chan K, Lee TW, Sejnowski TJ, Goldbaum MH, Sample PA, Crowston JG, Weinreb RN. Confocal scanning laser ophthalmoscopy classifiers and stereophotograph evaluation for prediction of visual field abnormalities in glaucoma-suspect eyes. Invest Ophthalmol Vis Sci. 2004;45:2255-2262.
30. Townsend KA, Wollstein G, Danks D, Sung KR, Ishikawa H, Kagemann L, Gabriele ML, Schuman JS. Heidelberg Retina Tomograph 3 machine learning classifiers for glaucoma detection. Br J Ophthalmol. 2008;92:814-818.
31. Zangwill LM, Chan K, Bowd C, Hao J, Lee TW, Weinreb RN, Sejnowski TJ, Goldbaum MH. Heidelberg retina tomograph measurements of the optic disc and parapapillary retina for detecting glaucoma analyzed by machine learning classifiers. Invest Ophthalmol Vis Sci. 2004;45:3144-3151.
32. Uchida H, Brigatti L, Caprioli J. Detection of structural damage from glaucoma with confocal laser image analysis. Invest Ophthalmol Vis Sci. 1996;37:2393-2401.

33. Adler W, Peters A, Lausen B. Comparison of classifiers applied to confocal scanning laser ophthalmoscopy data. Methods Inf Med. 2008;47:38-46.
34. Weinreb RN, Zangwill L, Berry CC, Bathija R, Sample PA. Detection of glaucoma with scanning laser polarimetry. Arch Ophthalmol. 1998;116:1583-1589.
35. Medeiros FA, Jammal AA, Thompson AC. From Machine to Machine: An OCT-Trained Deep Learning Algorithm for Objective Quantification of Glaucomatous Damage in Fundus Photographs. Ophthalmology. 2019;126:513-521.
36. Brigatti L, Hoffman D, Caprioli J. Neural networks to identify glaucoma with structural and functional measurements. Am J Ophthalmol. 1996;121:511-521.

DOI: 10.4274/tjo.galenos.2021.83704
Turk J Ophthalmol 2022;52:201-207

Original Article

Effectiveness, Sensitivity, and Specificity of Intraocular Lens Power Calculation Formulas for Short Eyes

Wiktor Stopyra

MW-med Eye Centre, Cracow, Poland

Abstract

Objectives: To compare intraocular lens (IOL) power calculation formulas in terms of absolute error (AE) and receiver operating characteristic curves in eyes with axial length (AL) shorter than 22.0 mm.

Materials and Methods: The data of hyperopic patients who underwent uneventful phacoemulsification with IOL implantation in MW-med Eye Centre, Cracow, Poland between October 2015 and June 2019 were retrospectively reviewed. IOL power was calculated using Holladay1, SRK/T, Hoffer Q, Holladay2, Haigis, and Barrett Universal II formulas. The power of the implanted lens was based on Hoffer Q. Three months after phacoemulsification, refraction was measured and AE was calculated. The percentage of patients with full visual acuity without any correction and the percentage of hyperopic patients was determined for each formula. Receiver operating characteristic curves with cut-off points for AL were drawn for each formula and the area under the curve was evaluated.

Results: Fifty-six patients (62 eyes) whose ocular AL ranged between 20.58 mm and 21.97 mm were included in the study. Hoffer Q formula yielded the lowest mean AE (0.09±0.08 D), the highest percentage of patients with full visual acuity without correction (75.8%), and the lowest rate of postoperative hyperopia (8.1%). However, the SRK/T formula had the largest area under the curve (0.667).

Conclusion: The Hoffer Q formula gave the lowest level of AE in the study and seems to be recommendable for IOL power calculation for hyperopic eyes. Further studies are needed on the use of receiver operating characteristic curves in assessing the effectiveness of IOL power calculation formulas.

Keywords: Phacoemulsification, hyperopia, intraocular lenses, ROC curve

Address for Correspondence: Wiktor Stopyra, MW-med Eye Centre, Cracow, Poland
E-mail: wiktorstopyra@gmail.com **ORCID-ID:** orcid.org/0000-0002-3919-8339
Received: 02.05.2021 **Accepted:** 17.08.2021

Cite this article as: Stopyra W. Effectiveness, Sensitivity, and Specificity of Intraocular Lens Power Calculation Formulas for Short Eyes. Turk J Ophthalmol 2022;52:201-207

Introduction

Accurate intraocular lens (IOL) power calculation is a very important aspect of cataract surgery because patients' expectations for perfect vision after surgery are still increasing.[1] Therefore, new IOL power calculation formulas based on more parameters are still being developed. Historically, first-generation formulas like the Binkhorst or SRK (Sanders-Retzlaff-Kraff) were based on axial length (AL), corneal power (K), and lens constant (A) only. In second-generation formulas like the SRK II, A was modified based on AL. Third-generation formulas (Holladay 1, SRK/T, Hoffer Q) incorporated more variables such as anterior chamber depth (ACD).[2] Later came fourth-generation formulas like the Haigis (which uses three constants [a0, a1, a2] that are analogous to surgeon factor [SF], ACD, and AL, respectively) and the Holladay 2, which added further parameters like lens thickness and corneal white-to-white, leading to the fifth-generation formulas (Olsen, Barrett Universal II, Hill-Radial Basis Function).[3] While the Barrett Universal II and the Olsen formulas are based on Holladay 2-like globe parameters, the Hill-RBF formula is a mathematical algorithm developed to select IOL power independent of an effective lens position estimation.[4]

It is well known that most IOL power calculation formulas perform well for eyes with AL between 22.0 and 25.0 mm.[5] The accuracy of IOL power calculation formulas for eyes shorter than 22.0 mm or longer than 25.0 mm is still questionable.[6,7] There have been many studies conducted on this. Most often the research methodology is based on calculation of absolute error (AE) using an absolute value of the difference between postoperative and predicted spherical equivalences of refractive error.[6,7,8,9,10,11,12] Only some studies have considered other aspects of the accuracy of IOL power calculation formulas, such as the percentage of patients with full visual acuity (VA) without any correction and the percentage of patients with postoperative hyperopia.[2,3,13,14,15] Although the receiver operating characteristic (ROC) curve method is widely used in medicine to assess the sensitivity and specificity of certain tests, the concept of using it to compare the accuracy of IOL power calculation formulas is new.[16]

This study aimed to compare IOL power calculation formulas in eyes shorter than 22.0 mm in terms of AE, the percentage of patients with full VA without any correction, and the percentage of hyperopic patients after phacoemulsification. Additionally, the study attempted to demonstrate the accuracy of IOL power calculation formulas using ROC curves, which is a novel approach.

Materials and Methods

Hyperopic patients (i.e., axial length of 22.0 mm or less) with Wisconsin grade 3 or 4 cataracts who underwent uneventful sutureless phacoemulsification with monofocal IOL implantation through a 2.4-mm clear corneal incision in MW-med Eye Centre, Cracow, Poland between October 2015 and June 2019 were included in the study.

The exclusion criteria were: corneal astigmatism greater than 2.0 diopters (D) or a history of other ophthalmic procedures such as vitrectomy, limbal relaxing incisions, and corneal refractive surgery.

The study was conducted adhering to the tenets of Declaration of Helsinki. Each patient signed an informed consent for a routine cataract surgery.

Preoperatively, all patients underwent a full ophthalmological examination including the evaluation of best corrected Snellen VA, intraocular pressure measurement, anterior biomicroscopy, and fundoscopy. Preoperative keratometry and ocular biometry were performed using a Zeiss IOLMaster 700 (Carl Zeiss Meditec AG, Jena, Germany) with partial coherence interferometry to measure K and AL. IOL power was calculated with six different formulas (Holladay 1, SRK/T, Hoffer Q, Haigis, Holladay 2, Barrett Universal II) but the Hoffer Q formula was chosen to predict the definite IOL power. All phacoemulsification (phaco) procedures were performed by the same eye surgeon who used a similar accumulated energy complex parameter (actual phaco power multiplied by time). Monofocal, single-piece, hydrophobic, acrylic foldable IOLs (AcrySof SA60AT, Alcon Laboratories, Fort Worth, TX, USA) were implanted during the surgery. Postoperative refraction was measured 3 months after the surgery using an autorefractor keratometer (Nidek ARK-1, Nidek Co Ltd, Tokyo, Japan) and at least three K measurements were taken for each patient.

Numerical error (NE) was defined as the difference between the real postoperative refractive outcome expressed as spherical equivalent (sum of spherical power and half of cylindrical power) and the refraction predicted by each formula. A positive value indicated a hyperopic error and a negative value referred to myopic error, while the absolute value is AE. Therefore, the mean AE for each formula was calculated as the average of the absolute value of the deviation from predicted postoperative refractive outcome for all cases. AE values were used to determine the percentage of patients with full VA without any correction (AE between 0 and 0.12 D), with correction up to ±0.25 D (AE between 0.13 D and 0.37 D), and with correction up to ±0.5 D (AE >0.37 D). Additionally, the percentage of hyperopic patients (NE ≥0.13) was calculated for each formula (patients with AE ≤ 0.12 were regarded as full VA without any correction, while NE ≤-0.13 corresponded to myopia).

Finally, ROC curves were drawn for each formula and cut-off points for AL (the highest true positive rate and the lowest false negative rate) were identified. To develop an ROC curve, the sensitivities and specificities for different values of a continuous test measure were first tabulated. Then, the graphical ROC curve was drawn by plotting sensitivity (true positive rate) on the y-axis against 1-specificity (false positive rate) on the x-axis for the various values tabulated. This allowed the area under the curve (AUC), which ranges from 0 to 1, to be calculated for each formula.

Statistical analysis was performed using the Statistica 13.1 package. P value <0.05 was considered statistically significant unless it was necessary to apply Bonferroni corrections for

multiple comparisons, which reduced the significance level to 0.003. Normality of data distributions was checked using the Shapiro-Wilk test. The non-parametric Kruskal-Wallis test was used to check for statistically significant differences between groups. The Mann-Whitey U test (for quantitative variables) and chi-square or Fisher exact test (for qualitative variables) were used for pairwise formula comparisons.

Results

The study included 62 eyes of 56 patients (30 women and 26 men) with a mean age of 71.2 years (range: 55-92). AL varied between 20.58 and 21.97 mm (median: 21.49 mm).

The Hoffer Q formula provided the lowest mean AE of 0.09±0.08 D. Detailed results of the AE calculated for each formula are listed in Table 1.

Considering the AE, which indicates the expected correction after cataract surgery, the studied group was divided into three subgroups. The first subgroup had expected emmetropia (AE ≤0.12 D), the second had expected correction of ±0.25 D (AE 0.13-0.37 D), and the third group had expected correction of ±0.5 D or more (AE >0.37 D). The percentage distribution of the subgroups is presented in Figure 1.

Due to non-normal data distribution, the non-parametric Kruskal-Wallis test was used to determine differences in AE values between formulas. As the achieved probability value was p<0.001, post-hoc analysis with chi-square test (or Fisher exact test in special cases) was performed to compare AE distribution between pairs of formulas. Due to multiple comparisons, Bonferroni correction was applied, thereby lowering the assumed level of significance to $\alpha = 0.05/15 = 0.003$. Statistically significant differences were found in the following pairs of variables: Hoffer Q versus all other formulas, Haigis versus Holladay 1, Haigis versus Holladay 2, and Barrett Universal II versus Holladay 1 (Table 2).

To calculate the expected hyperopia after cataract surgery, two additional groups of patients were formed. The first group had expected emmetropia or myopia (NE ≤0.12 D) and the second group had expected hyperopia (NE >0.12 D). The percentage distribution of these groups is presented in Figure 2.

Similarly, due to non-normal data distribution, Kruskal-Wallis test followed by post-hoc chi-square or Fisher exact test with Bonferroni correction was performed to compare percentage distribution of NE between pairs. Statistically significant differences were found in the following pairs of variables: Hoffer Q versus Barrett Universal II, Hoffer Q versus Holladay 1, and Hoffer Q versus SRK/T (Table 2).

Additionally, ROC curves were drawn for each formula and cut-off points for AL were determined as decision thresholds. The AUC value was also calculated for each formula, with higher AUC values reflecting better formula performance. The calculation results are presented in Table 3 and ROC curves with cut-off points are illustrated graphically in Figure 3.

Discussion

The exact prediction of IOL power for hyperopic eyes is still a problem in daily practice for a cataract surgeon. There are many studies investigating this problem[2-15,17] and assessing the accuracy of selected formulas basing on different variables, most frequently AE.[6-12] Only a few authors have proposed other criteria for assessing the effectiveness of IOL power calculation formulas, such as percentage of patients with ±0.25 D, ±0.5 D, ±0.75 D, and ±1.0 D refraction after phacoemulsification.[3,4,14,15] Such parameters are useful, but results can vary widely. For example, postoperative refraction up to ±0.5 D in short eyes using the Hoffer Q formula was reported in 42.5% of patients in a study by Doshi et al.,[1] 71% in a study by Aristodemou et al.,[13] and 84.9% of patients in a study by Gökce et al.[4] Even greater differences were obtained using the Haigis formula, with rates of 17.5% reported by Doshi et al.,[1] 62.8% by Gokce et al.,[4] and 72.0% by Moschos et al.[3] In the present study, postoperative refraction up to ±0.5 D ranged from 82.3% (Haigis) to 100%

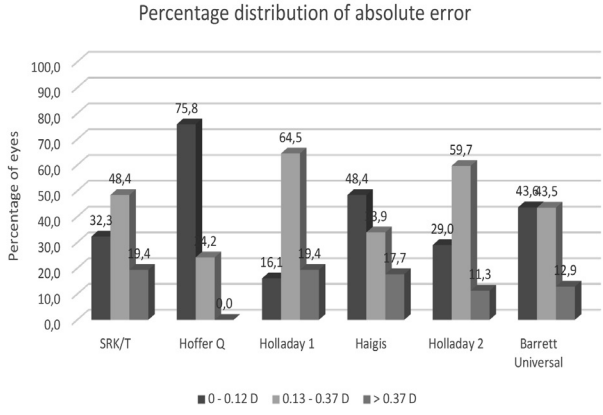

Figure 1. Percentage distribution of absolute error (AE) for all formulas. There was a significant difference among the groups (p<0.001, Kruskal-Wallis)

Table 1. Descriptive statistics of absolute error

	Absolute error (D)					
	SRK/T	**Hoffer Q**	**Holladay 1**	**Haigis**	**Holladay 2**	**Barrett Universal**
Mean ± SD	0.23±0.17	0.09±0.08	0.26±0.17	0.21±0.22	0.20±0.13	0.19±0.16
Median	0.20	0.06	0.23	0.13	0.19	0.14
Range	0.01-0.63	0.00-0.34	0.01-0.73	0.00-0.91	0.00-0.54	0.00-0.71

SD: Standard deviation

(Hoffer Q). In other studies, the percentage of patients with full VA without correction was also estimated.[2]

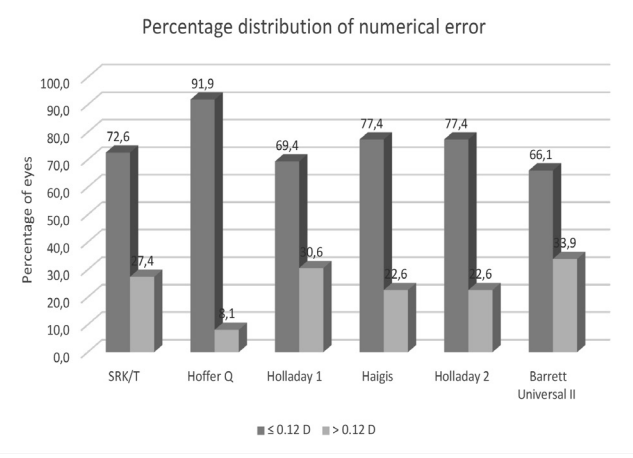

Figure 2. Percentage distribution of numerical error (NE) for all formulas. There was a significant difference among the groups (p<0.001, Kruskal-Wallis)

This study demonstrated that the Hoffer Q formula provided the lowest AE, the highest percentage of patients with full VA without correction, and the lowest percentage of hyperopic patients when used for IOL power calculation in eyes with AL smaller than 22.0 mm.

Consistent with the results of this study, the Hoffer Q is considered by many the most accurate formula for IOL power prediction in hyperopic eyes.[2,4,8,9,11,13] According to the literature, the second best in terms of accuracy would be the Haigis formula.[3,6,8,11,12] However, a 2018 meta-analysis based on 11 observational studies involving 1161 eyes demonstrated superiority of Haigis over Hoffer Q, whereas Holladay 2 gave the smallest mean AE but without a statistically significant difference.[6] The Holladay 2 formula was also shown to be the most accurate in IOL power prediction for short eyes in a few studies.[4,11] Single studies indicated the Holladay 1 formula,[13] Hill-RBF,[14] Barrett Universal II,[15] or Kane formula[17] as the most exact for IOL power calculation in hyperopic eyes. Hoffer and Savini's[11] analysis of studies published in the past 50 years revealed that the Hoffer Q, Haigis, and Holladay 2 formulas were the best options for IOL power prediction in short eyes.

Table 2. Results of pairwise comparisons of percentage distribution of absolute error (AE) and percentage distribution of numerical error (NE)

Chi-square test results	p (AE)	p (NE)
SRK/T vs. Hoffer Q.	<0.001	<0.001
SRK/T vs. Holladay 1	0.021	0.618
SRK/T vs. Haigis	0.054	0.433
SRK/T vs. Holladay 2	0.174	0.433
SRK/T vs. Barrett Universal II	0.199	0.319
Hoffer Q vs. Holladay 1	<0.001	<0.001
Hoffer Q vs. Haigis	<0.001	0.004
Hoffer Q vs. Holladay 2	<0.001	0.004
Hoffer Q vs. Barrett Universal II	<0.001	<0.001
Holladay 1 vs. Haigis	<0.001	0.200
Holladay 1 vs. Holladay 2	0.049	0.200
Holladay 1 vs. Barrett Universal II	<0.001	0.618
Haigis vs. Holladay 2	0.001	1
Haigis vs. Barrett Universal II	0.332	0.076
Holladay 2 vs. Barrett Universal II	0.062	0.076

Table 3. Area under the curve (AUC) values with two-sided confidence level

Formula	AUC	SE	95% lower confidence level	95% upper confidence level	p
SRK/T	0.667	0.076	0.518	0.815	0.028
Hoffer Q	0.645	0.096	0.458	0.833	0.129
Holladay 1	0.649	0.089	0.475	0.823	0.093
Haigis	0.493	0.075	0.347	0.639	0.928
Holladay 2	0.615	0.074	0.47	0.759	0.119
Barrett Univ. II	0.564	0.073	0.421	0.707	0.380

SH: Sayısal hata

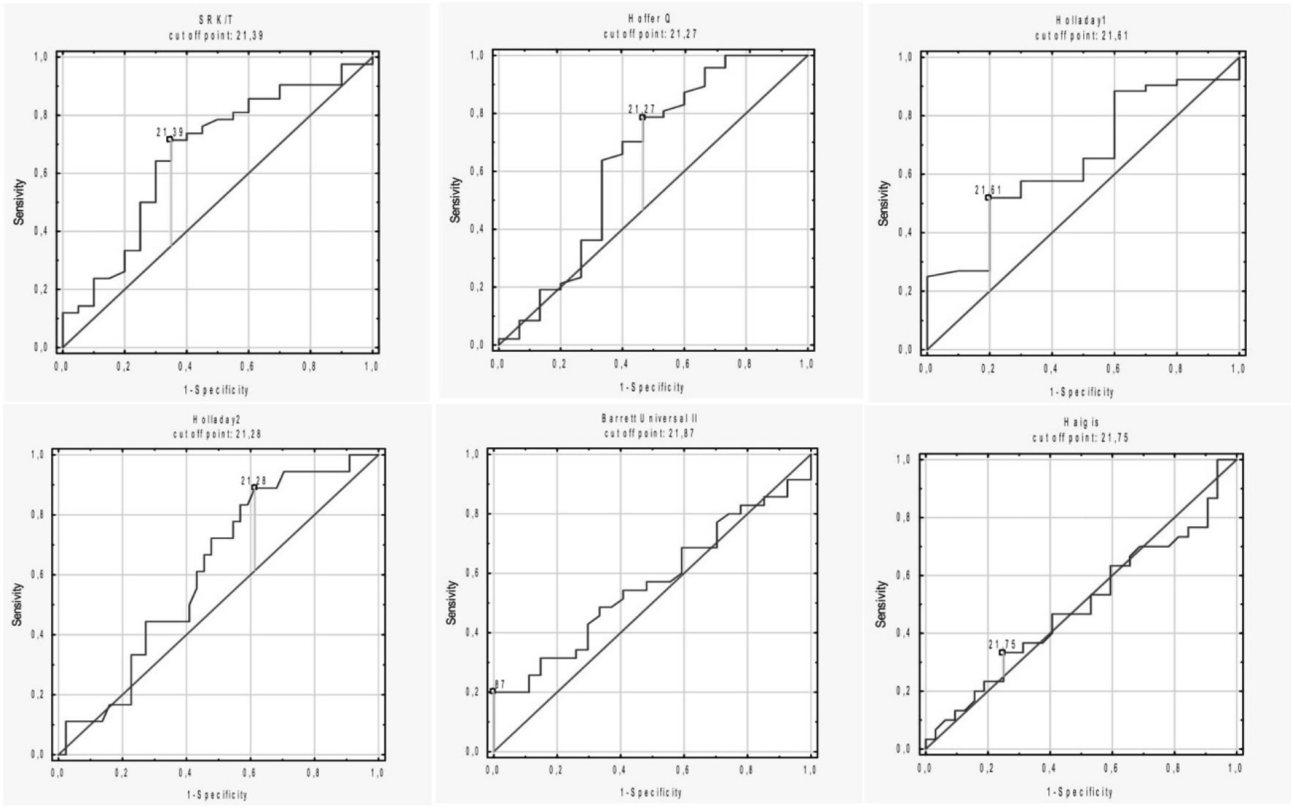

Figure 3. Receiver operating characteristic curves and cut off-points for each formula

Previous studies based on AE have shown the percentage of patients requiring both plus and minus correction after phacoemulsification. However, it is known that postoperative low myopia is less burdensome than hyperopia. Therefore, in this study I showed the percentage of hyperopic patients after cataract surgery based on NE, not only on AE. The Hoffer Q formula yielded the lowest outcomes in terms of postoperative hyperopia (8.1%). In a 2014 study of 69 patients, Moschos et al.[3]. showed that as many as 15% of patients required correction greater than ±1.0 D when IOL power was calculated according to the Hoffer Q formula. However, they used A-scan ultrasound to obtain AL, which is a less accurate method than IOLMaster. Studies based on preoperative and postoperative ultrasound biometry demonstrated that 54% of the errors in predicted refraction after IOL implantation can be attributed to AL measurement errors.[18] However, in the study by Gökce et al.,[4] after applying the method of optical low-coherence reflectometry to measure AL (Lenstar LS900), this rate was only 2.3% of 67 patients when using the Hoffer Q formula (and Holladay 1). The accuracy of AL, K, and ACD measurements is similar using Lenstar LS900 and IOLMaster 700. However, the IOLMaster 700 uses swept-source optical coherence tomography and demonstrates superior acquisition of biometric measurements compared with the widely used optical biometer IOLMaster 500.[19] On the other hand, there was reportedly no statistically significant difference in compared biometric parameters obtained with the IOLMaster 700 and the Pentacam AXL, which combines Scheimpflug technology with partial coherence interferometry.[20] In contrast, a recent study of 16 patients by Tang et al.[15] showed that up to 46.7% of patients (which was the best result, obtained with the Hill-RBF formula) required correction greater than ±0.5 D after phacoemulsification. However, the surgeries in their study were performed by resident ophthalmologists.

The methodology of this study is pioneering because of the use of ROC curve analysis. ROC curves are widely used to evaluate sensitivity and specificity in medicine.[16] However, they have not been used in previous studies of the effectiveness of IOL power calculation formulas. The ROC curve is plotted as:

ROC (·) = {(1-F (c), 1-G (c)): - ∞ ≤ c ≤ ∞}

It is a graph of variable x {x: x > c} with a changing threshold c. Since F (+1) = G (+1) = 1 and F (-1) = G (-1) = 0, the ROC curve joins the vertices (0, 0) and (1, 1) of the unit square (where F is the distribution function of the variable x in the group labeled 0 and G is the distribution function of the variable x in the group labeled 1). In practice, it is useful to calculate AUC.[16] Normally, an AUC of 0.5 represents a test with no discriminating ability (i.e., no better than chance), while an AUC of 1.0 represents a test with perfect discrimination.

In this study, the largest AUC (0.667) was obtained for the SRK/T formula and was statistically significant (p=0.028).

However, the AUC values achieved by Holladay 1 (0.649) and Hoffer Q (0.645) were very close to that obtained for SRK/T. Additionally, a cut-off point for AL was marked for each formula and ranged from 21.27 mm (the Hoffer Q formula) to 21.87 mm (the Barrett Universal II formula). The cut-off point for the Hoffer Q formula was the smallest, demonstrating that the Hoffer Q was more accurate for even shorter eyes than those tested. On the other hand, the median AL of the examined eyes was 21.49 mm and was the closest to the cut-off point of the SRK/T formula, which could favor this formula in terms of AUC. However, there are some papers proving the accuracy of the SRK/T formula in IOL power calculation. Doshi et al.[1] reported that the SRK/T formula achieved the largest percentage of patients with refraction up to ±0.5 D, while the Hoffer Q formula had the largest percentage with refraction up to ±1.0 D in short eyes. Aristodemou et al.[13] obtained the highest percentage of patients with refraction up to ±0.25 D and up to ±1.0 D for eyes with AL ranging from 21.5 mm to 21.99 mm using the SRK/T formula. The cut-off points determined in this study are very similar due to the small AL range of the studied eyes, although theoretically, based on these cut-off points one can try to determine the ranges of AL for which the given formula is the most accurate. The concept will probably work better with myopic eyes, where length differences are much larger. Although the ROC curve method seems intriguing, it did not give unequivocal results when assessing the sensitivity and specificity of the IOL power calculation formulas.

Study limitations

I recognize certain limitations of this study. The first one is the relatively small range of AL in the operated eyes (20.58-21.97 mm). Aristodemou et al.[13] obtained different mean AE results for certain length ranges, reporting the smallest mean AE in eyes with a length of 20.00-20.99 mm for the Holladay 1 formula, 21.00-21.49 mm for the Hoffer Q formula, and 21.50-21.99 mm for the SRK/T formula (AE=0.67, 0.50, and 0.43, respectively). In the present study, the median AL of the operated eyes was 21.49 mm, which could have resulted in the Hoffer Q formula obtaining the highest accuracy in terms of AE and the SRK/T formula in terms of ROC curve. This interpretation of the discrepancy in my results is similar to the observations of Aristodemou et al.[13] in their large study (457 eyes). Although the patient group in my study does not seem large, there are many published papers with even smaller samples.[9,12,18,21,22] Cook at el.[21] and Gavin et al.[22] studied 41 eyes, Wang et al. included 33 eyes,[18] Carifi et al. evaluated 28 eyes,[9] and Roh et al.[12] studied only 25 eyes. On the other hand, there have been a few studies with more eyes: 457 in the study by Aristodemou et al.,[13] 86 in the study by Gökce et al.,[4] and 75 in the study by Eom et al.[23] Another limitation of this study is that all patients received the same model of IOL, so these results may not be generalizable to IOL models of a different design. Similarly, all procedures being performed by the same eye surgeon limits generalization. Additionally, six patients participating in this study had both eyes operated on, which may also be a limitation of the study. However, they accounted for only 10% of operated eyes and should not affect the final result. Finally, pupil dilatation was not considered in the study. There are reports on the influence of pupil dilation on the accuracy of IOL power calculation formulas.[24]

Conclusion

In summary, this study shows that the Hoffer Q formula can be recommended for IOL power calculation for eyes with AL smaller than 22.0 mm in terms of AE, percentage of patients with full visual acuity without correction, and percentage of hyperopic patients. However, considering the results of ROC curve analysis, the SRK/T formula is the most accurate for these cases, followed by Holladay 1 and Hoffer Q. Although the reliability of the presented results may be limited due to the small sample size, the concept of using the ROC curve method seems promising.

Ethics

Ethics Committee Approval: It is retrospective study based on patients data.

Peer-review: Externally peer reviewed.

Financial Disclosure: The author declared that this study received no financial support.

References

1. Doshi D, Limdi P, Parekh N, Gohil N. A Comparative Study to Assess the Predictability of Different IOL Power Calculation Formulas in Eyes of Short and Long Axial Length. J Clin Diagn Res. 2017;11:NC01-NC04.
2. Stopyra W. Accurate intraocular lens power calculation formulas for eyesballs with the axial length smaller than 22.0 mm. Okulistyka. 2017;3:29-31. http://old.okulistyka.com.pl/_okulistyka/index.php?strona=artykul&wydanie=170&artykul=1815.
3. Moschos M, Chatziralli IP, Koutsandrea C. Intraocular lens power calculation in eyes with short axial length. Indian J Ophthalmol. 2014;62:692-694.
4. Gökce SE, Zeiter JH, Weikert MP, Koch DD, Hill W, Wang L. Intraocular lens power calculations in short eyes using 7 formulas. J. Cataract Refract Surg. 2017;43:892-897.
5. Chen C, Xu X, Miao Y, Zheng G, Sun Y, Xu X. Accuracy of Intraocular Lens Power Formulas Involving 148 Eyes with Long Axial Lengths: A Retrospective Chart-Review Study. J Ophthalmol. 2015;2015:976847.
6. Wang Q, Jiang W, Lin T, Wu X, Lin H, Chen W. Meta-analysis of accuracy of intraocular lens power calculation formulas in short eyes. Clin Exp Ophthalmol. 2018;46:356-363.
7. Wang Q, Jiang W, Lin T, Zhu Y, Chen C, Lin H, Chen W. Accuracy of intraocular lens power calculation formulas in long eyes: a systemic review and meta-analysis. Clin Exp Ophthalmol. 2018;46:738-749.
8. Batkov EN, Pashtayev NP, Mikhaylova VI. Raschet opticheskoĭ sily intraokuliarnoĭ linzy pri refraktsionnoĭ khirurgii 'ékstremal'noĭ' gipermetropii [Calculation of intraocular lens power in surgical treatment of extreme hyperopia]. Vestn Oftalmol. 2019;135:21-27.
9. Carifi G, Aiello F, Zygoura V, Kopsachilis N, Maurino V. Accuracy of the refractive prediction determined by multiple currently available intraocular lens power calculation formulas in small eyes. Am J Ophthalmol. 2015;159:577-583.
10. Karabela Y, Eliacik M, Kava F. Performance of the SRK/T formula using A-Scan ultrasound biometry after phacoemulsification in eyes with short and long axial lengths. BMC Ophthalmol. 2016;16:96.

11. Hoffer KJ, Savini G. IOL power calculation in short and long eyes. Asia Pac J Ophthalmol (Phila). 2017;6:330-331.
12. Roh YR, Lee SM, Han YK, Kim MK, Wee WR, Lee JH. Intraocular lens power calculation using IOLMaster and various formulas in short eyes. Korean J Ophthalmol. 2011;25:151-155.
13. Aristodemou P, Knox Cartwright N, Sparrow JM, Johnston RL. Formula choice: Hoffer Q, Holladay 1, or SRK/T and refractive outcomes in 8108 eyes after cataract surgery with biometry by partial coherence interferometry. J Cataract Refract Surg. 2011;37:63-71.
14. Kane JX, Van Heerden A, Atik A, Petsoglou C. Accuracy of 3 new methods for intraocular lens power selection. J Cataract Refract Surg. 2017;43:333-339.
15. Tang KS, Tran EM, Chen AJ, Rivera DR, Rivera JJ, Greenberg PB. Accuracy of biometric formulae for intraocular lens power calculation in a teaching hospital. Int J Ophthalmol. 2020;13:61-65.
16. Hoo ZH, Candlish J, Teare D. What is an ROC curve? Emerg Med J. 2017;34:357-359.
17. Darcy K, Gunn D, Tavassoli S, Sparrow J, Kane JX. Assesment of the accuracy of new and updated intraocular lens power calculation formulas in 10 930 eyes from the UK National Health Service. J Cataract Refract Surg. 2020;46:2-7.
18. Wang JK, Chang SW. Optical biometry intraocular lens power calculation using different formulas in patients with different axial lengths. Int J Ophthalmol. 2013;6:150-154.
19. Song JS, Yoon DY, Hyon JY, Jeon HS. Comparison of ocular biometry and refractive outcomes using IOL Master 500, IOL Master 700, and Lenstar LS900. Korean J Ophthalmol. 2020;34:126-132.
20. Shajari M, Cremonese C, Petermann K, Singh P, Müller M, Kohnen T. Comparison of axial length, corneal curvature, and anterior chamber depth measurements of 2 recently introduced devices to A known biometer. Am J Ophthalmol. 2017;178:58-64.
21. Cooke DL, Cooke TL. Comparison of 9 intraocular lens power calculation formulas. J Cataract Refract Surg. 2016;42:1157-1164.
22. Gavin EA, Hammond CJ. Intraocular lens power calculation in short eyes. Eye (Lond). 2008;22:935-938.
23. Eom Y, Kang SY, Song JS, Kim HM. Use of corneal power-specific constants to improve the accuracy of the SRK/T formula. Ophthalmology. 2013;120:477-481.
24. Teshigawara T, Meguro A, Mizuki N. Influence of pupil dilation on the Barrett Universal II (new generation), Haigis (4th generation), and SRK/T (3rd generation) intraocular lens calculation formulas: a retrospective study. BMC Ophthalmol. 2020;20:299.

DOI: 10.4274/tjo.galenos.2022.01057
Turk J Ophthalmol 2022;52:208-211

Case Report

Descemet Stripping Endothelial Keratoplasty for Congenital Aniridia: An Interesting and Challenging Story

Michael Tsatsos*, Ioannis Athanasiadis**, Nikolaos Ziakas*

*Moorfields Eye Hospital NHS Foundation Trust at Bedford Eye Clinic, Bedford, UK
**Second Department of Ophthalmology, Aristotle University of Thessaloniki, Thessaloniki, Greece

Abstract

Congenital aniridia is a rare condition affecting a wide range of ocular structures, from the ocular surface to the retina. We present the case of a 59-year-old woman with PAX6- and WT1-negative congenital aniridia who developed aniridia-associated keratopathy and progressive endothelial dysfunction with corneal decompensation after cataract surgery. The patient underwent successful ultrathin Descemet stripping endothelial keratoplasty. Despite the challenges faced with an unstable iridolenticular diaphragm, we were pleasantly surprised to see improvement not only of corneal edema and endothelial function but also of the whole cornea, including anterior corneal anatomy and appearance. In conclusion, endothelial transplantation in a patient with aniridia resulted in improvement of all the corneal structures from the endothelium to the stroma, epithelium, and possibly even the ocular surface.
Keywords: Aniridia, ocular surface, endothelium, keratoplasty

Introduction

Congenital aniridia (CA) is a rare panocular condition with different inheritance patterns and phenotypic expression. The *PAX6* gene on chromosome 11p13 is a crucial factor in its pathogenesis. The most common form is autosomal dominant CA, which involves only the eyes and has complete penetrance but variable expressivity. Sporadic cases are less frequent and are associated with a de novo mutation. This form of CA can correlate with Miller/WAGR (Wilms tumor, aniridia, genitourinary anomalies, and mental retardation) syndrome. Autosomal recessive CA is the least common variant and can be associated with cerebellar ataxia and mental retardation (Gillespie syndrome).[1]

CA affects a wide range of eye structures, from the ocular surface to the cornea, iris, lens, optic nerve, and macula. The cornea and ocular surface are characteristically affected, and the term aniridia-associated keratopathy is used to describe the progressive ocular surface pathology that greatly contributes to the reduction of the visual acuity of these patients.[2]

Case Presentation

A 59-year-old woman with bilateral CA was referred to our corneal unit for progressive reduction in visual acuity in the right eye associated mainly with endothelial dysfunction. She had previously undergone cataract surgery in the right eye and received an Ophtec aniridia sutured intraocular lens (IOL)

Address for Correspondence: Ioannis Athanasiadis, Second Department of Ophthalmology, Aristotle University of Thessaloniki, Thessaloniki, Greece
E-mail: athana1972@yahoo.com **ORCID-ID:** orcid.org/0000-0002-6236-7540
Received: 01.11.2021 **Accepted:** 12.02.2022

Cite this article as: Tsatsos M, Athanasiadis I, Ziakas N. Descemet Stripping Endothelial Keratoplasty for Congenital Aniridia: An Interesting and Challenging Story. Turk J Ophthalmol 2022;52:208-211

(Ophtec, Netherlands). Fundus examination was challenging, as expected in CA, but we were able to confirm the presence of foveal hypoplasia. This was confirmed with optical coherence tomography.

On examination, the patient had a best corrected visual acuity (BCVA) of hand movements, photophobia, aniridia-associated keratopathy, ptosis, nystagmus, and intraocular pressure of 12 mmHg. There was obvious corneal opacity and edema associated with stromal striae in Descemet's membrane as well as superficial and deep pannus suggesting chronicity of the corneal edema and ocular surface disease (Figure 1). Corneal thickness was measured as 857 μm, but endothelial cell count could not be obtained due to the marked corneal swelling. Genetic testing was negative for *PAX6* and *WT1* gene mutations, indicating sporadic CA with no other systemic involvement.

The patient underwent thin manual Descemet stripping endothelial keratoplasty (TM-DSEK) with 90% air fill on the operating table and developed partially detach of the graft tissue the following day. CA poses a great challenge when performing DSEK surgery, as air bubble management is much more complicated than usual due to the lack of a stable lens/iris diaphragm, even after the use of an aniridia IOL.

An excellent quality corneal graft with an endothelial cell count of 3227 cells/mm^2 was supplied by the Hellenic Eye Bank. An ultrathin endothelial graft was prepared as previously described.[3,4] In brief, a small temporal clear corneal incision of 4.0 mm was made with a keratome blade. A circle was marked on the recipient corneal epithelium with an 8.75-mm disc marker densely coated with gentian violet. A reverse Sinskey hook was then used to score the Descemet's membrane on the posterior side of the host cornea. This was performed under continuous balanced salt solution (BSS) flow through a Simcoe cannula (Sterimedix, Redditch, UK) inserted through a side port. The endothelial graft was inserted correct/stromal side up using the Endoserter device (Ocular Systems Inc., Winston-Salem, North Carolina, USA) and was unfolded by gently sliding the Simcoe into its fold and introducing BSS. It was centered using peripheral pressure from the flow of BSS into the chamber. The wound was closed with three 10-0 nylon sutures and filtered air was injected under the graft to 90% fill. The patient recovered in supine position and was encouraged to avoid standing or sitting as much as possible for the first 2 days.

On the first postoperative day, the graft was partially detached with most of the air escaping posteriorly, probably due to a small crescentic gap between the aniridia IOL and iris remnants (Figure 1), as noted during the postoperative review. As this was a complicated case, we opted to proceed with rebubbling using a 20% SF_6/air mix on the operating table. The endothelial graft remained attached and led to an improvement of visual acuity to 0.55 ETDRS at 6 months postoperatively.

We were surprised to see that 3 months after DSEK surgery, there was a marked improvement of the whole corneal appearance and aniridia-associated keratopathy (Figures 2a,b)

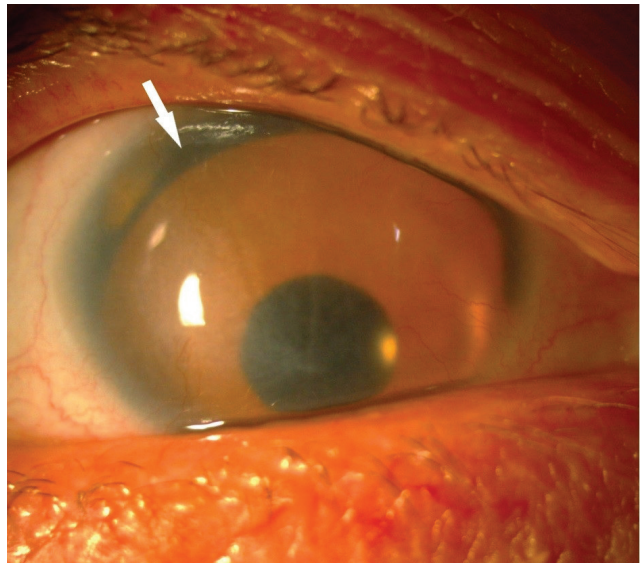

Figure 1. Congenital aniridia preoperatively with a crescentic gap between the aniridia intraocular lens and iris remnants (white arrow)

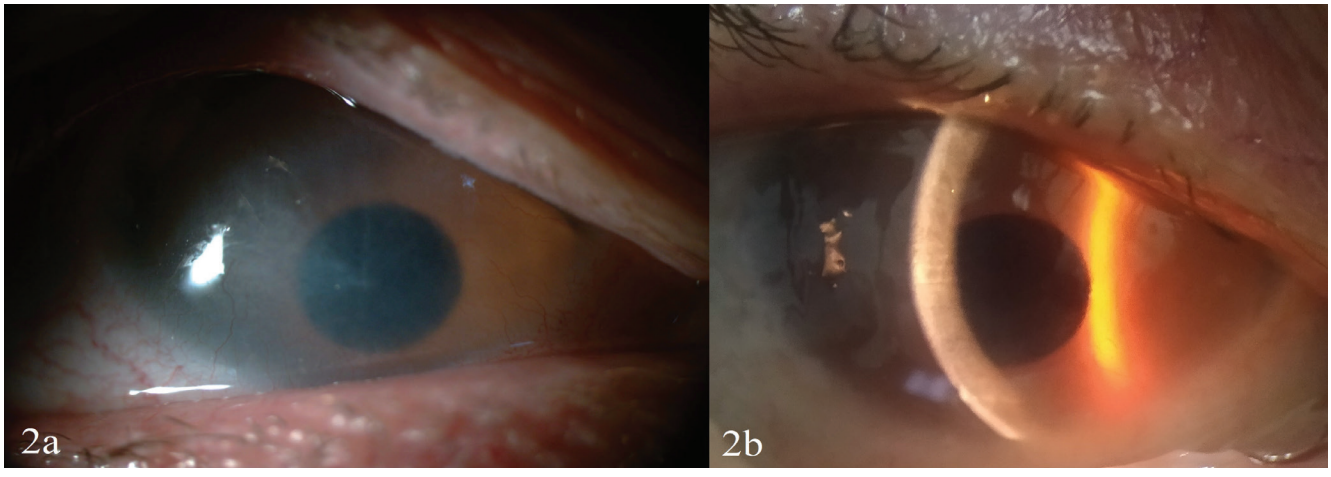

Figure 2. Congenital aniridia preoperatively (a) and 3 months after Descemet stripping endothelial keratoplasty (b)

that remains to date (Figures 3 and 4a,b). Intraocular pressure ranged between 10 and 14 mmHg at postoperative visits. The graft showed a minimum central thickness of 70 µm with total corneal thickness measuring 651 µm at 12 months after DSEK (Figure 5). Graft endothelial cell count reached 2169 cells/mm^2 12 months after surgery. BCVA further improved to 0.52 at postoperative 12 months and the patient maintained this level of vision throughout the follow-up period.

Discussion

Patients with CA pose a great challenge for surgeons because it is a panocular condition with range of pathologies in most of the eye structures. The ocular surface is particularly and characteristically affected, termed aniridia-associated keratopathy. Most patients with CA have a mutation in the *PAX6* gene. The remaining patients seem to have a slightly milder pathology and disease course, as in our patient.[1] Aniridia keratopathy is usually associated with superficial corneal alterations due to limbal stem cell insufficiency. Although endothelial dysfunction is not common, cases of histopathology-proven Descemet's membrane/endothelial damage have previously been reported with subendothelial fibrous membrane present in some cases.[5] Whether this was the case in our patient or the compromised endothelium was partly or totally associated with the previous cataract surgery cannot be ascertained.

DSEK is currently the preferred method for endothelial replacement in cases of aniridia as it offers minimal risk of posterior dislocation and easier manipulation compared to Descemet's membrane endothelial keratoplasty.[6]

We noticed that in our patient, the corneal stroma and ocular surface showed improvement after DSEK despite being significantly affected preoperatively. This was associated with a marked improvement in BCVA from hand movements to 0.55 LogMAR, reduced fluorescein staining, and an increase in tear film break-up time to 5-6 seconds from 2-3 seconds preoperatively (Figure 4a,b). This great visual outcome and improvement in the appearance of the whole cornea was maintained throughout the 2-year follow-up period. Although this improvement could be related to the reduction of corneal swelling and epithelial edema after restoring corneal endothelial function, the extent of improvement in the corneal surface could not be fully explained.

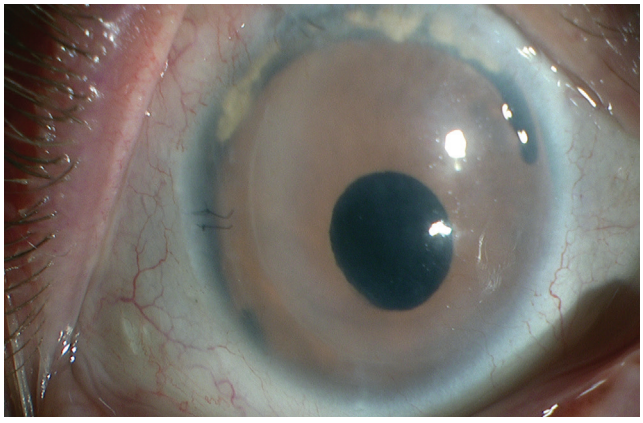

Figure 3. Appearance 12 months after Descemet stripping endothelial keratoplasty

Figure 5: Corneal optical coherence tomography of the right eye 12 months after Descemet stripping endothelial keratoplasty

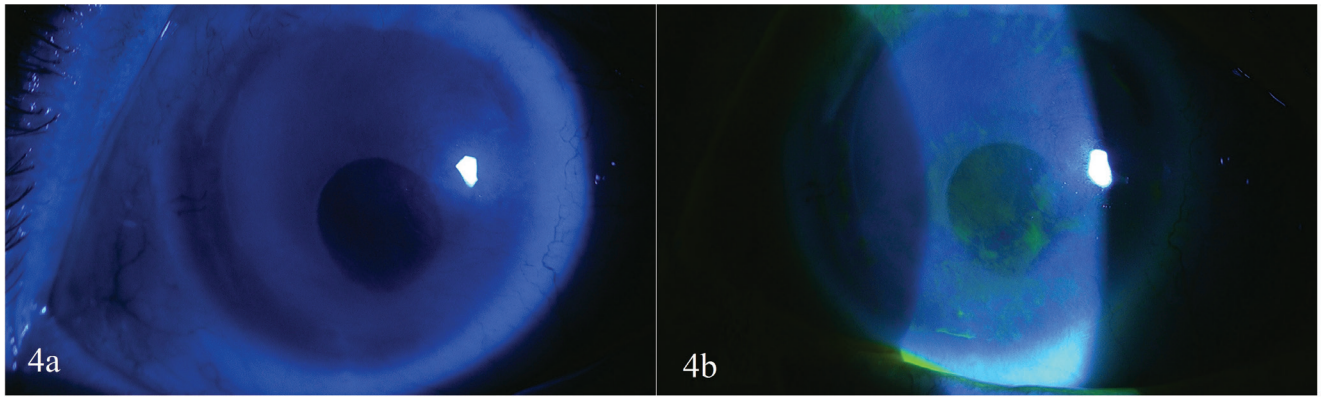

Figure 4. Postoperative cobalt blue light images of the right eye without (a) and with (b) fluorescein staining

This is the first reported case in which endothelial transplantation in a patient with aniridia resulted in improvement of the whole corneal appearance. CA is a complex pathology affecting all of the corneal (and other) structures. We observed improvement of the whole corneal appearance and function, including improved tear break-up time and superficial staining following successful TM-DSEK. A number of explanations for this can be suggested, but the mechanism remains to be elucidated. Interestingly, Zola et al.[7] demonstrated improved corneal clarity and reduced density of anterior subepithelial fibrosis following endothelial keratoplasty in non-aniridic eyes. They proposed a cascade of corneal remodeling following resolution of stromal edema after Descemet stripping automated endothelial keratoplasty, amongst other factors, as a possible mechanism for this improvement, which suggests that a similar interaction could be the reason behind the great improvement seen in our case. Although the preoperative endothelial dysfunction may have contributed to the worsening of the ocular surface disease, the improvement noted after restoration of endothelial function cannot be fully explained. There may still be an underlying association or synergistic interaction between stromal keratocytes, limbal stem cells, and corneal endothelium that is responsible for the health of the whole cornea and hence of corneal integrity.

Ethics

Informed Consent: Obtained.

Peer-review: Externally peer reviewed.

Authorship Contributions

Surgical and Medical Practices: M.T., Concept: M.T., Design: M.T., Data Collection or Processing: M.T., I.A., Analysis or Interpretation: M.T., I.A., N.Z., Literature Search: M.T., I.A., N.Z., Writing: M.T., I.A., N.Z.

Conflict of Interest: No conflict of interest was declared by the authors.

Financial Disclosure: The authors declared that this study received no financial support.

References

1. Tripathy K, Salini B. Aniridia. In: StatPearls [Internet]. Treasure Island (FL): StatPearls Publishing; 2020.
2. Ihnatko R, Eden U, Fagerholm P, Lagali N. Congenital Aniridia and the Ocular Surface. Ocul Surf. 2016;14:196-206.
3. Tsatsos M, Konstantopoulos A, Hossain P, Anderson D. Presoaking with BSS used for thin manually dissected DSEK (TMDSEK): a viable option for thin DSEK. Eye (Lond). 2014;28:701-704.
4. Tsatsos M, Athanasiadis I, Kopsachilis N, Krishnan R, Hossain P, Anderson D. Comparison of the Endosaver with noninjector techniques in Descemet's stripping endothelial keratoplasty. Indian J Ophthalmol. 2017;65:1133-1137.
5. Bausili MM, Alvarez de Toledo J, Barraquer RI, Michael R, Tresserra F, de la Paz MF. Histopathology Findings of Corneal Buttons in Congenital Aniridia Patients. Ophthalmic Res. 2016;56:202-206.
6. Veldman PB, Terry MA, Straiko MD. Evolving indications for Descemet's stripping automated endothelial keratoplasty. Curr Opin Ophthalmol. 2014;25:306-311.
7. Zola M, Kim J, Petrelli M, Schmutz L, Hashemi K, Kymionis G. Resolution of Corneal Fibrosis After Descemet's Stripping Automated Endothelial Keratoplasty: A Case Report. Ophthalmol Ther. 2020;9:349-354.

DOI: 10.4274/tjo.galenos.2022.86681
Turk J Ophthalmol 2022;52:212-215

Case Report

Asymptomatic Unilateral Full-Thickness Macular Hole in a Patient with Bietti Crystalline Dystrophy During 13-Year Follow-up with Optical Coherence Tomography

Ali Osman Saatci*, Mustafa Kayabaşı*, Remzi Avci**

*Dokuz Eylül University Faculty of Medicine, Department of Ophthalmology, İzmir, Turkey
**Retina Eye Hospital, Bursa, Turkey

Abstract

A 39-year-old woman with progressive bilateral visual decline was diagnosed as having Bietti crystalline dystrophy in 2008. The disease course was monitored with optical coherence tomography until 2021. During the last routine eye examination in 2021, a full-thickness, slightly eccentric, visually asymptomatic macular hole with an intact foveola was noted in the left eye. No surgical treatment was recommended. The pathogenesis of full-thickness macular hole remained unclear as there were only subtle signs of prior very mild macular edema and vitreomacular interface abnormality. A degenerative process was also possible.

Keywords: Bietti crystalline dystrophy, macula, macular hole, optical coherence tomography

Introduction

Bietti crystalline dystrophy (BCD) is a rare, genetically determined retinal dystrophy characterized by shiny yellow crystalline deposits in the retina and less frequently in the limbus, together with progressive chorioretinal atrophy mainly commencing at the posterior pole.[1,2,3]

Rare macular complications previously reported in patients with BCD include macular hole,[4,5,6,7] cystoid macular edema,[8] subfoveal neurosensorial detachment,[9] and macular neovascular membrane.[10,11,12]

We hereby report the longitudinal optical coherence tomography (OCT) follow-up of a woman who developed a unilateral full-thickness macular hole 13 years after the first examination.

Case Presentation

In 2008, we examined a 39-year-old otherwise healthy woman who presented with bilateral progressive visual decline of at least 10 years' duration. There was no family history, consanguinity, or similarly affected family member. On examination, best corrected visual acuity was 6/10 on Snellen chart bilaterally. Crystalline deposits were observed in the superior corneal limbus of both eyes. Intraocular pressure was 16 mmHg bilaterally. Fundus examination and fluorescein angiography revealed scattered, refractile retinal deposits at the posterior pole and surrounding retina in association with areas of retina pigment epithelium (RPE) atrophy in both eyes (Figure 1 A-D). On OCT, intraretinal hyperreflective dots, bright plaques over the Bruch's membrane-RPE complex, and outer retinal tubulations were

Address for Correspondence: Ali Osman Saatci, Dokuz Eylül University Faculty of Medicine, Department of Ophthalmology, İzmir, Turkey
E-mail: osman.saatci@yahoo.com **ORCID-ID:** orcid.org/0000-0001-6848-7239
Received: 27.01.2022 **Accepted:** 28.03.2022

Cite this article as: Saatci AO, Kayabaşı M, Avci R. Asymptomatic Unilateral Full-Thickness Macular Hole in a Patient with Bietti Crystalline Dystrophy During 13-Year Follow-up with Optical Coherence Tomography.. Turk J Ophthalmol 2022;52:212-215

detected (Figure 1 E,F). Our clinical diagnosis was BCD and we examined the patient several times between 2008 and 2018 and obtained consecutive OCT images (Figure 2 A-H).

The patient recently underwent an ophthalmic examination in December 2021 following a long COVID-related interruption. However, she denied any recent visual symptoms. Her best-corrected visual acuity was Snellen 4/10 in the right eye with correction of -2.00 -2.25x15 and 6/10 in the left eye with correction of -3.75 -1.00x150 (sphere, cylinder x axis). Anterior segment examination was unremarkable bilaterally. We noted advanced chorioretinal atrophy and reduced number of retinal crystalline deposits at the both posterior pole (Figure 3 A-D). However, serial OCT sections and en-face OCT angiography slabs revealed a slightly eccentric full-thickness macular hole with an intact foveola in the left eye (Figure 4 A-G). As the patient was asymptomatic and the appearance of hole was only observed in two consecutive B-scans 132 µm apart, surgery was not recommended, and we advised her to have more frequent visits.

Discussion

Partial and full-thickness macular defects can by caused by tractional forces on the fovea or may arise from anomalous posterior vitreous detachment and contraction of an epiretinal membrane. In addition, cystoid macular edema and high myopia can also lead to macular hole formation.[13]

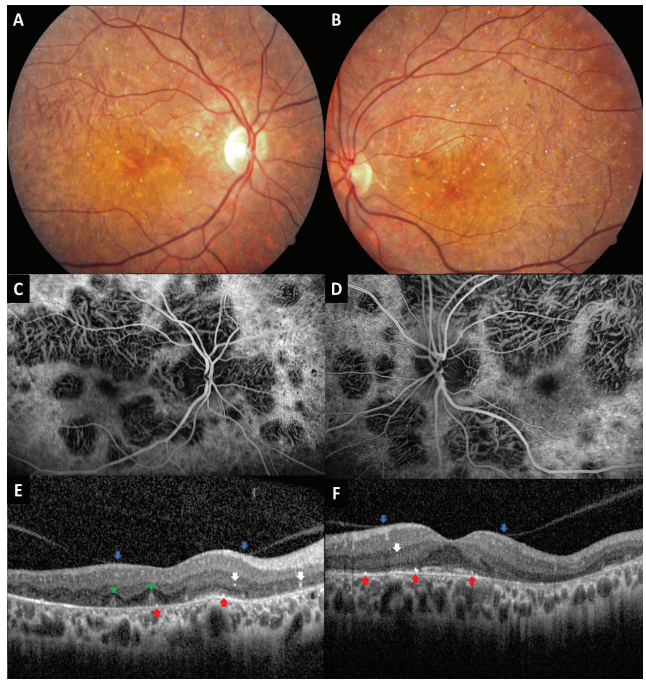

Figure 1. Examination in 2008. Color fundus images of the right (A) and left (B) eyes show scattered intraretinal crystals at the posterior pole with subtle chorioretinal atrophy. Composite venous phase fluorescein angiogram of the right (C) and left (D) eyes reveal patchy hypofluorescent areas corresponding to areas of chorioretinal atrophy. Optical coherence tomographic sections from the right (E) and left (F) eyes demonstrate a few hyperreflective dots corresponding to intraretinal crystals (white arrows), vitreoretinal adhesions (blue arrows), outer retinal tubulations (green arrowheads) and bright plaques on top of the

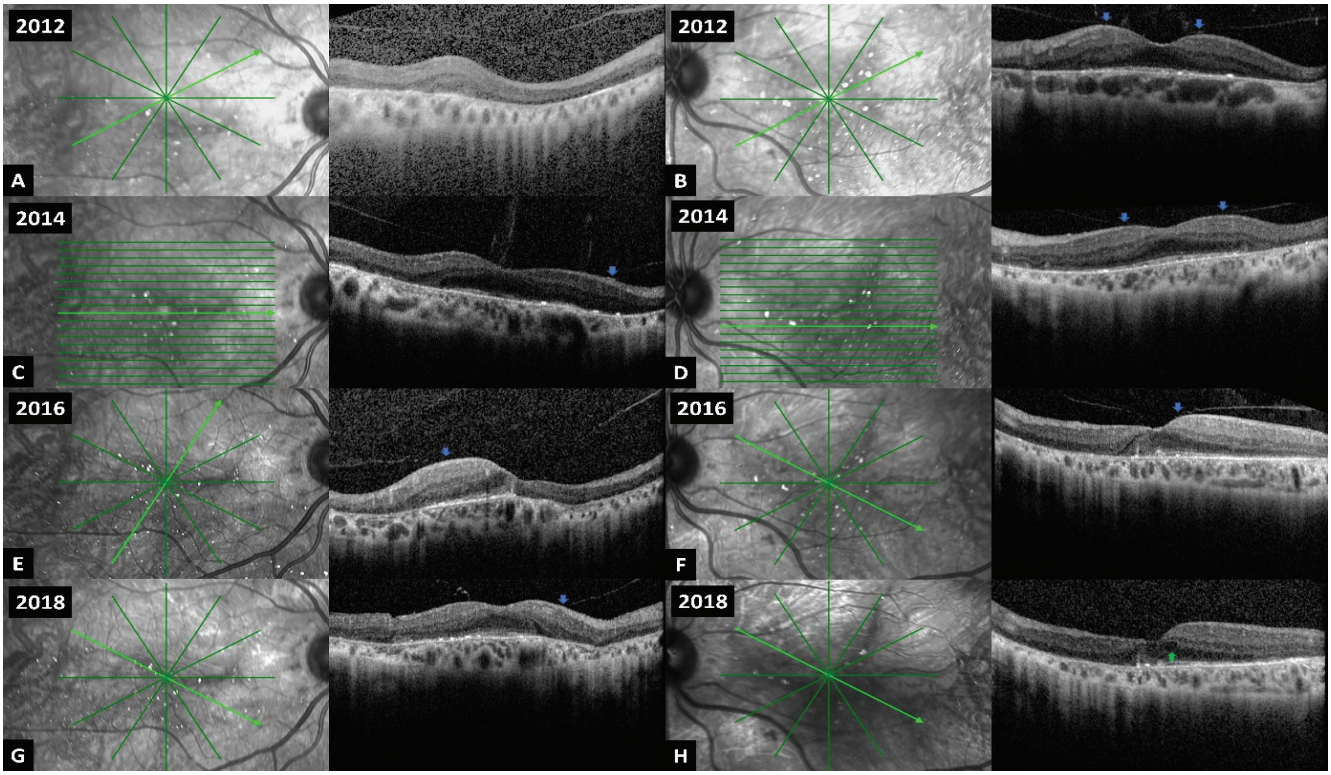

Figure 2. Consecutive optical coherence tomographic sections with related reflectance images taken from the right (A, C, E, G) and left (B, D, F, H) eyes between 2012 and 2018. Note the subtle cystic macular changes in the left eye (green arrow). Vitreoretinal adhesions are marked with blue arrows

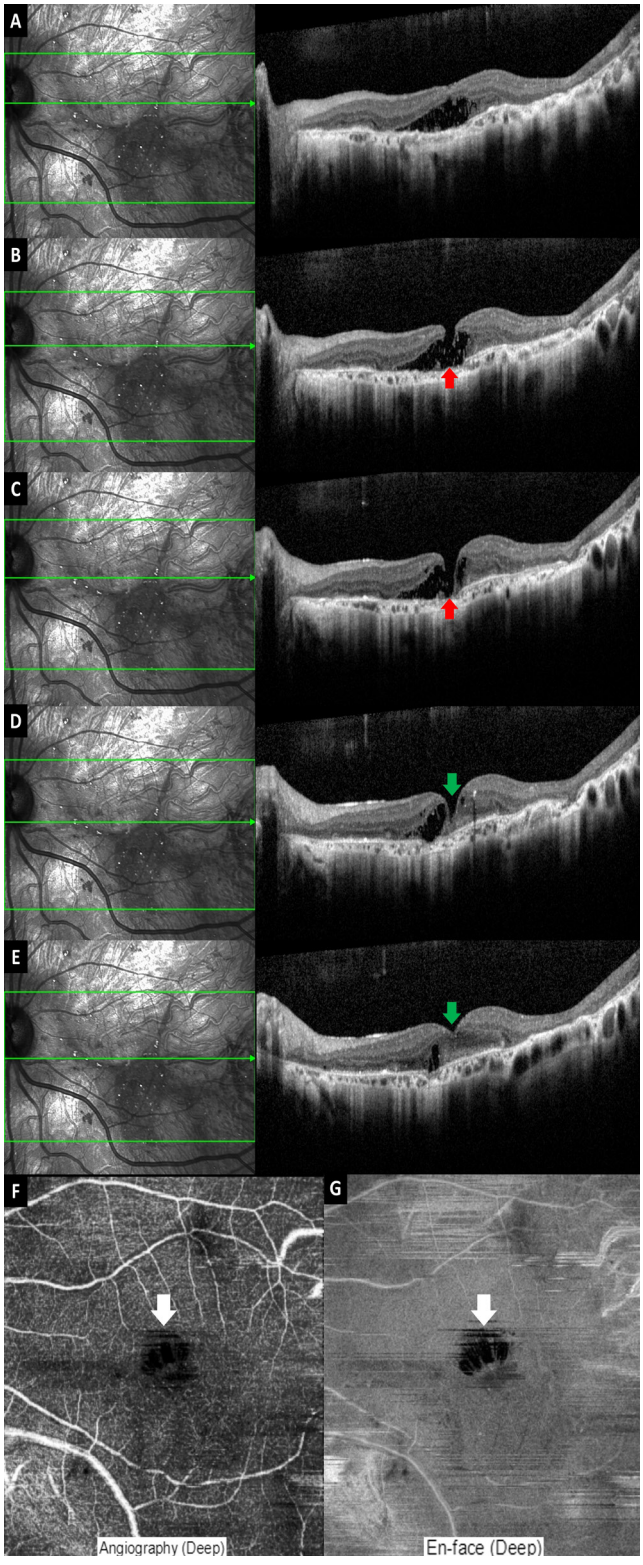

Figure 4. Consecutive optical coherence tomographic sections taken in the left eye at 132-µm intervals (A-E) show the full-thickness eccentric hole (red arrows) with the intact foveola (green arrows). Optical coherence tomography angiographic section (F) and en-face image (G) of deep vascular plexus slabs reveal a central flow void corresponding to the hole (white arrows)

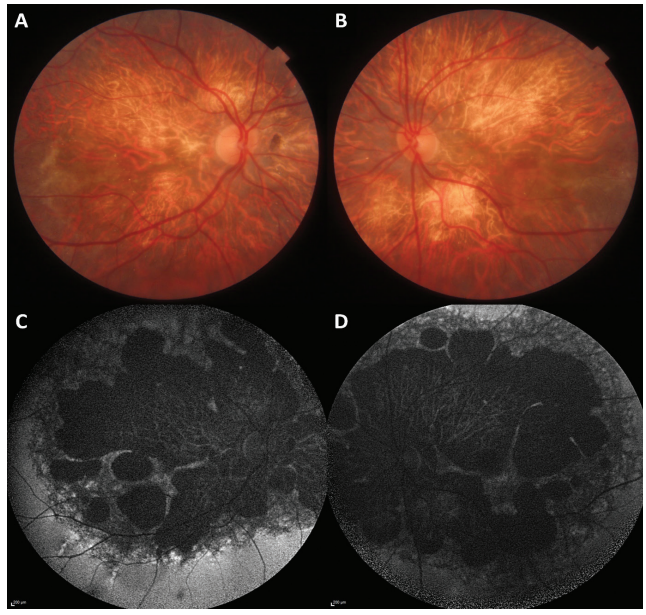

Figure 3. Examination in 2021. Color fundus images of the right (A) and left (B) eyes show marked chorioretinal atrophy and near complete absence of intraretinal crystals at the posterior pole. Fundus autofluorescence images of the right (C) and left (D) eyes demonstrate extensive hypoautofluorescent areas

There are only a few anecdotal reports of macular holes in patients with BCD and thus, its pathogenesis is still somewhat obscure. Bagolini and Ioli-Spada[4] reported a series of eight patients with BCD, of whom two were previously followed by Bietti. One of these patients was a 31-year-old highly myopic woman with bilateral retinal detachment and a unilateral macular hole. We previously reported a 21-year-old man who developed a stage 4 full-thickness unilateral macular hole with surrounding macular detachment three years after initial examination.[5] Ji et al.[6] reported bilateral macular holes in a 32-year-old man with stage 3 BCD according to Yuzawa's[1] clinical disease staging. No surgery was performed, and the authors did not elaborate on the pathogenetic mechanism of the macular hole development. Nourinia et al.[7] described a 42-year-old man who was followed for 10 years and developed a unilateral full-thickness macular hole. Pars plana vitrectomy with internal limiting membrane peeling and gas injection was performed, and the hole was closed successfully following the surgery.

The pathogenesis of full-thickness macular hole formation is not clear in the present case. We reanalyzed all of the previous OCT sections from the left eye and noticed very mild macular edema and vitreomacular interface abnormality in some of the sections. It is likely that a degenerative process might have also been a factor in the hole formation. Talib et al.[14] shared their observations in a case with choroideremia and unilateral full-thickness macular hole and argued that chronic low-grade inflammation originating from the outer retinal cells might have contributed to the hole formation. On the other hand, Müller cells might have a role as they transmit the traction forces from the inner to outer retina, leading to central photoreceptor layer defects and even neurosensorial retinal detachment.[13]

We elected to follow the patient for the time being as the patient was asymptomatic, most likely due to slight eccentric location of the full-thickness hole with the intact foveola. Her left eye had also less chorioretinal atrophy when compared to the fellow eye and was the better-seeing eye.

Full-thickness macular hole is very rarely observed in association with BCD and has a yet undetermined and possibly multifactorial pathogenesis. We recommend frequent ophthalmic examinations and careful tomographic monitoring in patients with BCD to detect any macular changes, including macular hole.

Ethics

Informed Consent: Obtained.

Peer-review: Externally and internally peer reviewed.

Authorship Contributions

Concept: A.O.S., M.K., R.A., Design: A.O.S., M.K., R.A., Data Collection or Processing: A.O.S., M.K., R.A., Analysis or Interpretation: A.O.S., M.K., R.A., Literature Search: A.O.S., M.K., R.A., Writing: A.O.S., M.K., R.A.,

Conflict of Interest: No conflict of interest was declared by the authors.

Financial Disclosure: The authors declared that this study received no financial support.

References

1. Yuzawa M, Mae Y, Matsui M. Bietti's crystalline retinopathy. Ophthalmic Paediatr Genet. 1986;7:9-20.
2. Osman Saatci A, Can Doruk H. An Overview of Rare and Unusual Clinical Features of Bietti's Crystalline Dystrophy. Med Hypothesis Discov Innov Ophthalmol. 2014;3:51-56.
3. Bozkurt B, Ozturk BT, Kerimoglu H, Irkec M, Pekel H. In vivo confocal microscopic findings of 2 patients with Bietti crystalline corneoretinal dystrophy. Cornea. 2010;29:590-593.
4. Bagolini B, Ioli-Spada G. Bietti's tapetoretinal degeneration with marginal corneal dystrophy. Am J Ophthalmol. 1968;65:53-60.
5. Saatci AO, Yaman A, Berk AT, Söylev MF. Macular hole formation in Bietti's crystalline retinopathy. A case report. Ophthalmic Genet. 1997;18:139-141.
6. Ji SX, Yin XL, He XG, Yuan RD, Ye J, Liu SZ, Gan XM, Dong Y. Bietti crystalline dystrophy with bilateral macular holes. Retin Cases Brief Rep. 2009;3:361-363.
7. Nourinia R, Dehghan MH, Fekri S. Outcome of Macular Hole Surgery in Bietti Crystalline Dystrophy. J Ophthalmic Vis Res. 2017;12:338-341.
8. Saatci AO, Doruk HC, Yaman A. Cystoid Macular Edema in Bietti's Crystalline Retinopathy. Case Rep Ophthalmol Med. 2014;2014:964892.
9. Padhi TR, Kesarwani S, Jalali S. Bietti crystalline retinal dystrophy with subfoveal neurosensory detachment and congenital tortuosity of retinal vessels: case report. Doc Ophthalmol. 2011;122:199-206.
10. Atmaca LS, Muftuoglu O, Atmaca-Sonmez P. Peripapillary choroidal neovascularization in Bietti crystalline retinopathy. Eye (Lond). 2007;21:839-842.
11. Nachiappan K, Krishnan T, Madhavan J. Ranibizumab for choroidal neovascular membrane in a rare case of Bietti's crystalline dystrophy: a case report. Indian J Ophthalmol. 2012;60:207-209.
12. Kobat SG, Gul FC, Yusufoglu E. Bietti crystalline dystrophy and choroidal neovascularization in childhood. Int J Ophthalmol. 2019;12:1514-1516.
13. Bringmann A, Unterlauft JD, Barth T, Wiedemann R, Rehak M, Wiedemann P. Müller cells and astrocytes in tractional macular disorders. Prog Retin Eye Res. 2022;86:100977.
14. Talib M, Koetsier LS, MacLaren RE, Boon CJF. Outcome of Full-Thickness Macular Hole Surgery in Choroideremia. Genes (Basel). 2017;8:187.

DOI: 10.4274/tjo.galenos.2022.05860
Turk J Ophthalmol 2022;52:216-219

Case Report

Sheath-Preserving Complete Optic Nerve Avulsion Following Closed-Globe Injury: A Case Report

Seray Şahin, Onur Furundaoturan, Mine Esen Barış, Elif Demirkılınç Biler

Ege University Faculty of Medicine, Department of Ophthalmology, İzmir, Turkey

Abstract

A 29-year-old man presented with a sudden loss of vision after a closed-globe injury. At presentation, he had no light perception in the right eye and the right pupil was dilated and nonreactive to light. On ophthalmological examination, the area of the optic nerve head was excavated, suggesting optic nerve avulsion. Magnetic resonance imaging scan showed optic nerve avulsion without rupture of the optic nerve sheath. Four months after the injury, the patient's visual acuity remained unchanged. Gliosis developed at the avulsion site. Closed-globe injuries may cause severe posterior injury even if there is no anterior damage in the eye. To prevent unnecessary treatment, trauma patients should be examined carefully appropriate imaging to confirm the diagnosis.

Keywords: Traumatic optic nerve avulsion, closed globe injuries, complete optic nerve avulsion, optic nerve sheath

Introduction

Optic nerve avulsion is the forced disinsertion of the optic nerve from the retina, choroid and vitreous, characterized by retraction of the lamina cribrosa from the scleral rim while the optic nerve sheath is preserved.[1] It is a rare and severe complication of ocular blunt trauma. Optic nerve damage may be complete or partial. In complete avulsion, the damage usually occurs in the optic canal or orbit; the intracranial part of the nerve is rarely involved because of its mobility.[2] Previously published reports and observations of traumatic optic nerve avulsion suggested that a sudden rise in the intraocular pressure, sudden rotation of the globe, anterior luxation, and other factors might be responsible for this unique complication.[1,2,3,4] In this case report, we describe a young man with complete optic nerve avulsion and intact sheath caused by compressed air hose injury.

Case Presentation

A 29-year-old man was referred to the emergency department with periorbital edema, pain, and sudden loss of vision in the right eye following blunt trauma with a compressed air hose. In ophthalmological examination, visual acuity in the right eye was no light perception. The right pupil was dilated and nonreactive to light. Proptosis, chemosis, conjunctival laceration, and subconjunctival air bubbles were observed on anterior segment examination of the right eye. The cornea and lens were clear. Posterior segment examination revealed the presence of retinal

Address for Correspondence: Mine Esen Barış, Ege University Faculty of Medicine, Department of Ophthalmology, İzmir, Turkey
E-mail: mine.baris@yahoo.com **ORCID-ID:** orcid.org/0000-0003-1341-6737
Received: 16.08.2021 **Accepted:** 17.02.2022

Cite this article as: Şahin S, Furundaoturan O, Barış ME, Demirkılınç Biler E. Sheath-Preserving Complete Optic Nerve Avulsion Following Closed-Globe Injury: A Case Report. Turk J Ophthalmol 2022;52:216-219

ischemia affecting all quadrants of the fundus with vitreous hemorrhage located inferiorly and preretinal hemorrhages. The area of the optic nerve head was excavated, suggesting optic nerve avulsion, and filled with hemorrhage, with blood emanating into the vitreous and a ring of peripapillary hemorrhage (Figure 1).

Intraocular pressures (IOP) were 12 mmHg in the right eye and 18 mmHg in the left eye. Visual acuity of the left eye was 20/20 without correction and the light reflex of the left pupil was normal. Anterior and posterior segment examinations of the left eye were also normal.

Normal IOP of the right eye suggested that the sclera was intact, but due to excessive chemosis and subconjunctival hemorrhage, urgent explorative surgery was planned in order to search for a rupture site. Otorhinolaryngology and neurosurgery consultations were requested. Neurosurgery recommended a 24-hour follow-up cranial computed tomography (CT) scan for pneumocephalus. The explorative surgery was canceled due to suspected cerebrospinal fluid fistula.

On CT, fractures were observed in the medial wall of the right orbit and ethmoidal cell walls. Magnetic resonance imaging (MRI) and CT scan showed optic nerve avulsion without rupture of the optic nerve sheath and posttraumatic pneumocephalus (Figures 2 and 3).

Flash visual evoked potentials (VEP) revealed delayed latency and decreased P wave amplitude in the right eye.

Four months after injury, the patient's visual acuity remained unchanged. Gliosis developed at the avulsion site (Figure 4)

Discussion

In cases of high-velocity injuries to the periorbital structures, the impact of blunt trauma plays a vital role in the displacement of tissues within the orbit. During blunt trauma to the orbital margin, Bell's phenomenon occurs as a natural protective mechanism. This induces certain changes in the anatomical orientation of the globe with respect to the horizontal, vertical, and anteroposterior axes.[5] The loss of myelin and absence of supportive connective tissue septae make the axons at the lamina cribrosa particularly vulnerable.[6]

There are several mechanisms reported to be responsible for this rare entity. Pujari et al.[5] reported that anterior globe luxation is more important in the pathomechanism of traumatic optic nerve avulsion, whereas a sudden rise in IOP leading to posterior rupture of the optic nerve appears to be of lesser significance since most cases of ocular blunt trauma are not accompanied by optic nerve avulsion. In our case, we suspect that the whiplash motion of the hose combined with its high velocity might have caused a sudden rotation and perhaps anterior displacement of the globe, resulting in optic nerve avulsion. Optic nerve avulsion is defined as a traumatic disinsertion of the nerve fibers at the disc margin.[4] Although preservation of the optic nerve sheath has rarely been reported in cases in the literature, MRI demonstrated an intact optic nerve sheath in this case.

Optic nerve avulsion mainly presents as a dense hemorrhagic manifestation along the optic nerve head with or without other vascular complications.[5] Retinal ischemia is also observed because of associated central retinal arterial injury. In the literature, avulsion of the optic nerve occurred mostly at the junction of the nerve and globe, but there are cases reported with different avulsion sites. Tamase et al.[7] reported a case in which the optic nerve was split distal to the optic chiasm and temporal hemianopsia developed in the contralateral eye. In our case, the avulsion site was similar to the literature and the fellow eye was

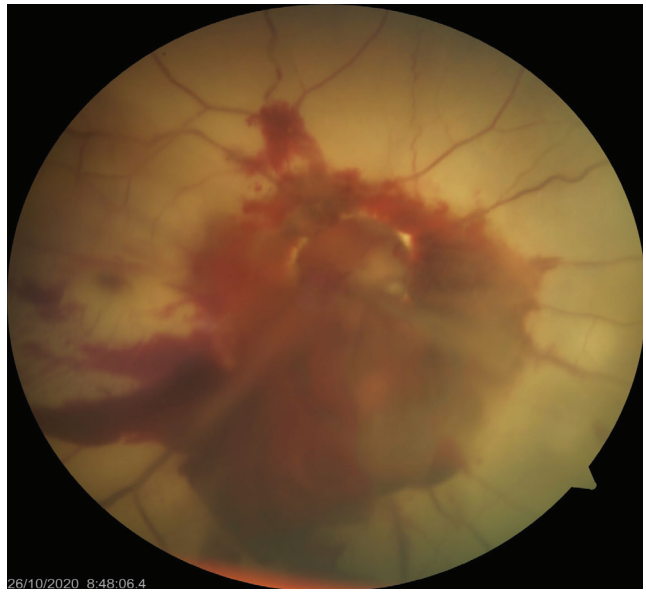

Figure 1. Image of total optic nerve avulsion showing an empty optic disc, vitreous hemorrhage, and ischemic retina

Figure 2. Initial computed tomography scan showing optic nerve avulsion (red arrow) without rupture of the optic nerve sheath and posttraumatic pneumocephalus (yellow arrow)

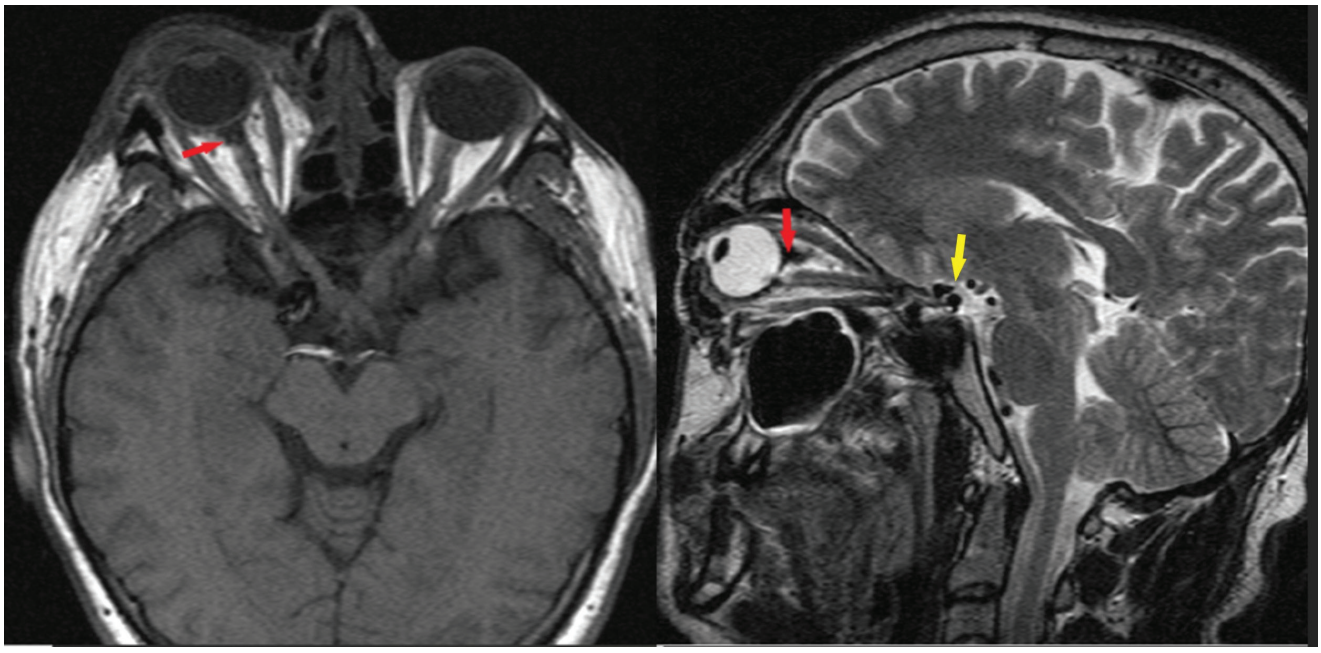

Figure 3. T1-weighted axial MRI and T2-weighted sagittal MRI showing the site of optic nerve avulsion (red arrows) and pneumocephalus (yellow arrow)
MRI: Magnetic resonance imaging

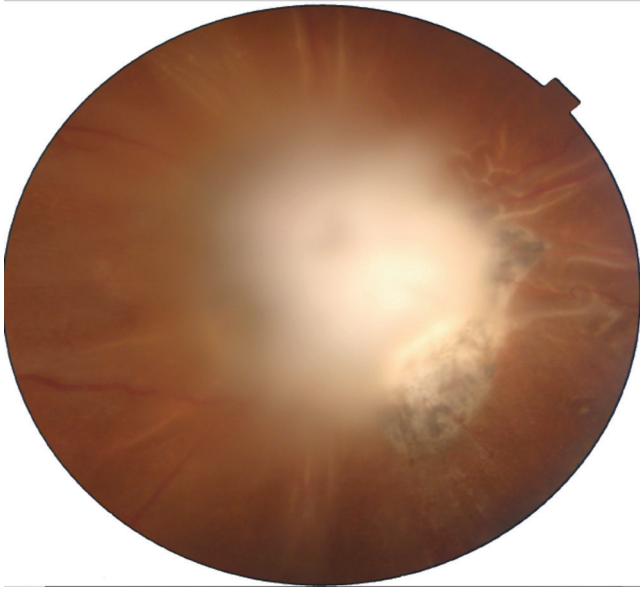

Figure 4. Gliosis developed months after the incident

not affected.

Optic nerve avulsion has been reported after injuries with various causes, such as iron bars, bear attack, or falling from a tree.[7,8,9] Complete optic nerve avulsion occurred in all of these cases, but the optic nerve sheath was not intact. Mumcuoglu et al.[10] reported a case of partial optic nerve avulsion with preservation of the sheath.

In the present case, the injury was a result of blunt trauma caused by a compressed air hose. Complete avulsion of the optic nerve rarely occurs with preservation of the optic nerve sheath, as in our case.

Blunt orbital trauma may cause severe posterior injury even if there is no anterior damage in the eye.

Sawhney et al.[1] reported optic disc excavation in traumatic avulsion cases, but the diagnosis can be hidden because of vitreous hemorrhage. It is essential to confirm the diagnosis so that the patient is not subjected to unnecessary treatment such as optic nerve decompression or high-dose steroids.

Patients can be monitored for complications including phthisis bulbi and secondary neovascularization or rubeotic glaucoma.[11]

Lastly, this case once again demonstrates the importance of using safety goggles.

Ethics

Informed Consent: Obtained.

Peer-review: Externally peer reviewed.

Authorship Contributions

Concept: S.Ş., O.F., M.E.B., Design: S.Ş., O.F., M.E.B., E.D.B., Data Collection or Processing: S.Ş., M.E.B., Analysis or Interpretation: S.Ş., O.F., M.E.B., E.D.B., Literature Search: S.Ş., O.F., M.E.B., Writing: S.Ş., M.E.B.

Conflict of Interest: No conflict of interest was declared by

the authors.

Financial Disclosure: The authors declared that this study received no financial support.

References

1. Sawhney R, Kochhar S, Gupta R, Jain R, Sood S. Traumatic optic nerve avulsion: role of ultrasonography. Eye (Lond). 2003;17:667-670.
2. Mackiewicz J, Tomaszewska J, Jasielska M. Optic nerve avulsion after blunt ocular trauma - Case report. Ann Agric Environ Med. 2016;23:382-383.
3. Lohmror I, Hada M, Agarwal V, Khilnani K. Optic nerve avulsion associated with central retinal artery occlusion following rotational globe injury. Indian J Ophthalmol. 2018;66:1040-1041.
4. Foster BS, March GA, Lucarelli MJ, Samiy N, Lessell S. Optic nerve avulsion. Arch Ophthalmol. 1997;115:623-630.
5. Pujari A, Saxena R, Phuljhele S, Bhaskaran K, Basheer S, Sharma P. Pathomechanism of optic nerve avulsion. Med Hypotheses. 2019;125:28-30.
6. Anand S, Harvey R, Sandramouli S. Accidental self-inflicted optic nerve head avulsion. Eye (Lond). 2003;17:646-647.
7. Tamase A, Tachibana O, Iizuka H. Usefulness of MRI Slices Parallel to the Optic Chiasma in a Case with Traumatic Optic Nerve Avulsion after a Bear Attack. Neurol Med Chir (Tokyo). 2019;59:357-359.
8. Değirmenci MFK, Yalçındağ N, Atilla H. Optic Nerve Avulsion and Retinal Detachment After Penetrating Ocular Trauma: Case Report. Turk J Ophthalmol. 2018;48:89-91.
9. Liu Y, Wang J, Zhu D. Avulsion of Optic Nerve and Peripapillary Retina. Retina. 2020;40:e22-e23.
10. Mumcuoglu T, Durukan HA, Erdurman C, Hurmeric V, Gundogan FC. Functional and structural analysis of partial optic nerve avulsion due to blunt trauma: case report. Indian J Ophthalmol. 2010;58:524-526.
11. Davidson A, Jackson D, Painter S, Parmar B. Traumatic optic nerve head avulsion. BMJ. 2017;359:j4881.

DOI: 10.4274/tjo.galenos.2022.53484
Turk J Ophthalmol 2022;52:220

Letter to the Editor re: "Refractive and Vision Status in Down Syndrome: A Comparative Study"

Pathum Sookaromdee*, Viroj Wiwanitkit**

*Private Academic Consultant, Bangkok, Thailand
**Department of Community Medicine, DY Patil University, Pune, India

Keywords: Down syndrome, refractive, vision

Dear editor,

We would like to share our ideas on the publication "Refractive and Vision Status in Down Syndrome: A Comparative Study."[1] Hashemi et al.[1] concluded that *"In DS patients, the prevalence rates of refractive errors, amblyopia, and visual impairment are higher than those in non-DS individuals."* Regarding DS and refractive/vision problems, there should be a hypothesis for the clinical association. How DS might contribute to ocular problems should be proposed. In a recent report, the possible mechanism was cerebral visual impairment, not an intraocular problem.[2] This might not be concluded based on the findings of the present study. An important concern is about the control group. The control group is only a group of non-DS cases but not healthy controls. For example, "candidates for refractive surgery" must have an ocular problem. Additionally, Hashemi et al.[1] mentioned "age- and gender-matched normal controls," but there were unequal numbers of subjects in the patient and control groups. Hence, there might be a methodological flaw and bias.

Peer-review: Internally peer reviewed.

Authorship Contributions

Concept: P.S., V.W., Design: P.S., V.W., Data Collection or Processing: P.S., V.W., Analysis or Interpretation: P.S., V.W., Literature Search: P.S., V.W., Writing: P.S., V.W.

Conflict of Interest: No conflict of interest was declared by the authors.

Financial Disclosure: The authors declared that this study received no financial support.

References

1. Hashemi H, Mehravaran S, Asgari S, Dehghanian Nasrabadi F. Refractive and Vision Status in Down Syndrome: A Comparative Study. Turk J Ophthalmol. 2021;51:199-205.
2. Wilton GJ, Woodhouse R, Vinuela-Navarro V, England R, Woodhouse JM. Behavioural Features of Cerebral Visual Impairment Are Common in Children with Down Syndrome. Front Hum Neurosci. 2021;15:673342.

Address for Correspondence: Pathum Sookaromdee, Private Academic Consultant, Bangkok, Thailand
E-mail: pathumsook@gmail.com **ORCID-ID:** orcid.org/0000-0002-8859-5322
Received: 01.09.2021 **Accepted:** 09.03.2022

Cite this article as: Sookaromdee P, Wiwanitkit V. Letter to the Editor re: "Refractive and Vision Status in Down Syndrome: A Comparative Study". Turk J Ophthalmol 2022;52:220

DOI: 10.4274/tjo.galenos.2022.46037
Turk J Ophthalmol 2022;52:221-222

Reply to Letter to the Editor re: "Refractive and Vision Status in Down Syndrome: A Comparative Study"

Hassan Hashemi*, Shiva Mehravaran**, Soheila Asgari*, Farzaneh Dehghanian Nasrabadi***

*Noor Eye Hospital, Noor Ophthalmology Research Center, Tehran, Iran
**School of Computer, Mathematical, and Natural Sciences, Morgan State University, Baltimore, MD, USA
***Iran University of Medical Sciences, School of Rehabilitation, Department of Optometry, Tehran, Iran

Keywords: Down syndrome, visual impairment, refractive error

We are grateful for your kind attention to our manuscript.[1] This paper presented the prevalence of amblyopia and refractive errors in patients with Down syndrome (DS), however, we did not investigate their types and causes. In other words, this paper provides a description of visual dysfunction in this population, but no causal inference can be drawn regarding the relationship between DS and cerebral visual impairment (CVI). On the other hand, the study conducted by Wilton et al.[2] did not have a causality design. They only carried out a cross-sectional study using a questionnaire rather than neurologic assessment to find that 38.0% of the DS patients were suspected CVI cases. Even with predictive models, only 62.0% of the suspected CVI was correctly detected. For these reasons, the results of our study and those of Wilton et al.[2] are not contradictory.[1]

The second comment was related to the control group. As reported in the other paper of this project, the DS population comprised known cases (according to genetic testing results in the medical records) regardless of refractive error status.[3] Therefore, the control group must have included non-DS subjects regardless of their refractive error status. If the criteria used to select the control group included normal subjects without refractive errors, matching would have been biased. Considering the objective of the study, matching was only done for age and sex. Your comment would apply to the assessment of the association between DS and the type of visual impairment (cerebral or ocular). The reason for the unequal number of participants in the two groups is that we performed group-matching, not individual matching, and the number of subjects may not necessarily be equal in the two groups in group-matching.

Peer-review: Internally peer reviewed.

Authorship Contributions

Concept: H.H., S.M., S.A., F.D.N., Design: H.H., S.M., S.A., F.D.N., Data Collection or Processing: H.H., S.M., S.A., F.D.N., Analysis or Interpretation: H.H., S.M., S.A., F.D.N., Literature Search: H.H., S.M., S.A., F.D.N., Writing: H.H., S.M., S.A., F.D.N.

Conflict of Interest: No conflict of interest was declared by the authors.

Financial Disclosure: The authors declared that this study received no financial support.

Address for Correspondence: Hassan Hashemi, Noor Eye Hospital, Noor Ophthalmology Research Center, Tehran, Iran
E-mail: research@norc.ac.ir **ORCID-ID:** orcid.org/0000-0002-2109-0856
Received: 15.02.2022 **Accepted:** 09.03.2022

Cite this article as: Hashemi H, Mehravaran S, Asgari S, Nasrabadi FD. Reply to Letter to the Editor re: "Refractive and Vision Status in Down Syndrome: A Comparative Study". Turk J Ophthalmol 2022;52:221-222

References

1. Hashemi H, Mehravaran S, Asgari S, Dehghanian Nasrabadi F. Refractive and Vision Status in Down Syndrome: A Comparative Study. Turk J Ophthalmol. 2021;51:199-205.
2. Wilton GJ, Woodhouse R, Vinuela-Navarro V, England R, Woodhouse JM. Behavioural Features of Cerebral Visual Impairment Are Common in Children with Down Syndrome. Front Hum Neurosci. 2021;15:673342.
3. Makateb A, Hashemi H, Farahi A, Mehravaran S, Khabazkhoob M, Asgari S. Ocular alignment, media, and eyelid disorders in Down syndrome. Strabismus. 2020;28:42-48.